

EXPLORING THE MECHANISMS BY WHICH THE
KYNURENINE PATHWAY METABOLITE QUINOLINIC
ACID INDUCES PHOSPHORYLATION OF TAU PROTEIN.

By

Ali Asgher Ali

A THESIS SUBMITTED TO MACQUARIE UNIVERSITY
FOR THE DEGREE OF MASTERS OF RESEARCH
FACULTY OF MEDICINE AND HEALTH SCIENCES
DEPARTMENT OF BIOMEDICAL SCIENCES

OCTOBER 2020



EXAMINER'S COPY

This thesis is submitted to Macquarie University in fulfilment of the requirement for the Degree of Master of Research.

The work presented in this thesis is, to the best of my knowledge and belief, original except as acknowledged in the text. I hereby declare that I have not submitted this material, either in full or in part, for a degree at this or any other institution.

Ali Asgher Ali

Declaration of contributions to publication

The work presented in this study was conducted by Ali Asgher Ali under the supervision of Dr David B. Lovejoy who formulated the working hypothesis of this study and provided assistance in writing, mentoring, and editing. Dr David Lovejoy, Dr Kelly Jacobs, Dr Ben Heng, and Dr Edwin Lim assisted with elements of the experimental work. Prof. Gilles Guillemin also provided supplementary support.

Acknowledgements

There is no knowledge and science
like pondering and thought; and
there is no prosperity and
advancement like knowledge and
science.

Ja'far al-Sadiq

Bihar al-Anwar

What was supposed to be a 10-month long marathon became a last-minute sprint, which would not have been possible without the guidance and support I received throughout the year.

To everyone at the Guillemain Group who helped me from start until the final end: a huge thanks.

My work with cell culture, Western blots, and UHPLC would have been made more difficult had it not been for the support provided by Ben, who also gave me the primary human neurons used in my experiments. While I am mentioning the UHPLC, I also wanted to acknowledge the assistance that Ed provided in training me in using the UHPLC, and thank Ananda for helping me with all the trouble-shooting with what became the most frustrating equipment in this study. I also wanted to thank Sharron, who so kindly provided the macrophages, as well as her support throughout the year both inside and outside the lab. I also want to take the time to acknowledge each time

Vanessa kept reminding me to not spend too many weekends in the lab. Thank you Kelly, whose early training and support helped me catch-up to lost time - many of my first lab technique attempts during HDR were with you. I also must acknowledge Gilles, who aside from helping me with my first set of ICC experiments, was readily available to provide his insight, especially during the latter stages of my ROS and Ca^{2+} influx experiments. I also wanted to thank Abid, whose suggestions really helped me in my last weeks of experiments. Most importantly, I want to thank you all for you welcoming me into your group.

I also wanted to take the time and mention the Connor Group, in particular Marina, who provided not only her insight into Ca^{2+} influx assays but also supplied us with a sample of the FLIPR and Fura-2AM dyes that helped shape the earlier stages of the experiments. I am also thankful for members of the Dementia Research Centre, Magda and Holly from the van Eersel and Fath Groups in particular, who supplied me with the primary mouse cells and the GCamp virus that ended up being a part of some critical experiments. All the microscopic imaging of my ICC and live-cell imaging experiments would not have been so easily achieved without the support and guidance of Arthur, who was so readily available to answer all my questions. I also wanted to acknowledge that my thesis was supported by the MQ-MRES RTP and MQ-MRES 2 scholarships, which partially funded my experiments, and the Motor Neuron Disease Research Centre, which provided most of the supplies for the Western blot experiments.

Of course, I wanted to especially thank David, my supervisor whose help eased my research experience. We had many set-backs but I was finally able to make it because of *your* great ideas. Thank you.

The support I received outside the lab makes me feel most grateful for those around me. I want to acknowledge the support provided to me by Jen, who was willing to spend as much time on me as I needed. Thank you for having my back. I also wanted to acknowledge my friends, both the old friends that came with me into the MRes program, and to the new friends I made along the way. Thank you for keeping me company during those late nights and weekends, especially to my Western blot

buddy. The biggest blessing is that there are so many I can name. Thank you for your motivation. I also want to thank my friends from outside the university, who didn't really understand my "brain stuff" but were there for me throughout the year.

Most importantly, I wanted to thank my family, especially my parents, whose quiet resilience throughout the year left me inspired and motivated. There can never be enough words to describe how much your patience has meant to me. Tolerating my late nights, supporting me through my ups and downs, dealing with my frustrations, and keeping me grounded; all despite everything else... words are just not enough.

I am very lucky.

And very thankful.

Conference Submissions

- Ali A. Ali, Gilles J. Guillemin, David B. Lovejoy; *A cell model to investigate the mechanisms by which tau phosphorylation is modulated in the Kynurenine Pathway.* (Accepted for poster presentation at the Australia and New Zealand Cell and Developmental Biology Meeting, 2019)

Abstract

Quinolinic acid (QUIN) is a well-described neurotoxin produced in excess by chronic induction of the kynurenine pathway of tryptophan metabolism. Indeed, clinical evidence supports a role for QUIN in the progression of Alzheimer's disease (AD). Several studies have also shown that QUIN is associated with Tau phosphorylation. QUIN was found to be co-localised with phosphorylated Tau (pTau) in AD brain clinical samples and treatment of primary neurons with QUIN increased the expression of pTau. However, no studies have yet examined the mechanism by which QUIN causes Tau phosphorylation.

The work reported in this thesis aimed to better understand this mechanism. Considering that QUIN has been reported to mediate cellular calcium influx by stimulation of the N-methyl D-aspartate receptor (NMDAR) stimulation and that calcium influx also has been shown to lead to Tau phosphorylation, it was hypothesized that QUIN might mediate Tau phosphorylation by increasing intracellular calcium influx. Using a variety of experimental strategies, we investigated whether this was the case. We further explored this mechanistic link by examining the effects of a calcium chelator, an inhibitor of kynurenine-3-monooxygenase (KMO; the enzyme that leads to QUIN production) and NMDAR blockers on the expression of pTau.

Contents

Declaration	v
Acknowledgements	vii
Conference Submissions	xi
Abstract	xiii
Abbreviations	xix
List of Figures	xxi
List of Tables	xxv
1 Introduction	1
1.1 Overview	1
1.2 Tau and Tauopathies	3
1.2.1 Understanding Tauopathies	3
1.2.2 Neurotoxic Tau Formation	7
1.3 The Role of Enzymes in Tau Phosphorylation	9
1.4 Tauopathy and Reactive Oxygen Species (ROS)	10
1.5 N-methyl-D-aspartate receptors (NMDARs) in AD	12
1.6 Calcium in Tauopathies	13

1.7	The Kynurenine Pathway (KP) in Tauopathies	14
1.7.1	Kynurenine Metabolites in Tauopathies	16
1.7.2	KP Enzymes in Tauopathies	19
1.8	Aims	20
2	Methodology	21
2.1	Tissue Culture	21
2.2	Cellular IDO and KMO Expression in N2a and SH-SY5Y Cell Lines . .	22
2.3	Baseline Tau Phosphorylation in HEK-293 peZ Cells	23
2.4	<i>In vitro</i> Calcium Imaging of Primary Mouse Neurons in Response to KP Modulation	23
2.5	Tau Phosphorylation in Response to KP Metabolite Modulation	24
2.6	ROS Production in Cells as determined by the DCF-DA Assay	24
2.7	Ca ²⁺ Influx in Cells as determined by the Fura 2-AM Assay	26
2.8	Western Blot Analysis	27
2.9	Immunocytochemistry	28
2.10	KP Metabolite Quantification via Ultra High Performance Liquid Chro- matography (UHPLC)	28
2.11	Statistical Analysis	29
3	Results	31
3.1	Cellular IDO-1 and KMO Expression in N2a and SH-SY5Y Cell Lines .	31
3.2	KP Stimulation Increases Tau Phosphorylation in N2a Cells	34
3.3	KYNA Inhibits QUIN-Driven ROS	35
3.4	ROS Production in a KMO Over-expressing Cell Model	36
3.5	QUIN Increases Cellular Ca ²⁺ Influx	38
3.6	KMO Over-Expression Increases Baseline Tau Phosphorylation in HEK peZ Cells	45
3.7	KP Metabolite Modulation Alters Tau Phosphorylation	46
3.8	Attempted Optimisation of High-Throughput ROS and Ca ²⁺ Influx As- says in Various Cell Lines	56

4	Discussion	63
4.1	Interplay Between KP Metabolites, ROS and Ca^{2+} Influx	63
4.2	Calcium Signalling in Tau Phosphorylation	67
4.3	The Role of the KP and KMO Inhibition in Tauopathy	71
4.4	Conclusion	73
A	Appendix	75
A.1	Real-Time Videos of Ca^{2+} Influx	75
	References	77

Abbreviations

3HK	3-hydroxy kynurenine
AA	Anthranilic acid
Aβ	Amyloid- β
AD	Alzheimer's disease
APP	Amyloid precursor protein
BBB	Blood-brain barrier
BDNF	Brain-derived neurotrophic factor
BSA	Bovine serum albumin
CDK	Cyclin-dependent kinase
CNS	Central nervous system
DCF-DA	2',7'-dichlorofluorescein diacetate
GSK	Glycogen synthase kinase
HEK	Human Embryonic Kidney
IDO	Indoleamine-pyrrole 2,3-dioxygenase
KAT	Kynurenine aminotransferases
KMO	Kynurenine-3-monooxygenase
KP	Kynurenine pathway
KYN	Kynurenine
KYNA	Kynurenic acid
MAPK	Mitogen-activated protein kinase
MAPT	Microtubule-associated protein tau

NFT	Neurofibrillary tangles
NMDA	N-methyl-D-aspartate
NMDAR	N-methyl-D-aspartate receptor
PBS	Phosphate buffered saline
PFA	Paraformaldehyde
PKA	Protein kinase A
PKC	Protein kinase C
PP	Protein phosphatase
p-Tau	Phosphorylated tau
PTMs	Post translational modifications
QUIN	Quinolinic acid
ROS	Reactive oxygen species
TRP	Tryptophan
UHPLC	Ultra high-performance liquid chromatography
VGCC	Voltage-gated calcium channel

List of Figures

1.1	Extensive NFT formation in the hippocampus of an AD patient.	2
1.2	Timeline of tau-centric research in neurodegeneration.	3
1.3	Various manifestations of tauopathies in the diseased human brain. . .	6
1.4	Hypothesised relationship between the Kynurenine Pathway and neurodegeneration.	15
1.5	Phosphorylation of tau induced by QUIN in a dose-dependent manner.	17
1.6	QUIN colocalises with NFTs in human hippocampal neurons.	18
3.1	Confirmation of KMO expression in mammalian N2A and SH-SY5Y cancer cell lines.	32
3.2	Confirmation of IDO-1 expression in mammalian N2A and SH-SY5Y cell line.	33
3.3	KP metabolites 3HK and QUIN induced tau phosphorylation in N2a cells	34
3.4	QUIN increases ROS production in N2a cells	35
3.5	KYNA pre-incubation decreases QUIN-derived ROS production in SH-SY5Y cells	36
3.6	KMO over-expression induces greater ROS production in HEK peZ cells	37
3.7	Live cell calcium imaging of primary hippocampal mouse neurons acutely treated with QUIN and calcium markedly induces increased Ca^{2+} influx.	39

3.8	Live cell calcium imaging of primary hippocampal mouse neurons chronically treated with QUIN markedly induces increased Ca^{2+} influx, inhibited by NMDAR antagonists and calcium chelation.	40
3.9	Live cell calcium imaging of primary hippocampal mouse neurons acutely treated with calcium	41
3.10	Live cell calcium imaging of primary hippocampal mouse neurons acutely treated with QUIN.	42
3.11	Live cell calcium imaging of primary hippocampal mouse neurons chronically treated with Glutamate, NMDAR antagonist Memantine, and calcium chelating agent EDTA.	43
3.12	Live cell calcium imaging of primary hippocampal mouse neurons chronically treated with QUIN and NMDAR antagonist KYNA.	44
3.13	Baseline Tau Phosphorylation in HEK peZ Cells.	45
3.14	IFN γ treatment as a model of inflammation across cell types.	47
3.15	Schematic diagram demonstrating how KMO inhibitor Ro-61-8048 modulates the KMO branch of the KP	48
3.16	3-hydroxykynurenine : Kynurenine ratio in human neurons following KP modulation	49
3.17	3-hydroxykynurenine : Kynurenine ratio in HEK peZ cells following KP modulation	50
3.18	3-hydroxykynurenine : Kynurenine ratio in human neurons following KP modulation	51
3.19	Altered tau phosphorylation in primary human neurons after chronic KP modulation and Ca^{2+} chelation.	53
3.20	Altered tau phosphorylation in primary human macrophages after chronic KP modulation and Ca^{2+} chelation.	54
3.21	Altered tau phosphorylation in primary human macrophages after chronic KP modulation and Ca^{2+} chelation.	55
3.22	Time-course of a DCF-DA assay in various cell lines	57
3.23	End-point DCF-DA assay in HEK peZ [-] cells	58

3.24	Time-course of a Fura-2AM assay in N2a cells	60
3.25	Short-term end-point of a Fura-2AM assay in N2a cells	61
3.26	End-point Fura-2AM assay in SH-SY5Y and N2a cells	62

List of Tables

1.1	Available treatments for taupathies.	7
-----	--	---

1

Introduction

1.1 Overview

Alzheimer's Disease (AD) is the most common form of brain degeneration, responsible for 70% of dementia cases [1]. It is considered a global public health priority by the World Health Organization because of its associated comorbidities (diabetes, obesity and hypertension) [2] which are also known to exacerbate AD hallmarks, namely neurofibrillary tau tangles (NFT) and amyloid-beta ($A\beta$) plaques. The amyloid hypothesis states that AD pathology is triggered by $A\beta$ aggregation in response to disrupted β or γ secretase-driven APP cleavage, resulting in plaque formation [3]. The tau hypothesis postulates that upon phosphorylation, tau is detached from microtubules, resulting in microtubule instability and NFT formation [3].

Accumulation of A β plaques may drive tau phosphorylation [4], even though NFT formations are visible prior to A β plaque development [5]. There is also evidence to suggest that NFTs are the intermediary between A β plaque formation and tau pathology [6], with post-mortem human brain samples showing A β plaque co-localisation with NFTs within the AD hippocampus (Fig. 1.1) [7, 8]. However, animal studies have shown that extensive A β does not lead to tau pathology, even with signs of inflammation [9–11]. Protein phosphatases have also been linked to tau phosphorylation by acting through the NMDA receptors (NMDARs), a process that may be interrupted by quinolinic acid (QUIN). QUIN is a metabolite from the Kynurenine Pathway (KP) of tryptophan metabolism associated with neurodegeneration. It is known to be co-localised with NFTs [12–16], and its production is controlled by the kynurenine 3-monooxygenase (KMO) which is also implicated in neurodegeneration [17, 18]. It is believed that QUIN deregulates NMDAR-PP (N-methyl-D-aspartate receptor - protein phosphatase) pathways by inducing calcium (Ca²⁺) influx at NMDAR to promote ROS activity.

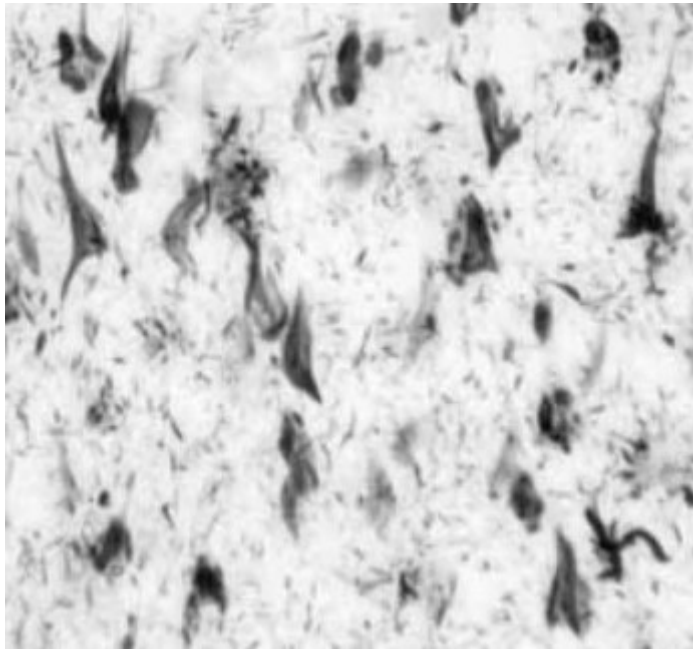


FIGURE 1.1: Extensive NFT formation in the hippocampus of an AD patient. Sourced from [7].

Ca^{2+} influx and ROS production are associated with phosphorylated tau (p-Tau) formation, but there are no studies on the mechanisms by which these phenomena produce p-Tau. This project aims to directly investigate whether QUIN-mediated Ca^{2+} influx is responsible for tau phosphorylation and further investigate the role of ROS on the production of p-Tau.

1.2 Tau and Tauopathies

1.2.1 Understanding Tauopathies

Studies show that phosphorylated tau (p-Tau) is the key component in the development of intracellular filamentous inclusions, known as neuro-fibrillary tangles (NFTs), that characterise many human neurodegenerative diseases, collectively referred to as tauopathies. Tau phosphorylation is known to be associated with disease symptoms [5] and may likely mediate mechanisms of neurodegeneration. Tau has long been implicated in neurodegeneration (Fig. 1.2) since NFTs were first identified in 1985 [19].

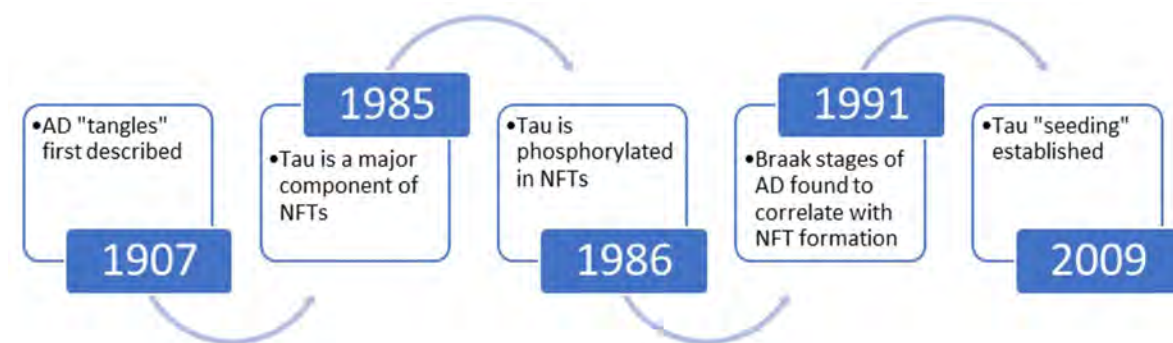


FIGURE 1.2: Timeline of tau-centric research in neurodegeneration. Adapted from [19].

The tau protein is an intrinsically disordered protein with six isoforms [20] unfolded in standard physiological conditions [21]. The ratio of tau isoforms and level of phosphorylation define physiological and pathological tau activity. These isoforms range from 58-110 kDa [19] and are derived from multiple splicing of the *MAPT* gene (which contains 5 exons) [22]. Tau isoforms then also undergo variable post-translational modifications (PTMs) and have different assemblies which can give rise to NFTs [23]. These modifications are prone to cross-talk [20], which further influence tauopathy [24]. Additionally, these PTMs may feed forward changes from oxidative stress [4], resulting in a positive feedback system that increases NFT formation alongside increased tau phosphorylation [25]. Various PTMs, including acetylation, ubiquitination, nitration, proteolytic cleavage, among others, are responsible for the heterogeneity of tauopathies [24]. It should be noted that the functions of these PTMs remain largely unknown [24] and that tau phosphorylation also has physiological benefits. For example, most tau phosphorylation occurs reversibly in early childhood and is critical for foetal brain development [5]. Aside from PTMs, there are more than 50 known mutations of *MAPT* which give rise to tauopathies [24].

Traditionally, tau has been thought to be responsible for cellular integrity and molecular transport [5]. However, these early studies were conducted in vitro in non-neuronal cells which limit their physiological relevance. Recent experiments challenge this tau dogma with results suggesting that tau in fact enables axonal microtubules to have more labile domains [21]. Modern advances lead to the consensus that tau is multi-functional, contributing to microtubule-related features of nerve cells and to non-microtubule features of these cells. Interestingly, where tau is depleted from the neurons, microtubules don't destabilise. Rather, the labile domains of the protein become shorter and more stable due to competing binding by MAP6 [21]. This irreversible stabilisation is likely achieved via tau phosphorylation, which decreases tau availability to the labile domain of microtubules, leaving stabilising factors such as MAP6 to bind in its place. Furthermore, knockdown and knockout models of tau have demonstrated no effects on microtubule assembly and axonal support [19].

It has been difficult to ascertain which tau species contribute most to tauopathies and by which mechanisms. Controversy remains as to whether it is the loss of tau function or the modification of tau function that results in disease manifestation [24]. A review into the molecular structure of tau [20] postulated that this may be because most studies have used recombinant tau constructs that confound results with their inherent biases which include 1) using arbitrary cofactors, 2) using constructs with no post-translational modifications, or 3) using arbitrary tau segments, all which make it difficult to ascertain their biological relevance. This is demonstrated where tau aggregates excised from post-mortem tissue showed varied composition and morphology depending on tauopathy, the heterogeneity of which is not matched in the present constructs (Fig. 1.3) [26]. Further complexity arises considering that tauopathies are not characterised by specific phosphorylation sites, and that tau phosphorylation is not characterised by increased phosphorylation at a specific epitope, rather it is characterised by either an overall increase in phosphorylation across multiple epitopes, or by an increase in the p-Tau:Tau ratio [24].

Consensus within the literature shows that regardless of mechanism, reducing overall tau levels may show benefit. Strategies identified to achieve this are yet to be tested in human trials and include:

- Anti-tau antisense oligonucleotides to inhibit Tau mRNA synthesis [27].
- Tau kinase and acetylase inhibition to inhibit proteasomal degradation [28].
- Anti-tau antibodies and tau aggregation inhibitors to limit NFT production [29].
- Autophagy enhancers to kill damaged cells [30].

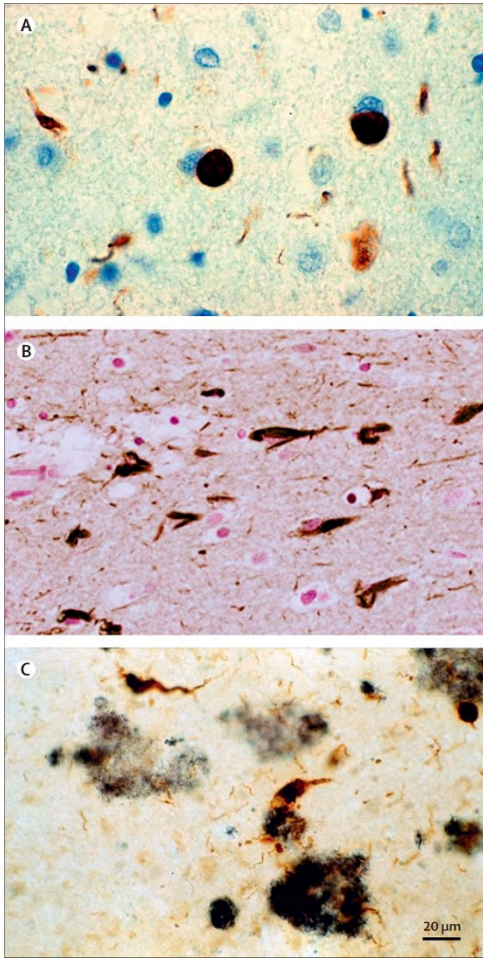


FIGURE 1.3: Various manifestations of tauopathies in the diseased human brain. (A) Pick bodies made of tau (brown) in Pick's disease. (B) NFTs made of tau (brown) in chronic traumatic encephalopathy. (C) Neuritic plaques made of amyloid β (blue), and NFTs (brown) in AD. Sourced from [5].

While there are treatments available (Table 1.1), there is a lack of successful disease modifying/disease ameliorating therapy for tauopathies. Challenges to treat tauopathies include the inability to diagnose early and discriminate between types of tauopathies, as well as an incomplete understanding of the cellular mechanisms involved in this process [31].

TABLE 1.1: Treatments available for tauopathy patients. Adapted from [31].

Drug	Disease stage	Mechanism
Donepezil/Rivastigmine	All Stages	Cholinesterase inhibition
Galantamine	Mild-Moderate	
Memantine	Moderate-Severe	NMDAR Antagonism

1.2.2 Neurotoxic Tau Formation

Many factors behind phosphorylation have been identified and include phosphatase and kinase deregulation, secreted $A\beta$, and oxidative stress [22]. Most tau phosphorylation occurs in dendrites and these tau species play an important role in loss of synaptic function and cognition mediated by NMDA. Dendritic tau has been shown to mediate $A\beta$ -dependent excitotoxicity by triggering NMDA receptor (NMDAR) phosphorylation [19]. This phosphorylation has been associated with impaired synaptic plasticity [19].

The resulting NFTs produced from phosphorylation and consequential aggregation was thought to be associated with the induction of cell apoptosis, since its formation matched clinical parameters for disease severity and cognitive decline [5, 19]. Post-mortem brain also showed NFT inclusions in multiple tauopathies (Fig. 1.3) [5]. Traditionally, it was believed that aggregation of insoluble, phosphorylated tau aggregates in the form of NFTs were the only toxic manifestation of tau. It is now accepted that soluble, prefibrillar tau oligomers are also responsible [24]. Gene silencing of *MAPT* to reduce tau oligomer expression has been known to recover memory in mouse models of tauopathies despite NFT formation [24].

Furthermore, studies show living neurons despite NFT inclusions, so it is now believed that small tau oligomers, rather than NFTs, are related to neuronal cell death [21]. This pathology seems to spread through intracellular propagation in a “prion-like” manner, where phosphorylated tau converts native tau into aggregates under oxidising conditions that form intermolecular disulphide bonds [32]. This process, termed “seeding”, requires increased ROS activity, thought to be initiated by extracellular tau uptake, but non-cell based mechanisms are now also being identified [33].

Evidence also shows that the seeding process is facilitated by tau phosphorylation [34–37], suggesting a positive feedback loop. This is best demonstrated in a study where NFTs sourced from different tauopathies were injected into mice, with tau from progressive supranuclear palsy and corticobasal degeneration showed glial tau inclusions, suggesting glial transmission, unlike neuronal transmission seen in AD [38]. This suggests that different tau strains determine seeding potency and cell-type specificity of tau aggregation that underlie the diversity of human tauopathies. Stimulating neuronal activity has been known to encourage tau release, but this extracellular tau is also known to modulate neuron behaviour, creating a positive feedback loop [33]. The uptake of extracellular tau by other neurons cannot yet be inhibited and may be a useful therapeutic strategy.

Patterns of phosphorylation differ - some sites are more phosphorylated in the diseased brain, or others are only phosphorylated in the diseased brain. Indeed, phosphorylation positions must be considered alongside degree of overall phosphorylation. Depending on the epitope, dephosphorylation may also produce NFTs [20]. Phosphorylation at Ser202 and Thr205 has been known to be sufficient to form aggregates when combined with phosphorylation at Ser119/208 but will not form aggregates if Ser262 is phosphorylated [39–42]. Together, these sites of phosphorylation are hypothesised to be the most relevant for conformational changes seen in tauopathies [39]. Combined phosphorylation at Ser202/Thr205/Ser208 epitopes results in readily formed NFT-like structures, supporting the hypothesis that the Ser202 and Thr205 epitopes of tau are crucial for NFT formation and protein destabilisation, similar to that seen in tauopathies.

It is noteworthy that phosphorylation of various tau epitopes relies on PTMs at other epitopes. Examples include acetylation on Lys321, which is responsible for inhibiting aggregation. Deacetylation at this epitope was shown to cause downstream phosphorylation at the Ser324 residue, which interfered with microtubule stability and was found to be up-regulated in AD patients [43]. It must be reiterated however, that tauopathies are not defined by phosphorylation at certain epitopes, rather, they are defined by an overall increase in phosphorylation across multiple epitopes, or an increase in the p-Tau:Tau ratio [24].

1.3 The Role of Enzymes in Tau Phosphorylation

Phosphorylation of tau has been known to play a crucial role in neurodegenerative diseases such as Alzheimer's, Parkinson's, and Huntington's diseases, as well as Motor Neuron Disease (MND), Down's Syndrome and various forms of cancer [5, 44]. Both *in vivo* and *in vitro* studies have revealed multiple sites of phosphorylation [5] which lead to the detachment of tau from microtubules to form aggregates [20]. In patients with neurodegenerative disease, tau appears nine times more phosphorylated relative to healthy individuals [5]. Additionally, normal tau contains 2-3 mol phosphate per mole of tau, but in patients with tauopathies, this is increased by at least 3-4-fold [32].

Phosphorylation is regulated by various kinases that phosphorylate and phosphatases that dephosphorylate the tau protein. They include protein kinase A (PKA), glycogen synthase kinase 3 β (GSK3 β), cyclin-dependent kinases (CDK), protein phosphatases (PP), and calcineurin. Tauopathies demonstrate kinase activation of PKA, GSK3 β , and CDK5 and decreased expression of phosphatases PP2A, PP2B, and PP5 [45, 46], with a chronic inhibition of calcineurin [46].

PKA is directly triggered by insulin deficiency in diabetic patients [47]. CDK5 and CDK1 are known to act on the most relevant sites of tau phosphorylation, with CDK1 also being known to promote A β plaque formation [39]. GSK3 β has been identified to be heavily involved in the phosphorylation of tau at Ser and Thr residues.

Insulin deficiency is also known to directly trigger PP2A [48], although the mechanism of discrimination between kinase and phosphatase activity remains to be elucidated. While PP2B is decreased in many tauopathies, it is increased in the AD brain [45]. However, the primary phosphatase that regulates tau phosphorylation in AD is PP2A [45]. First identified in this capacity as a tau phosphorylation mediator in 1996, it is responsible for 71% of phosphatase activity in the brain [49, 50]. It acts on Thr205, a site of phosphorylation known to be involved in conformational change, by acting upon GSK3 β through an unidentified mechanism [51, 52].

1.4 Tauopathy and Reactive Oxygen Species (ROS)

ROS and phosphorylation appear to be crucial for the manifestation of tauopathies, although the mechanistic causes remain poorly understood. While the literature supports the notion that accumulation of phosphorylated tau increases ROS activity, the reverse is also appear to be the case - that ROS production stimulates tau phosphorylation. ROS is balanced by antioxidant systems, which when disrupted lead to ROS accumulation and oxidative stress [40]. There is growing evidence that ROS activity either leads to, or is a component of, tauopathies, and has been implicated in many neurodegenerative diseases. Particularly in AD, the correlation between A β plaque formation and ROS production is well documented [24]. This is further supported by the Oxidative Stress Theory of Ageing [24], which suggests that brain neurons are the primary target of oxidative stress. Studies show that over-expression of tau can lead to increased ROS production and induce cell apoptosis. Seeding has also been implicated in ROS production, where primary rodent neurons expressing tau oligomers displayed high ROS production and increased mortality [24].

Evidence shows tau over-expression leaves cells vulnerable to oxidative stress, and that this is one of the leading biomarkers of tauopathies that can be detected in early onset, before A β plaque formation [40]. For example, pathological tau concentrations in murine N2a neuroblastoma cells demonstrated increased susceptibility to oxidative stress, leading to eventual apoptosis via the JNK pathway [24]. Whether it is a cause

or consequence of tau phosphorylation remains to be confirmed [46]. While increased ROS production correlation with increased tau phosphorylation is well recorded, controversy remains as to whether ROS production is a consequence of tauopathy or is an early cellular marker of "seeding". Several key enzymes have been implicated in both processes.

As previously described, PKA and PP2B are directly triggered by insulin deficiency in diabetic patients [47]. Additional oxidative stress further decreases insulin secretion, thereby increasing sensitivity to ROS [24]. Low insulin secretion has been known to increase tau phosphorylation in mice models of AD [24]. These observations directly link ROS production and tau phosphorylation to increased PP2B and PKA activity, which are in turn involved in Ca^{2+} influx via NMDAR. The anti-diabetic drug Metformin has been shown to mitigate this effect [53]. These findings give credence to the increasingly debated suggestion that AD is simply a new type of diabetes, Diabetes Type 3 [54].

PP2A is unusual in that it is down-regulated in most tauopathies, but up regulated in AD. While we see an interesting correlation between insulin deficiency, PP up-regulation, and ROS production, the literature also reports PP down-regulation with ROS activity. This correlates with their known enzymatic activity during tau phosphorylation - namely that PP2A is only responsible for 7% of all PP activity in the AD brain [45], while other PPs responsible for 93% of tau dephosphorylation, such as PP2B are down-regulated in AD and other tauopathies. PP activity has been closely linked with GSK3 β . The interaction of both these enzymes in tau phosphorylation has been linked to neurprotective conformational changes in the tau protein [51, 52].

GSK3 β itself has a dual role in tauopathies. In *in vitro* studies on primary cortical neuronal cultures have shown that ROS production resulted in increased tau phosphorylation, which reduced after GSK3 β inhibition [24]. Notably, the experiment was conducted in a low-GSK3 β expressing paradigm. When repeated with higher concentrations, the enzyme showed no protective effects. This suggests that the GSK3 β enzyme may have therapeutic benefits for ROS-induced cell apoptosis at low concentrations.

Intracellular mitochondrial A β accumulation has been well described in AD [55]. A β -induced mitochondrial dysfunction is reportedly due to A β interactions impairing physiological phosphorylation at the outer mitochondrial membrane, intermembrane space, inner mitochondrial membrane, and the mitochondrial matrix, which increases ROS production [56]. Increased ROS activity correlates with tau phosphorylation and the translocation of the GSK3 β enzyme to the nucleus [24]. This may be a modulatory factor in PKA activation.

It is thought that the stimulation of NMDA receptors (NMDARs) may dissociate tau from PP2A to reduce overall phosphatase activity [57]. PP2A is an allosteric modulator of NMDARs, which anchor the protein in the central nervous system [13]. Following over-activation of NMDAR, tau shows a rapid increase in phosphorylation followed by a slower dephosphorylation mediated by PP2A, indicating that the protein binds back to the receptor through unknown means [58].

1.5 N-methyl-D-aspartate receptors (NMDARs) in AD

Indeed, studies in AD postmortem brain tissues and AD animal models support a role for disruption of synaptic Ca²⁺ regulation in the neurotoxic action of A β , which may serve as a trigger for synaptic deterioration driving the cognitive loss in AD [59]. This cognitive loss is promoted by long-term depolarisation, where prolonged release of pre-synaptic glutamate activates AMPA receptors, removing magnesium antagonism at NMDAR, which in turn, enables Ca²⁺ influx. This in turn activates CaMKII cascade. This excess long-term depolarisation results in post-synaptic Ca²⁺ influx and induces spine shrinkage and synaptic loss [60], which has been associated abnormal calcineurin activity and decreased glutamate receptor (e.g. NMDARs) expression [61].

Thus, pathological inhibition of NMDARs by elevated A β may shift NMDAR-dependent signalling cascades towards apoptotic pathways, the mechanisms of which are yet to be elucidated.

Of special note is the relationship between NMDA and A β . Simultaneous A β and NMDA markedly increased influx, mediated by the post-synaptic GluN2B NMDAR [59]. This, and other evidence, supports the notion that A β deregulates glutamate receptors resulting in early cognitive deficits. From this, it can be surmised that NMDA is either the downstream target of A β , acting upon synaptic transmission, or it may control the formation of A β .

1.6 Calcium in Tauopathies

Calcium homeostasis is also known to play a role in tauopathies. Increased cytosolic concentrations alter the metabolism of A/ β plaque precursors [62] and phosphorylate Ca²⁺/calmodulin-dependent protein kinase II (Ca/CAMK II) [63]. In turn, A β plaques destabilise calcium homeostasis by acting on all glutamate receptors, including NMDARs, to enhance cellular uptake of Ca²⁺, leaving neurons vulnerable to excitotoxicity [12]. Recent findings have also shown that tau phosphorylation at the Thr205 epitope increased Ca²⁺/CAMK IV phosphorylation and nuclear Ca²⁺ influx in the rat hippocampus [64]. This suggests a possible positive feedback loop between tau phosphorylation and Ca²⁺ influx.

To this end, Ca²⁺ channel blockers have been shown to reduce A β toxicity [65] by preventing Ca²⁺ influx at voltage-gated Ca²⁺ channels. Influx of Ca²⁺, causing mitochondrial dysfunction, is partly driven by A β peptides activating NMDARs [66] which leads to tauopathies.

Interestingly, NMDAR activation with protein-kinase C (PKC)-driven GSK3 β inhibition has been shown to diminish tau phosphorylation at the Ser202 epitope [67]. This suggests that NMDAR is an important factor in tau phosphorylation, where excess NMDAR activation increases tau phosphorylation, while inhibition of enzymes acting at the NMDAR decrease cell apoptosis, Ca²⁺ influx, and tau phosphorylation.

It is also noteworthy that Ca^{2+} influx driven by certain mechanisms has demonstrated neuroprotective effects. Specifically, GluN2A (NMDAR)-driven influx is known to induce brain-derived neurotrophic factor (BDNF), a neuroprotective agent. However, influx through the extra-synaptic GluN2B inhibits this response [59]. This pre-/post-synaptic interplay may explain the synaptotoxicity of $\text{A}\beta$ oligomers that contribute to AD cognitive deficits [68] and the aberrant excitatory and inhibitory responses involving learning and memory circuits driven by $\text{A}\beta$ [69].

Such pathological signalling disrupts NMDAR-MAPK cascades that are monitored by Ca^{2+} sensors in neurons and microglia, which in turn mediates production of pro-inflammatory cytokines [70] that can activate various pathways known to be involved in tauopathies.

1.7 The Kynurenine Pathway (KP) in Tauopathies

The kynurenine pathway (KP) has emerged as a key regulator of neuroprotective and neurotoxic metabolites, and is the subject of drug development initiatives to develop inhibitors to block certain enzymes in the pathway [71, 72]. Current evidence suggests the KP metabolites may be important biomarkers of neurodegenerative and other diseases [73, 74].

There is mounting evidence to suggest that the metabolites of the Kynurenine Pathway (KP), a component of the immune system responsible for the metabolism of the essential amino acid Tryptophan, may in part regulate the pathophysiology of AD [75]. Within the central nervous system, this takes place across multiple cell-types: neurons, microglia, and macrophage. The pathway metabolites (Fig. 1.4) are known to play both protective and degenerative roles in AD.

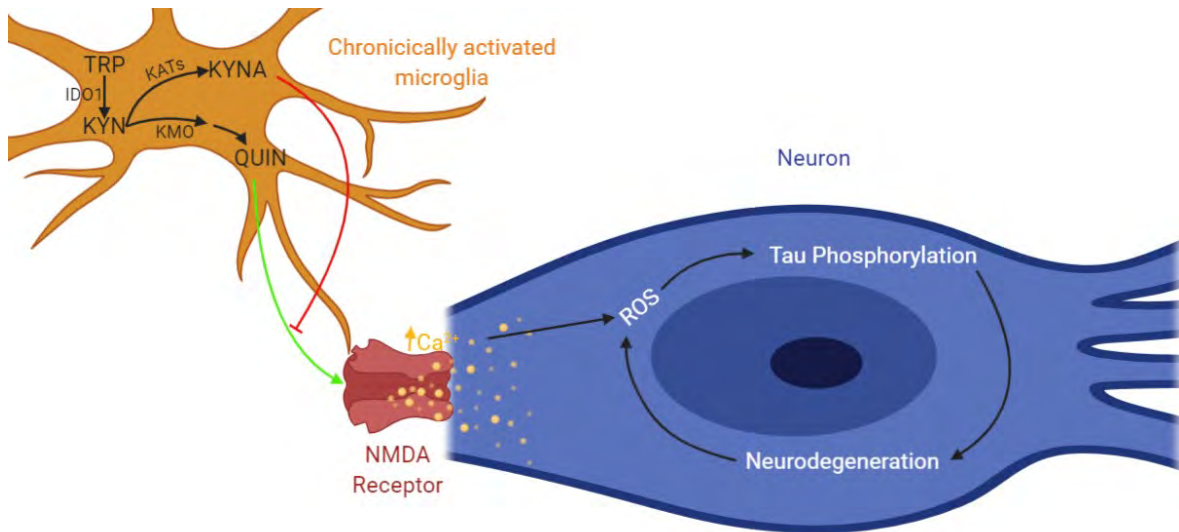


FIGURE 1.4: Hypothesised relationship between the Kynurenine Pathway and neurodegeneration. Chronically over-activated microglia produce excess QUIN, the accumulation of which correlates with p-Tau and ROS formation. IDO: Indoleamine-pyrrole 2,3-dioxygenase is the rate limiting enzyme of the Kynurenine Pathway. KMO: Kynurenine 3-monooxygenase favours the conversion of KYN to QUIN branch. KATs: Kynurenine aminotransferases favour the KYNA production branch of the pathway. TRP: Tryptophan. KYN: Kynurenine. KYNA: Kynurenic Acid. QUIN: Quinolinic acid. Image created using Biorender.com

The role of microglia in relation to the KP and neurodegeneration is noteworthy. Microglial over-activation in response to inflammation triggers the KP which may lead to neurotoxicity. Neuroinflammation derived from microglial over-activation is thought to contribute to tauopathies [76] and has associated with increased oxidative stress generated by microglia [76]. ROS activity is also known to be modulated by various kynurenine metabolites. Inhibiting the KP enzymes responsible may in part modulate microglial activity to hinder neurodegeneration. KP activation is also known to increase in tau phosphorylation at Ser202/Thr205, which produce NFTs upon phosphorylation, by inhibiting GSK3 β .

1.7.1 Kynurenine Metabolites in Tauopathies

Analytical studies show increased ratio of 3HK to Trp, increased quinolinic acid production, and quinolinic acid (QUIN)-derived production of NFTs and A β plaques [75]. High-Performance Liquid Chromatography (HPLC) evidence also suggests that tryptophan concentrations have an inverse relationship with the severity of cognitive deficit in AD patients, but not in disease duration [77]. Kynurenic acid (KYNA) has also been heavily implicated in AD [78, 79], with its synthetic analogues proving to have therapeutic effects [80]. Taken together, this strongly suggests a close relationship between KP metabolites and AD, with potential for identifying new potential targets for therapeutic intervention.

The KP was described in primary human neurons and human cancer cell lines in 2007, where the KP was implicated as a mechanism contributing to neurotoxicity [81]. A 2009 study of post-mortem brain tissue demonstrated the co-localisation of p-Tau with QUIN (Fig. 1.6, [15]). This study found a direct correlation between QUIN accumulation, tau phosphorylation and increased NFT formation in a dose-dependent manner (Fig. 1.5, [15]). NFTs have been shown to modulate cognitive impairment in AD-dementia patients [82].

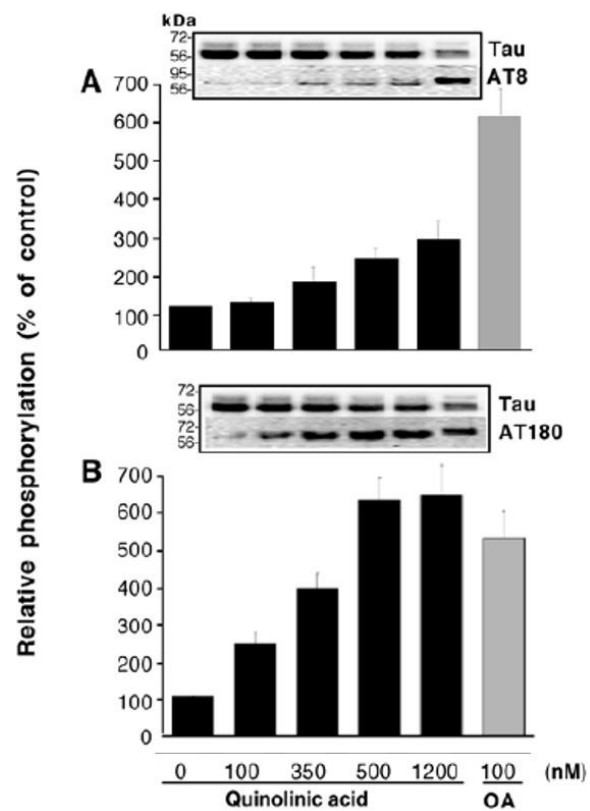


FIGURE 1.5: Phosphorylation of tau induced by QUIN in a dose-dependent manner. QUIN induces tau phosphorylation as determined by A) AT8 and B) AT180 antibodies. Image sourced from [15].

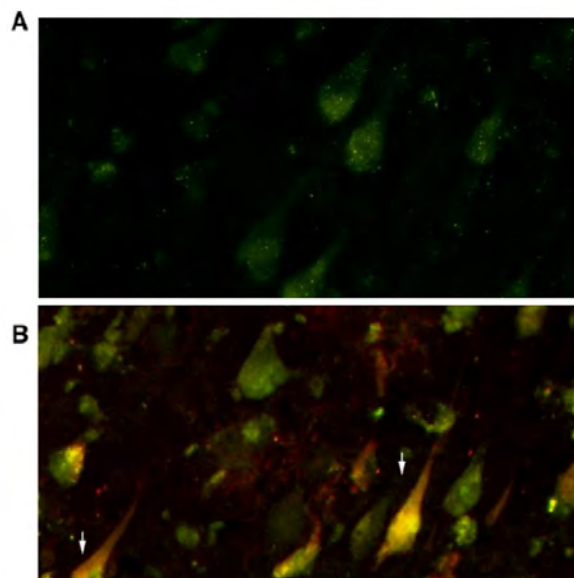


FIGURE 1.6: QUIN colocalises with NFTs in human hippocampal neurons. Deposition of QUIN (red) and p-Tau-derived tangles (green) in hippocampal neurons of A) a healthy control and B) Alzheimer's Disease brain. White arrows signify co-localisation of QUIN and p-Tau in the diseased brain. Image sourced from [15].

From the presently described literature, it can be summarised that microglial activation results in QUIN over-expression resulting in increased tau phosphorylation and ROS formation. Increased QUIN accumulation has been further shown to correlate with NFT formation and AD severity, mediated via QUIN interactions with NMDARs. QUIN activates NMDARs for glutamate release but inhibits glutamate re-uptake [77, 83]. The resulting accumulation of glutamate, referred to as excitotoxicity, contributes to cell apoptosis [57]. Conversely, KYNA demonstrates neuroprotective effects by antagonising QUIN activity at the NDMA receptor [75] which is favoured under basal conditions [83]. NMDARs are also closely linked to PP2A (see 1.4). This indicates the importance of KP metabolic homeostasis in the CNS. Both 3HK and 3HAA have also been shown to produce oxidative stress, although 3HK has been known to mitigate the neurotoxic properties of QUIN [72] by reducing oxidative stress, inline with the current belief that 3HK show milieu-specific effects on redox modulations.

1.7.2 KP Enzymes in Tauopathies

To further link the KP to tauopathy, IDO-1, the first rate-limiting enzyme in the KP was found to be colocalised with NFT formations [84]. Inhibition of the enzyme has shown neuroprotective effects [85], albeit at the expense of producing potentially neuroprotective metabolites, specifically KYNA, AA, and PIC.

KMO, another rate-limiting enzyme of the KP, is predominantly expressed within microglia and is known to be up-regulated during inflammation, leading to ROS production [83] and mitochondrial damage [86]. This is enacted through due to the KMO-facilitated production of 3HK leading to the production of the neurotoxin QUIN [83, 86].

Initially, 3HK was thought to be cytotoxic, though recent results indicate that 3HK is both antioxidant as well as pro-oxidant depending on the cell environment [18]. Regardless, the neuropathological role of 3HK remains unclear [83]. 3HK toxicity is inhibited by antioxidants, indicating its role in ROS generation [17]. Studies also indicate that 3HK synergistically enhances QUIN-mediated ROS production and neurotoxicity [77]. Conversely, low concentrations of 3HK have been known to mitigate QUIN toxicity [18]. Mechanisms of this action remain unclear, but it is known that the metabolite acts independently of NMDARs [87].

3HK conversion to QUIN is known to drive ROS production. In disease states, microglia are hyperactive resulting in overproduction and accumulation of the neurotoxic KP metabolite. Evidence for KP metabolite toxicity in tauopathies has been extensively reviewed [77]. Briefly, QUIN activates NMDARs in astrocytes to modulate Ca^{2+} influx in neurons, upstream of kinase activation (see above) [16].

The duality of the kynurenine pathway as a source for both neuroprotective and neurotoxic molecules needs to be further explored.

1.8 Aims

QUIN is known to mediate tau phosphorylation. It is known that QUIN activates the NMDAR receptor. It is also known that NMDAR activation stimulates Ca^{2+} influx, which is associated with ROS production, which in turn is associated with increased tau phosphorylation. Despite these observations, there is no present data linking these phenomena. For the first time, this project aims to mechanistically link QUIN-activated, NMDAR-driven Ca^{2+} influx and ROS production to tau phosphorylation.

To this end, tau phosphorylation will be studied across multiple cell lines with special focus on KMO over-expressing cell line HEK293 cells expressing stable pEZ[-] and pEZ [KMO] vectors [86] as a model of pathophysiological QUIN production. KMO inhibition and calcium chelation will be employed to observe effects on tau phosphorylation as well as calcium influx and ROS production. Tau phosphorylation will be confirmed using western blot analysis and ultra-High Performance Liquid Chromatography (UHPLC) will confirm KP metabolite modulation in response to enzyme inhibition. DCF and Fura-2AM assays will be utilised to assess metabolite-derived ROS production and Ca^{2+} influx.

2

Methodology

2.1 Tissue Culture

Mouse N2a and human SHSY5Y neuroblastoma cell lines, HEK-293 peZ [-] and HEK peZ [KMO] cells, and primary human macrophage and neurons were grown in 37°C at 5% CO₂ (g). Immortalised cell lines were previously cryogenically stored in -80°C in 90% FBS and 10% DMSO. N2a and HEK peZ cells were grown in Dulbecco's Modified Eagle Medium (DMEM) (Gibco reference: 11995-065). HEK peZ cells were further supplemented with 600 uM/mL Geneticin (G418 sulphate). Human SHSY5Y neuroblastoma cells were grown in a 1:1 Dulbecco's Modified Eagle Medium (DMEM)/F-12 (Ham) with GlutaMAX™ (Gibco reference: 10565-018). All immortalised cell lines were also supplemented with 10% foetal bovine serum (FBS) and 1% Penicillin Streptomycin.

Primary human monocytes were isolated from whole blood and converted to macrophage with Granulocyte-macrophage colony-stimulating factor (GM-CSF) in RPMI media. Primary human neurons were grown in Neurobasal media (Gibco reference: 21103-046) supplemented with 1% antibiotic/antimicrobial solution, 2% glutamate, 0.5% glucose, and 0.5% B27. Primary mouse neurons were co-cultured with 70, 000 hippocampal neurons and 300, 000 cortical neurons grown in neurobasal media supplemented with 1% Penicillin Streptomycin, 2% B27, and 0.25% Glutamax. Media was changed every 2-3 days, except for in primary mouse cells.

2.2 Cellular IDO and KMO Expression in N2a and SH-SY5Y Cell Lines

The Kynurenine Pathway was confirmed with the confirmation of IDO enzyme expression via immunocytochemistry (ICC) and KMO enzyme expression via western blots in N2a and SHSY5Y cell lines. Briefly, cells were seeded in EZ slides (Millipore catalogue no. PEZGS0416) at a seeding density of 0.04×10^6 cells/mL. Cells were processed in accordance to the ICC protocol. Cells were incubated with primary antibody mIDO-48 (dilution: 1/100, Biolegend, cat. #122402) and secondary antibody Goat anti-Rat IgG (H+L) Cross-Adsorbed Secondary Antibody, Alexa Fluor 555 (dilution: 1/200, Invitrogen, Cat. #A-21434).

Cells were visualised on the Axio Imager using the EC Plan Neofluar 20x/0.50 Ph 2 M27 objective and the HXP-120 lamp was used as a light source. DAPI staining was visualised using the 395 beam splitter at an excitation/emission range of 335-383/420-470 at 3.72 μ m depth of focus and 537.4 ms exposure time. Alexa Fluor 555 was visualised using the DS filter using the 570 beam splitter at an excitation/emission range of 533-558/570-640 with a 537.4 ms exposure time and 4.58 μ m depth of focus.

To establish KMO expression in N2a and SHSY5Y cells and over-expression in HEK peZ [KMO] and peZ [-] cells, cells were plated on a 6-well plate at a seeding density of 0.1×10^6 cells/well. Cells were grown to 80% confluency and lysed with RIPA

buffer and proteinase inhibitors for western blot analysis using Anti-kynurenine 3-monooxygenase antibody raised in rabbit (dilution: 1/1000, Abcam cat. #ab130959) with IRDye 680RD Goat anti-Rabbit IgG Secondary Antibody (dilution: 1/15000, Licore cat. #926-68071).

2.3 Baseline Tau Phosphorylation in HEK-293 peZ Cells

HEK peZ [KMO] and peZ [-] cells, cells were plated on a 6-well plate at a seeding density of 0.1×10^6 cells/well. Cells were grown to 80% confluency and lysed with RIPA buffer and proteinase inhibitors for western blot analysis using AT8 antibody raised in mouse (dilution: 1/1000, Invitrogen cat. #MN1020) with IRDye 700CW Goat anti-Mouse IgG Secondary Antibody (dilution: 1/15000, Licore cat. #926-32210).

2.4 *In vitro* Calcium Imaging of Primary Mouse Neurons in Response to KP Modulation

Primary mouse cells were grown in 30 mm glass-bottom dishes and transfected with GCAMP7f AAV-PHP.B (hsyn-JGCamp7-WPRE) in conditioned media at 11 DIV. After 13 days, neurons were then treated with either 250 μ M QUIN, 250 μ M QUIN and 50 μ M KYNA, 25 μ M Glutamate, 25 μ M Glutamate and 1.23 mM EDTA, or 20 μ M Glutamate and 20 μ M Memantine, for 24 hours to study chronic effects. Acute effects were studied using 250 μ M QUIN or 100 mM CaCl_2 .

The LSM 880 IndiMo AxioObserver with a Plan-Apochromat 40x/1.3 Oil DIC UV-IR M27 objective and MBS T80/R20 beam splitter was used to image cells. Laser ex/em was set to 514/546 nm (0.2% excitation power). Images were processed with a 0.86 AU pinhole using a unidirectional line sequential scanning (4.12 μ s pixel time, 30.00 μ s line time, 1.27 s frame time, 800 gain). At least 60 frames were recorded along the same focal plane for true comparisons across treatments.

Cell signalling was quantified using the Fiji software. Briefly, .CZI files generated during imaging were imported into the software. Regions with cellular activity were selected and added into the Region of Interest (ROI) Manager to calculate mean signal. Each frame incorporated at least 5 ROIs with a further 2 ROIs selected to account for background.

2.5 Tau Phosphorylation in Response to KP Metabolite Modulation

Preliminary tests were conducted on N2a cells treated with 10 μ M 3HK, 1200 nM QUIN, 100 μ M NMDA and 100 μ M NMDA + 10 μ M D-Ser. After a 24-h period, a Western blot analysis was conducted to determine changes in tau phosphorylation.

HEK peZ cells and primary neurons and macrophage were treated with 100 IU IFN γ /mL (Miltenyi Biotec #130-096-484) to up-regulate IDO-1 expression, over 24 or 72 hours. Cells were further supplemented with enzyme inhibitors and/or pre-incubation with other KP metabolites. UHPLC analysis was conducted to confirm IFN γ and enzyme inhibition activity.

2.6 ROS Production in Cells as determined by the DCF-DA Assay

Preliminary ROS assays were conducted in immortalised cell lines using Immunocytochemistry. Briefly, cells treated with 250 μ M QUIN or received a 2-h pre-incubation with 50 μ M KYNA followed by 24-h exposure period. After the 24-h treatment period, cells were given 2*5-min PBS washes followed by 10 μ M DCF-DA (Sigma-Aldrich cat #D6883) incubation prepared fresh in complete media. Incubation period was 30-min at 37°C at 5% CO $_2$ (g). Cells were visualised on the Axio Imager using a EC Plan Neofluar 20x/0.50 Ph 2 M27 objective and a HXP-120 lamp. DAPI was visualised with a 395 beam splitter with the excitation/emission range of 335-383/420-470 nm,

using 274.8 ms of exposure time and a depth of focus of 1.65 μm . DCF-DA is visualised within the green fluorescent range. The FITC filter was used, using a 495 beam splitter and an excitation/emission range of 450-490/500-550 nm, with a 274.8 ms exposure time and 1.85 μm depth of focus.

High through-put assays were conducted by seeding 20,000 cells in a 96-well black bottom microplate, using a live trace or end-point assays. Fluorescence was measured on the FLEX Station 3 with an excitation/emission of 504/529 nm with an internal temperature set at 37°C.

Live traces were conducted in the FLEX Station 3 with cells being pre-incubated with media or 100 μM KYNA. DCF loading was conducted using fresh 10 μM DCF-DA in complete media for 30 min at 37°C, 5% CO_2 (g). A final concentration of 1 mM QUIN or 1mM H_2O_2 was delivered using the FLEX station and fluorescence was recorded over a 180 s period. The PHERA Star was also used to measure fluorescence (data not shown), and a comparison of the results showed the FLEX Station to be more sensitive to fluorescence.

End-point assays also employed the FLEX Station for fluorescence measurements. HEK peZ [-] cells were treated with either 50 μM H_2O_2 for 5h, or 1 mM QUIN for 24h with either 2 mM EGTA, 100 μM KYNA or 50 μM APV 2-h pre-incubation. ROS production of only EGTA, KYNA, and APV were also measured. DCF-DA dye was loaded at 20 μM for 30 min at 37°C, 5% CO_2 (g) in FBS-free and phenol-red-free media.

The above protocol was improved from previous experiments not reported in this thesis for clarity. These conditions include used cells seeded at various densities ranging from full confluency to 20,000 cells cultured in media (DMEM), with and without phenol-red, and 10% FBS (data not shown). These methods also incorporated known methods from pre-existing literature [86, 88]. Assays were first trialled in N2a cell lines and then escalated to SH-SY-5Y and HEK peZ cell lines if successful.

2.7 Ca^{2+} Influx in Cells as determined by the Fura 2-AM Assay

High through-put assays were conducted by seeding 20,000 cells in a 96-well black bottom microplate, using a Live trace or end-point assays. 2.5 μM Fura 2-AM (Abcam cat #ab120873) was loaded into cells using loading solution and 4 mM probenecid [89] in phenol-red and FBS free media for 30 min at 37°C , 5% CO_2 (g). Fluorescence was measured on the FLEX Station 3. Free Ca^{2+} and bound, intracellular Ca^{2+} was measured at excitation wavelengths of 340 nm and 380 nm respectively. Emission was measured at 520 nm with an internal temperature set at 37°C . Ca^{2+} influx was calculated by taking the absorbance ratio of 340/380 nm. In both experiments, CaCl_2 was used as a positive control.

Live traces were conducted in the FLEX Station 3 with cells being pre-incubated with media, 100 μM KYNA, or 50 μM for 2 h. Fura 2-AM was loaded into the cells and a final QUIN concentration of 1 mM was delivered to the cells. A live trace was recorded for 30 min. A 4h end-point assay was also conducted on N2a and SH-SY5Y cell lines which further incorporated 100 μM as well as 10 μM D-Ser co-treatments with NMDA and QUIN to confirm NDA activity in the assay. Fluorescence was recorded on both the PHERA Star (data not shown) and the FLEX Station, the latter of which showed greater sensitivity.

End-point assays also employed the FLEX Station for fluorescence measurements. N2a and SH-SY5Y cells were pre-incubated in media or 50 μM KYNA for 2h followed by a 24h incubation with 1 mM QUIN.

The above protocol was improved from previous experiments not reported in this thesis for clarity. These conditions include used cells seeded at various densities ranging from full confluency to 20,000 cells cultured in media (DMEM or L-15), with and without phenol-red, at a range of FBS concentrations with and without glucose supplementation. These methods also incorporated known methods from pre-existing literature [89]. Assays were first trialled in N2a and then SH-SY-5Y and HEK peZ cell lines.

2.8 Western Blot Analysis

After treatment period, cells were washed in ice-cold PBS and rested on ice with cOmpleteTM, EDTA-free Protease Inhibitor Cocktail (Roche, cat. # 04693132001) and RIPA buffer (150 mM sodium chloride, 1.0% Triton X-100, 0.5% sodium deoxycholate, 0.1% SDS (sodium dodecyl sulfate), and 50 mM Tris (pH 8.0)). Cells were scraped for lysate which was frozen overnight, then thawed on ice and centrifuged (13.2 rpm, 15 min, 4°C). Protein content of the supernatant was quantified using the PierceTMBCA Protein Assay Kit (Thermo ScientificTMcat. # 23225). 20 µg protein with NuPAGE Sample Reducing Agent (10x) (InvitrogenTMcat. #NP0009)/4x Laemmli Sample Buffer (Bio-rad cat. # 1610747) in a ratio of 2.5:1, topped with milliQ water to a final volume of 20 µL. Samples were loaded into NuPAGETM4-12% Bis-Tris Midi Protein Gels (InvitrogenTM) and run at a constant 100 V on the PowerEaseTM300W Power Supply (230 VAC). All blots were run with 3 µL Precision Plus ProteinTMDual Color Standard (Bio-rad cat. # 1610374).

Proteins were transferred onto nitrocellulose membranes using the Trans-Blot Turbo Transfer System (25 V, 20 min). Membranes were blocked with 5% BSA (TBST) (2h, room temperature) and given 3x5-minute TBST washes. Primary primary antibodies [(GAPDH 14C10 (dilution: 1/1000, Cell Signalling Technology # 2118), β -actin AC-15 (dilution: 1/5000 Abcam cat. # ab6276), and AT8 (p-Tau) (Invitrogen cat. #MN1020)] and appropriate 700CW Licore secondary antibodies were diluted in 3% BSA (TBST) overnight at 4°C or at room temperature for 2h, respectively.

Membranes were imaged and quantified using the Odyssey CLx Imaging System. Briefly, the 700-nm channel independently selected to quantify the signal of the house-keeping proteins across various treatments which were normalised to the control to account for variable gel loading. This normalisation factor was also applied to p-Tau signals quantified by independently selecting the 800-nm channel. Odyssey CLx Imaging System signal detection is independent of the area of the membrane selected for signal quantification. Average tau phosphorylation across each treatment was taken as a percentage of phosphorylation compared to the media-only control cells.

2.9 Immunocytochemistry

Cells were seeded in EZ slides at a density of 0.04×10^6 cells/mL and fixed with 4% paraformaldehyde (PFA) in 1xPBS for 10 minutes at room temperature followed by 3x5-minute washes with ice-cold PBS. Cells were permeabilised with PBST (PBS, 0.1% Triton X-100) for 10 minutes at room temperature, followed by 3x5-minute washes with PBS. Cells were blocked with 1% BSA in PBS for 1h at room temperature. Primary antibody exposure was in a humidified chamber at 4°C in 1% BSA (PBS) overnight. This was followed by 3x5-minute PBS washes with a secondary antibody diluted in 1% BSA for 1 hour at room temperature. After another round of 3x5-minute PBS washes, the EZ Slides were mounted with ProLongTM Gold Antifade Mountant with DAPI (Invitrogen cat. #P36935) and rested at room temperature for 24 hours before being sealed with nail polish and stored at 4°C.

2.10 KP Metabolite Quantification via Ultra High Performance Liquid Chromatography (UHPLC)

Trp, KYN, 3-HK, 3-HAA and AA concentrations in cell supernatant were determined by UHPLC and quantified using a sequential diode-array (UV) and fluorescence detection as previously described with some modifications [81]. Cell supernatants were precipitated with 4°C TCA 10% (1:1 v/v), centrifuged (12,000 g; 25 min; 4°C), and filtered (0.20 µm PTFE syringe filter, Merck-Milipore, CA, USA). Supernatant was transferred to an HPLC vial for analysis.

The UHPLC analysis were carried out in UHPLC equipment (Agilent 1290 Infinity, Agilent, CA, USA) using an Agilent ZORBAX Rapid Resolution High Definition C18, reversed phase (2.1 x 150 mm, 1.8 µm). The temperature of column compartment was set at 40°C and flow rate set to 0.75 mL/min with an isocratic elution of 100% of sodium acetate (100 mM), pH 4.65.

The identification and quantification of KYN and 3-HK were performed by a UV detector (G4212A, Agilent, CA, USA) with absorbance at 365 nm (reference signal off) for KYN and 3-HK. The identification and quantification of Trp was performed by a fluorescence detector (G1321B xenon flash lamp, Agilent, CA, USA) with emission wavelength of 280 nm. The results were calculated by interpolation using 6-point calibration curve and expressed as μM for KYN and Trp, and nM for 3-HK.

2.11 Statistical Analysis

A two-tailed t-Test was used to determine statistical significance in immunocytochemistry ROS assays within cell lines and baseline tau phosphorylation within HEK peZ cell lines, and a one-way ANOVA was conducted to determine significance of various treatments on Ca^{2+} influx in primary mouse cells and all western blot comparisons. Key statistical details such as p-value, t-value, and n-value (replicates) are provided in the captions. Residual and Q-Q plots confirmed underlying assumptions of both statistical tests. Homoscedasticity plots demonstrated uneven distribution of standard deviations which was confirmed by Brown-Forsythe and Bartlett's tests. An even distribution of standard deviations is essential only where the n-value is not evenly matched across control and treatment groups, which was not the case in the present study. All graphs represent a mean value unless indicated, with error bars representing standard deviation.

3

Results

3.1 Cellular IDO-1 and KMO Expression in N2a and SH-SY5Y Cell Lines

Cellular KMO expression was confirmed in N2a and SH-SY5Y cells using standard Western blot technique (Fig. 3.1). Cellular IDO-1 expression was also confirmed using immunocytochemistry in the N2a and SH-SY5Y (Fig. 3.2) cell lines. Accordingly, both the key rate-limiting enzyme (IDO-1) and enzyme favouring the QUIN-production branch of the KP (KMO), were confirmed in N2a and SH-SY5Y cells, validating the cell line's use as a cell model to study the pathway.

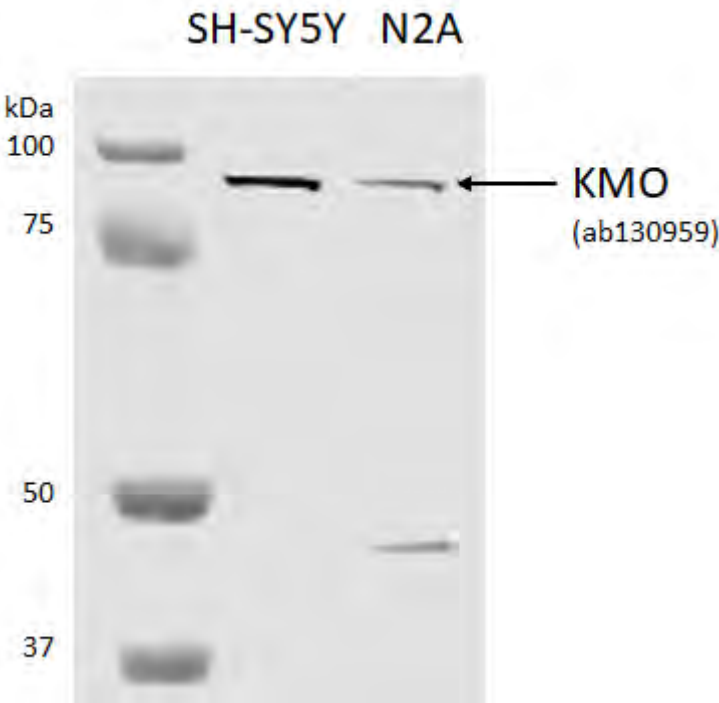


FIGURE 3.1: Confirmation of KMO expression in mammalian N2A and SH-SY5Y cancer cell lines.

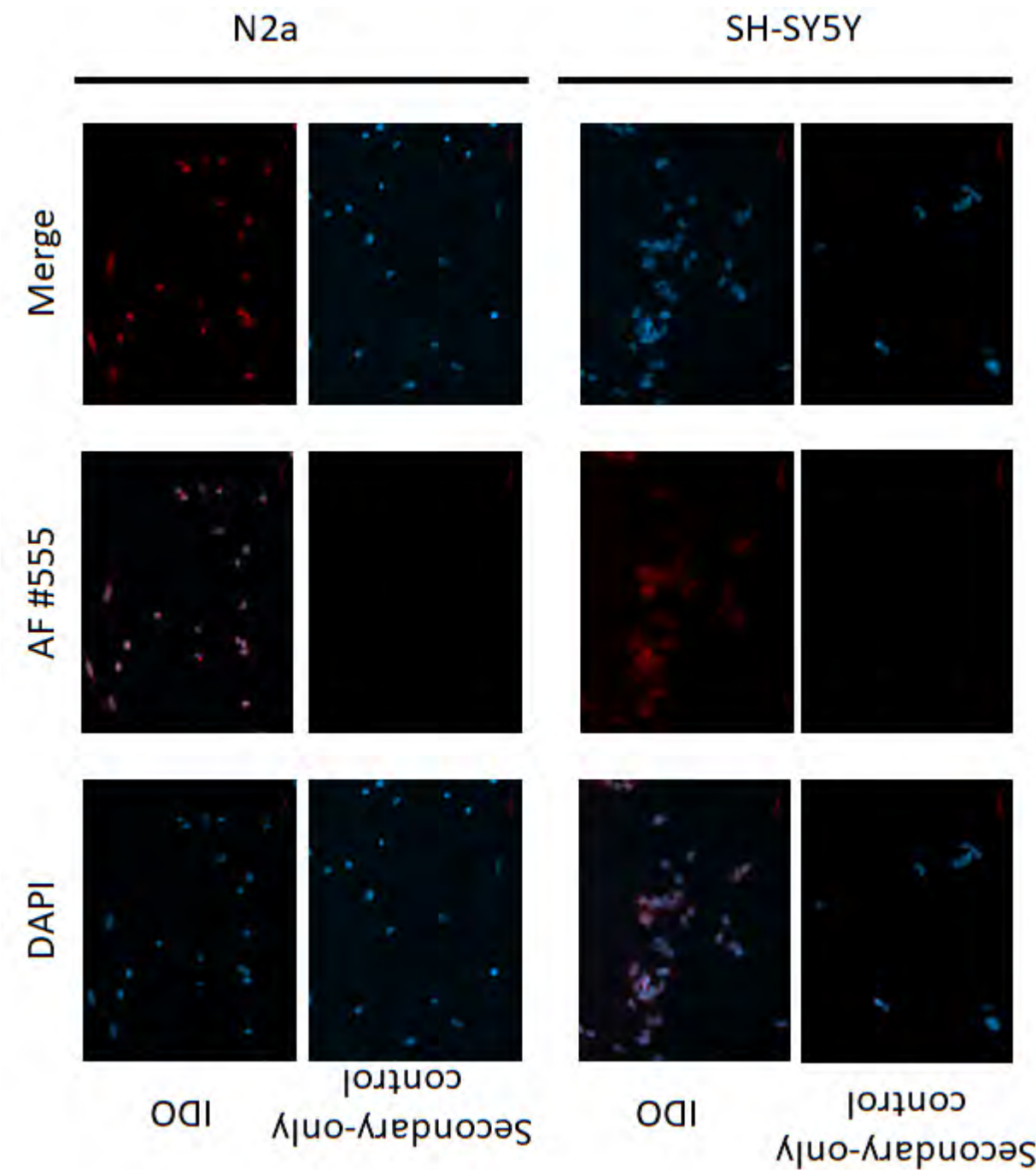


FIGURE 3.2: Confirmation of IDO-1 expression in mammalian N2A and SH-SY5Y cell line.

3.2 KP Stimulation Increases Tau Phosphorylation in N2a Cells

The Kynurenine pathway in SK-N-SH cells and its daughter cell line, SH-SY5Y, has been characterised and validated for various neurodegenerative tauopathies [81, 90–93]. However, effects of KP stimulation on N2a cells has not been previously assessed. Accordingly, N2a cells were treated with 3HK (to stimulate ROS) and QUIN. These experiments showed a >2-fold increase in tau phosphorylation, establishing N2a cells as a viable model for this study (Fig. 3.3). Notably, treatments of NMDA and D-Ser did not show any significant change in tau phosphorylation (data not shown).

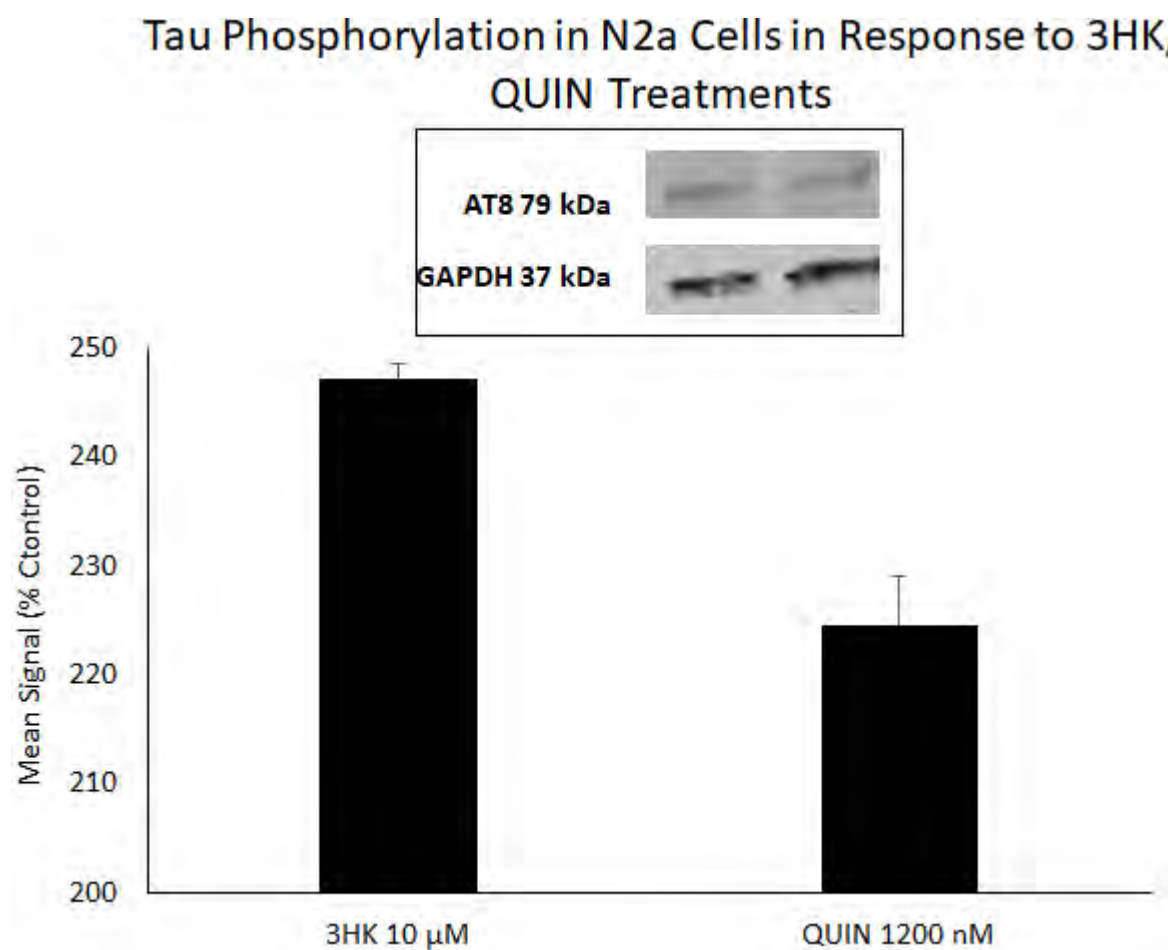


FIGURE 3.3: Stimulation of the KP with QUIN or 3HK supplementation demonstrated a 2-fold increase in tau phosphorylation in N2a cells; n=3 triplicates

3.3 KYNA Inhibits QUIN-Driven ROS

After validating both N2a and SH-SY5Y cell lines, the potency of QUIN activity on ROS production was assessed. Briefly, cells were treated with 10 μ M DCF-DA following QUIN treatment and KYNA pre-incubation. QUIN demonstrated a significant increase in ROS production compared to untreated in N2a cells (Fig. 3.4). This assay was repeated in the SH-SY5Y human cell line, which replicated these results. It was particularly noteworthy that a supplementary experiment incorporating KYNA pre-incubation demonstrated a significant reduction in QUIN-derived ROS activity (Fig. 3.5)

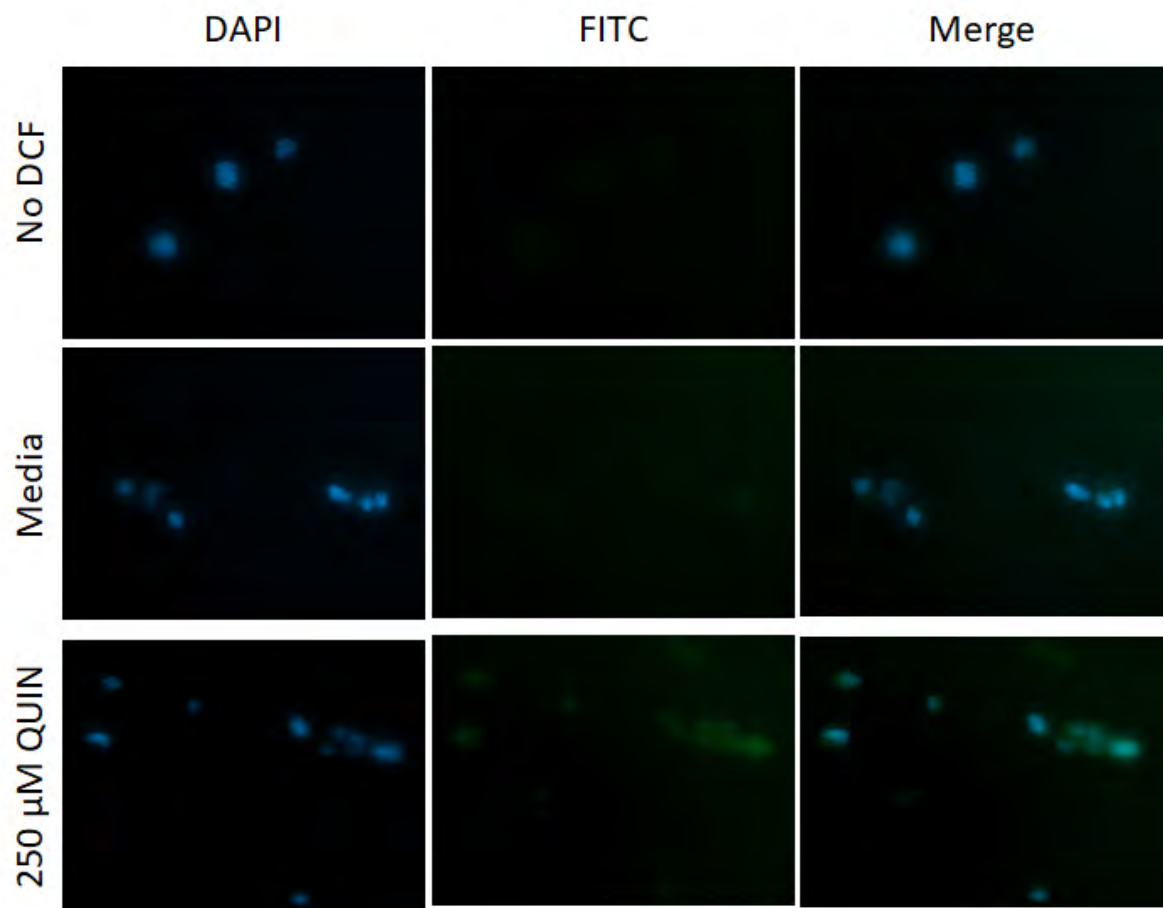


FIGURE 3.4: QUIN stimulated a significant increase in ROS production in N2a cells [Two-tailed t-Test: $p < 0.05$, $t = 3.8239$, $df = 6$; $n = 3$ triplicates].

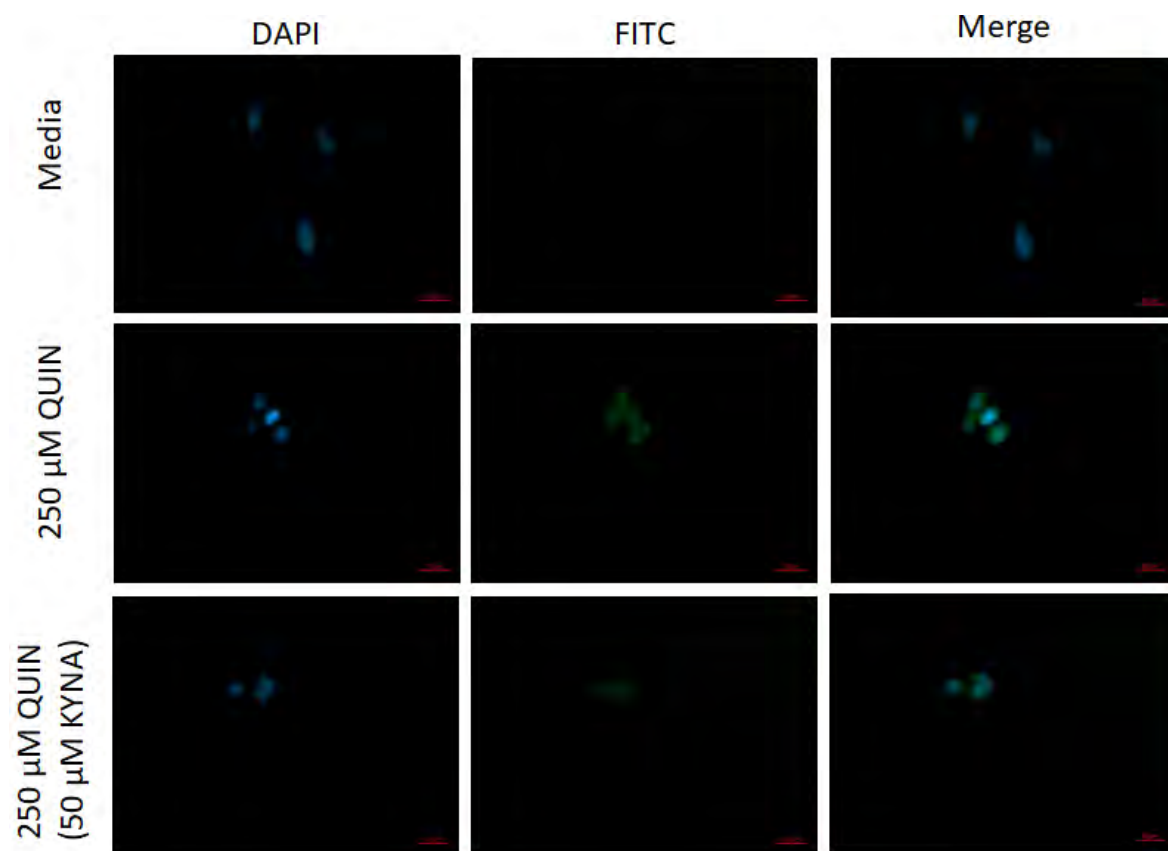


FIGURE 3.5: KYNA pre-incubation significantly inhibited the QUIN stimulated increase in ROS production in SH-SY5Y cells [Two-tailed t-Test: $p < 0.0001$, $t = 12.0710$, $df = 6$; $n = 3$ triplicates].

3.4 ROS Production in a KMO Over-expressing Cell Model

KMO is a key enzyme regulator in the KP which favours QUIN production. To better understand if KMO over-expression plays a role in ROS production, calcium influx, or tau phosphorylation, HEK-293 human embryonic kidney cells were genetically modified to over-express KMO as a model for excessive QUIN production [86]. DCF-DA loading demonstrated a significantly greater ROS activity in HEK peZ [KMO] than in HEK peZ [-] cells (Fig. 3.6). Notably, both cell lines showed no detectable ROS production without QUIN supplementation, which was unexpected for HEK peZ [KMO] cells.

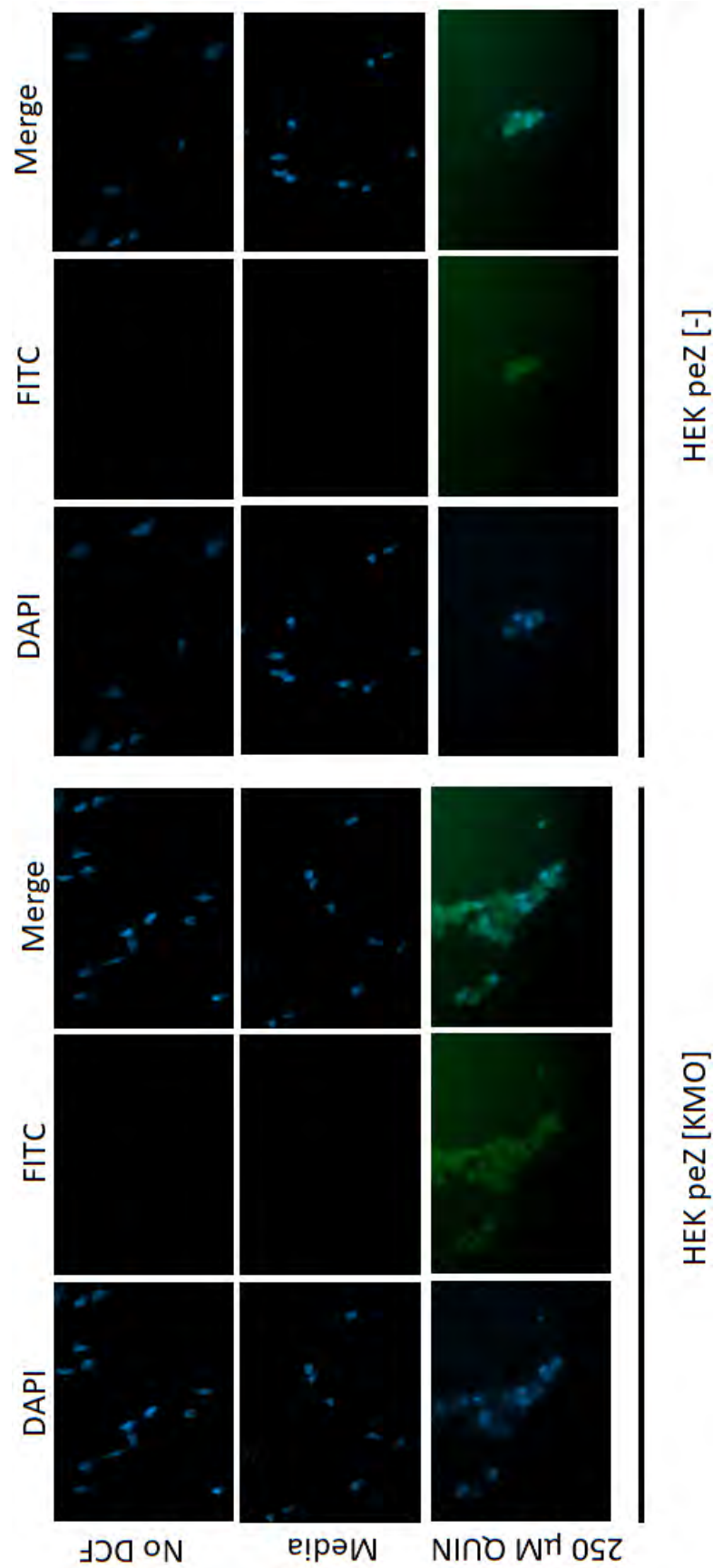


FIGURE 3.6: HEK peZ [KMO] cells showed greater ROS activity than HEK peZ [-] counterpart [Two-tailed t-Test: $p=0.0005$, $t=6.8351$, $df=6$; $n=3$ triplicates].

3.5 QUIN Increases Cellular Ca^{2+} Influx

DCF-DA assays established the role of KP metabolite QUIN in ROS production. Transfection of primary mouse neurons with the GCamp virus enabled the visualisation of both acute (Fig. 3.7) and chronic (Fig. 3.8) effects of KP modulation and calcium chelation on Ca^{2+} influx via fluorescent live-cell imaging.

Acute treatment of QUIN demonstrated a marked increase in Ca^{2+} influx increasing by 3-fold within 20 min. Chronic KP modulation and calcium chelation also showed remarkable effects. Glutamate supplementation (25 μM) to activate NMDAR resulted in an average >4-fold increase in calcium signal than the control. This signal was undetectable after independent treatments of calcium chelator EGTA (1.2 mM) and NMDAR antagonist Memantine (20 μM). Pre-incubation with KP metabolite, KYNA (50 μM), a known NMDAR antagonist, produced an almost 500-fold decrease in calcium signal at the comparable focal plane. A link to a compilation of real-time videos is provided in the Appendix (A.1), alternatively separate videos have been embedded in this document for CaCl_2 (Fig. 3.9) and QUIN stimulation (Fig. 3.10), and chronic Glutamate (Fig. 3.11) and QUIN (Fig. 3.12) co-treatments. All QUIN treatments prevented Ca^{2+} migration of calcium signals through the cells and localised them to the cell body, as compared to the control samples which showed calcium distribution along the entire neuron.

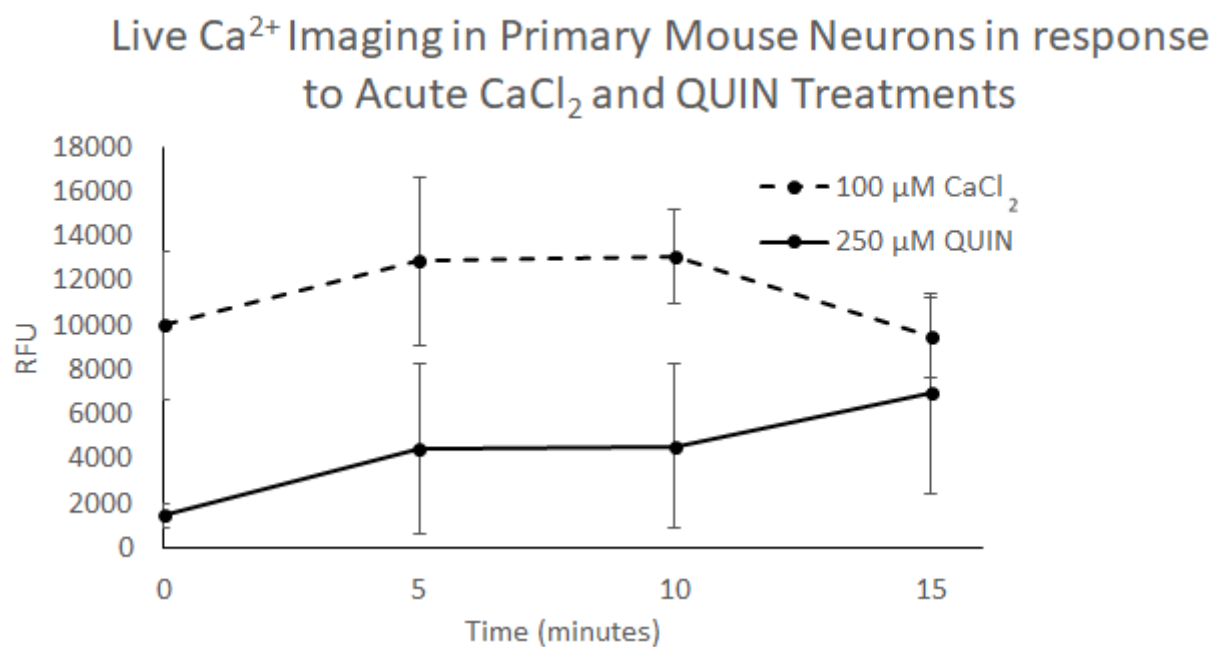


FIGURE 3.7: Treatment of primary mouse neurons with 250 μM QUIN and 100 μM of CaCl_2 showed a marked increase in calcium influx within 20 minutes of exposure.

Live Ca²⁺ Imaging in Primary Mouse Neurons in response to Various Chronic Treatments (24h)

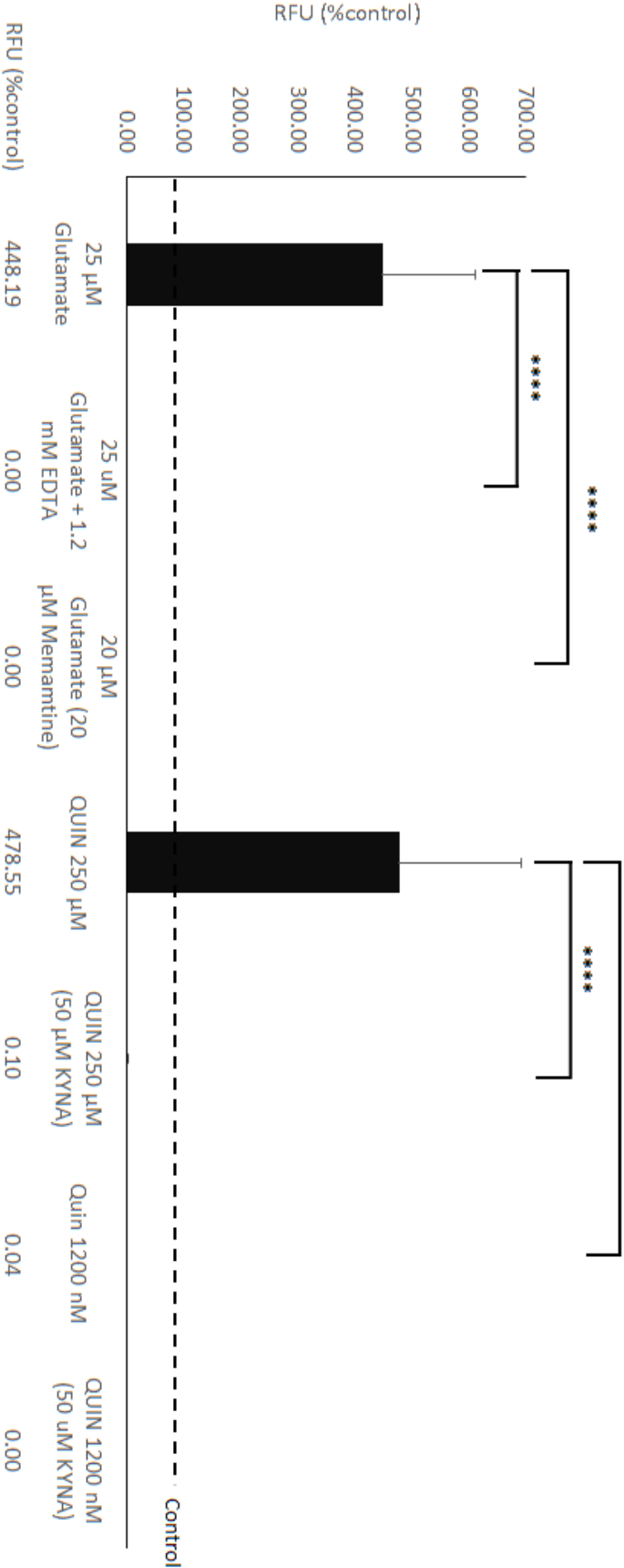


FIGURE 3.8: Chronic exposure of primary mouse neurons with Glutamate and QUIN showed marked calcium influx after a 24-hour exposure. Pre-incubation with known NMDAR antagonists and EGTA, Ca²⁺ chelator, demonstrated a statistically significant inhibition of calcium influx. [One-way ANOVA: ****p<0.0001; n=3 triplicates]

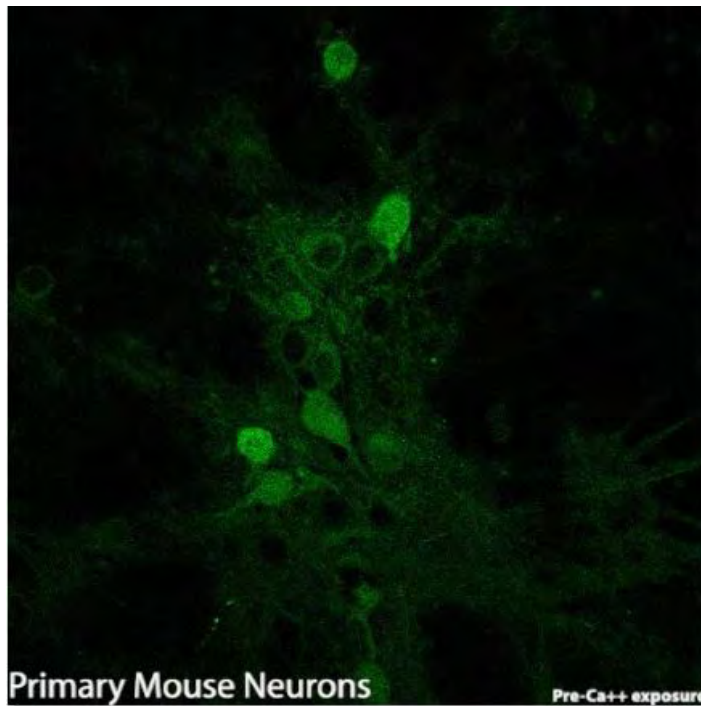


FIGURE 3.9: Live cell calcium imaging of primary hippocampal mouse neurons acutely treated with calcium. A compilation of all live-cell imaging videos are also compiled in the Appendix (Section [A.1](#)).

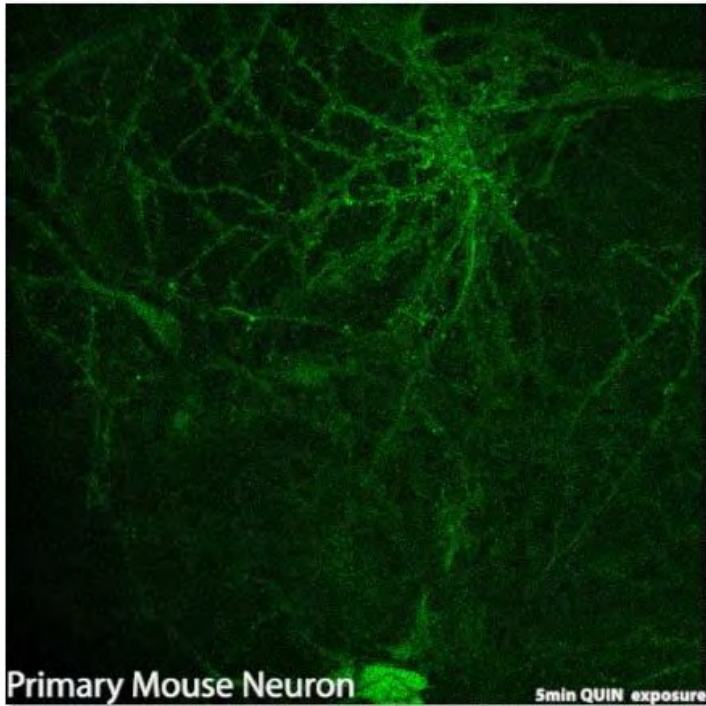


FIGURE 3.10: Live cell calcium imaging of primary hippocampal mouse neurons acutely treated with QUIN. A compilation of all live-cell imaging videos are also compiled in the Appendix (Section [A.1](#)).

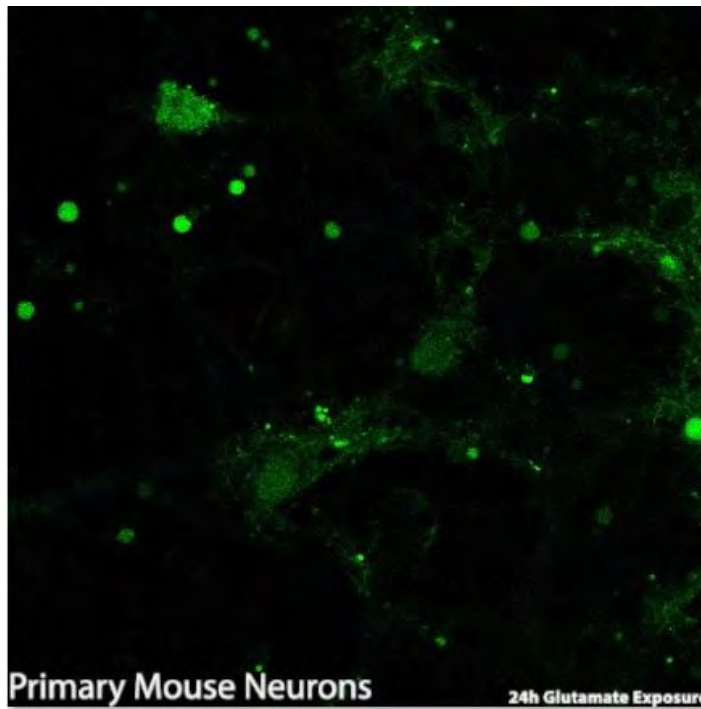


FIGURE 3.11: Live cell calcium imaging of primary hippocampal mouse neurons chronically treated with Glutamate, NMDAR antagonist Memantine, and calcium chelating agent EDTA. A compilation of all live-cell imaging videos are also compiled in the Appendix (Section [A.1](#)).

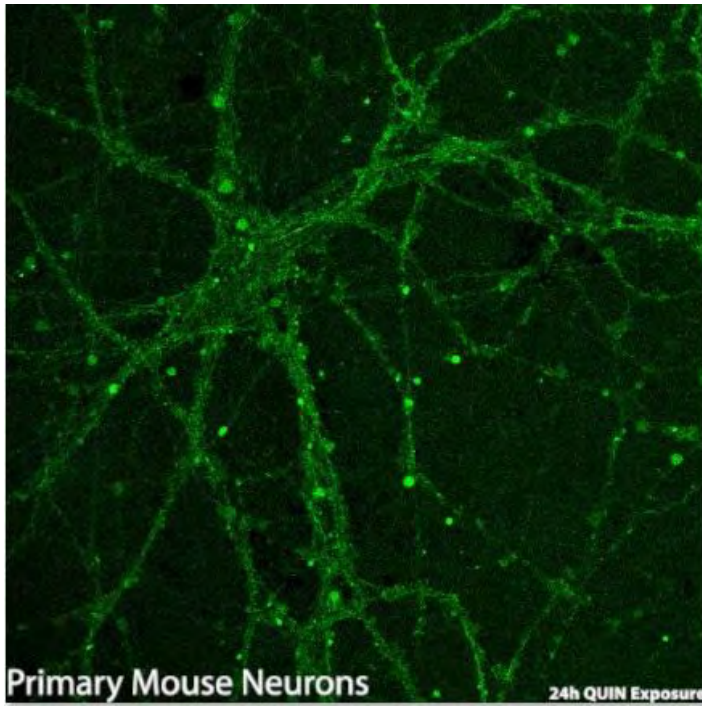


FIGURE 3.12: Live cell calcium imaging of primary hippocampal mouse neurons chronically treated with QUIN and NMDAR antagonist KYNA. A compilation of all live-cell imaging videos are also compiled in the Appendix (Section [A.1](#)).

3.6 KMO Over-Expression Increases Baseline Tau Phosphorylation in HEK peZ Cells

HEK peZ cells were used as cell models to investigate the effects of KP modulation with respect to ROS and Ca²⁺ influx on tau phosphorylation. Prior, baseline tau phosphorylation was assessed, with HEK peZ [KMO] cells showing 3-times greater tau phosphorylation than human-KMO-null HEK peZ [-] cells (Fig. 3.13).

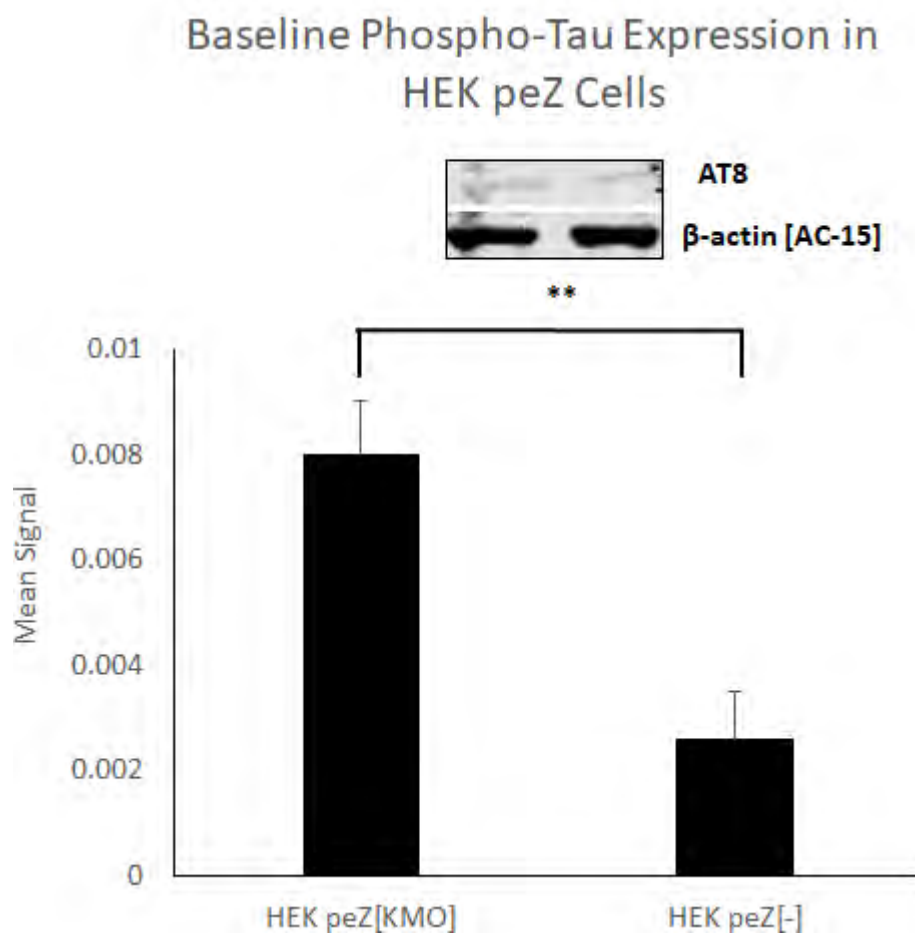


FIGURE 3.13: Baseline tau phosphorylation was significantly greater in HEK peZ [KMO] cells [Two-tailed t-Test: $P < 0.005$, $t = 6.8941$, $df = 4$; $n = 3$ technical replicates].

3.7 KP Metabolite Modulation Alters Tau Phosphorylation

Primary human neurons and macrophages, as well as HEK peZ cells, were employed to study the effects of KP modulation on tau phosphorylation, with particular emphasis on modulators of ROS and Ca^{2+} influx. To stimulate pathological KP activation, cells were treated with 100 IU/mL $\text{IFN}\gamma$ and treated with either Ro-61-8048 (KMO Inhibitor), or preincubated with kynurenine metabolites. UHPLC analysis of cell culture supernatant was conducted to determine Kynurenine : Tryptophan (K/T) ratio and 3-hydroxykynurenine : Kynurenine (3HK/KYN) ratio to determine success of KP activation and treatment KP modulation. Corresponding western blots were also conducted to determine impact on tau phosphorylation. Kynurenine : Tryptophan ratio increased in response $\text{IFN}\gamma$ treatment, as a model of inflammation, across all cell types except primary human neurons (Fig. 3.14).

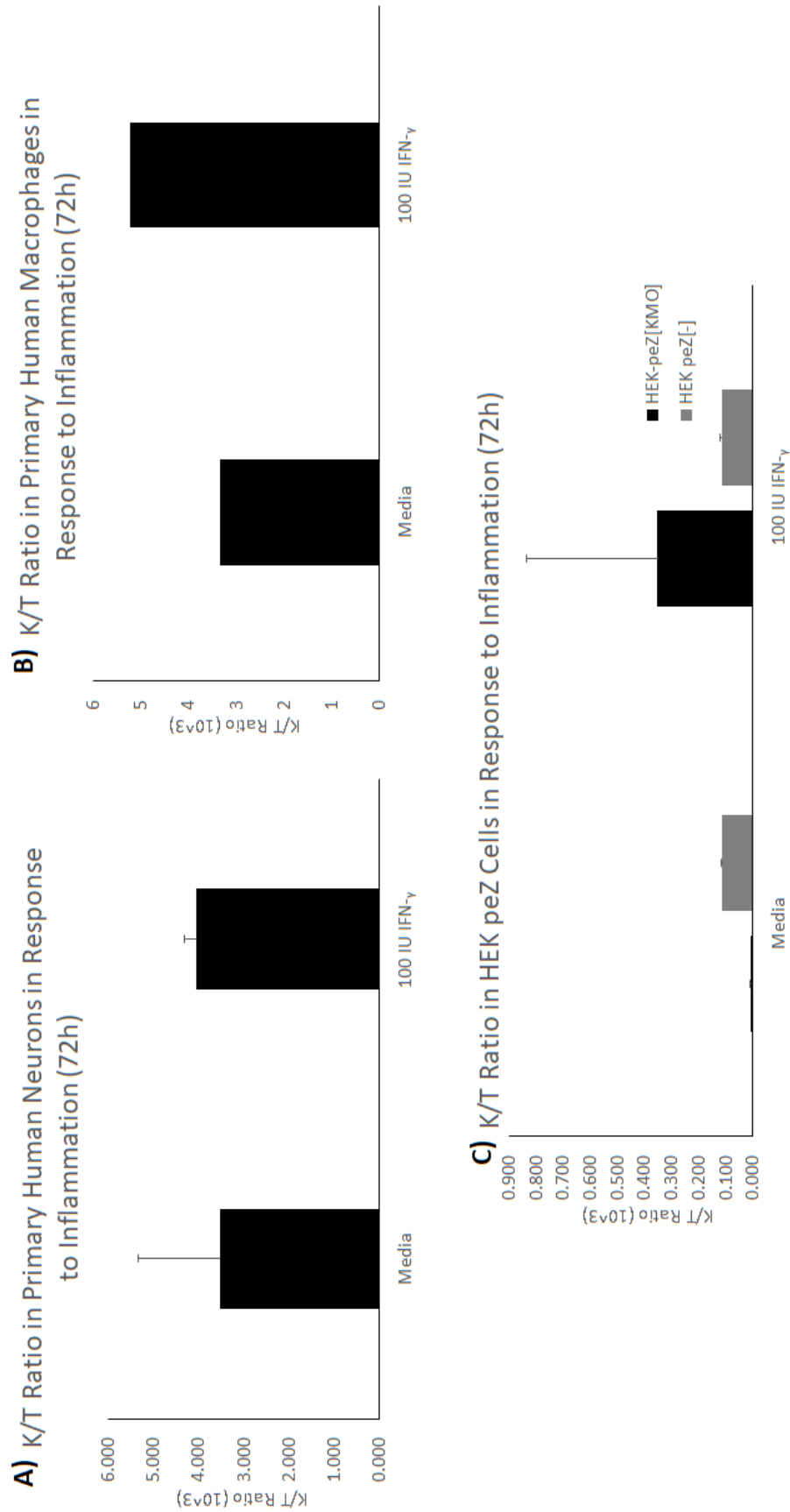


FIGURE 3.14: Kynurenine : Tryptophan ratio of A) primary human neurons, B), primary human macrophages, and C) HEK peZ [KMO] and [-] cells after IFN γ treatment as a model of inflammation; neurons and HEK cells n=2 duplicates, macrophages n=1.

IFN γ treatment allows us to use cells as a model to assess the effects of KP modulators. A particularly significant KP modulator was the KMO inhibitor Ro-61-8048. The KMO enzyme is responsible shuttling the KP towards the QUIN-producing branch. This inhibition drives the pathway towards the production of neuroprotective metabolites, converting KYN to KYNA instead of QUIN (Fig. 3.15). To determine success of KMO inhibition, the 3-hydroxykynurenine : Kynurenine ratio was calculated, which under successful KMO inhibition, would decrease.

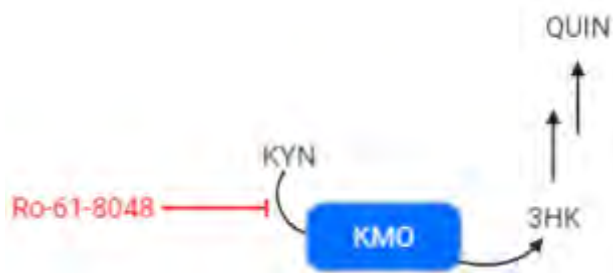


FIGURE 3.15: Schematic diagram demonstrating how KMO inhibitor Ro-61-8048 modulates the KMO branch of the KP

Primary human neurons showed no change in 3HK/KYN ratio following KMO inhibition. KMO activity was confirmed when the ratio increased 2-fold with KYN supplementation (Fig. 3.16). Interestingly, co-treatment with KYN and the KMO inhibitor did inhibit KMO, decreasing the 3HK/KYN ratio by more than 23-fold. In contrasting, both macrophages and HEK peZ cells showed potent KMO inhibition without KYN supplementation. In human macrophages, KMO inhibition decreased the ratio by almost 400% (Fig. 3.17), while both HEK peZ cell lines demonstrated less pronounced decrease (Fig. 3.18). Surprisingly, supplementing macrophages with KYN did not show the expected increase in 3HK/KYN ratio. Co-treatment with KYN and KMO inhibitor showed almost complete KMO inhibition in macrophages and both HEK peZ strains.

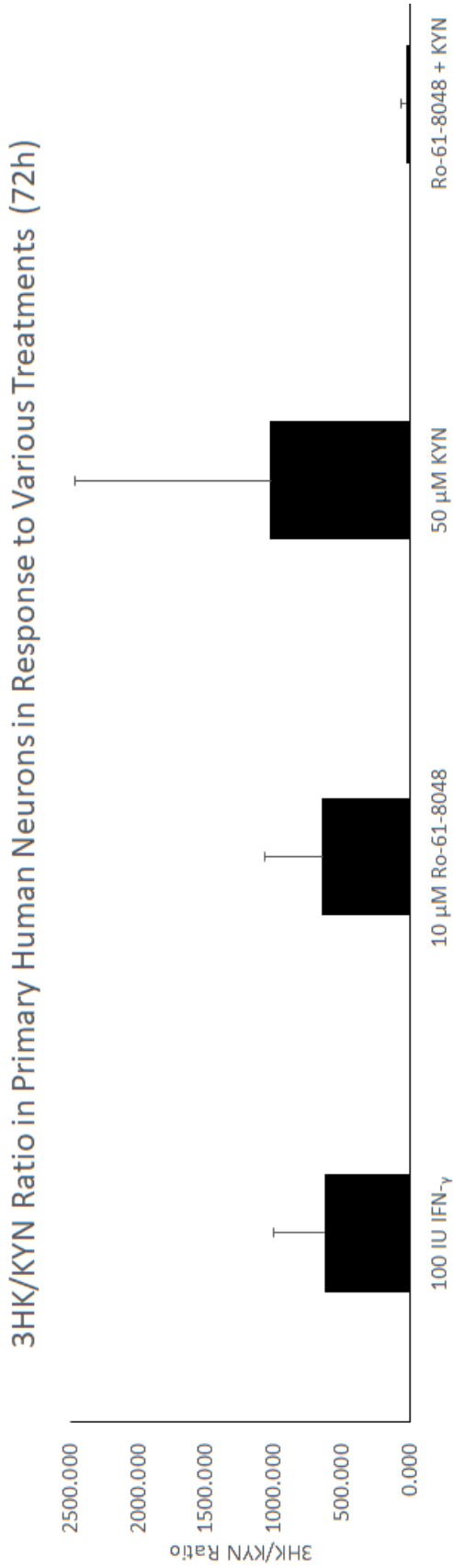


FIGURE 3.16: 3-hydroxykynurenine : Kynurenine ratio in primary human neurons as a response to KP modulation. All treatments included [IFN γ].

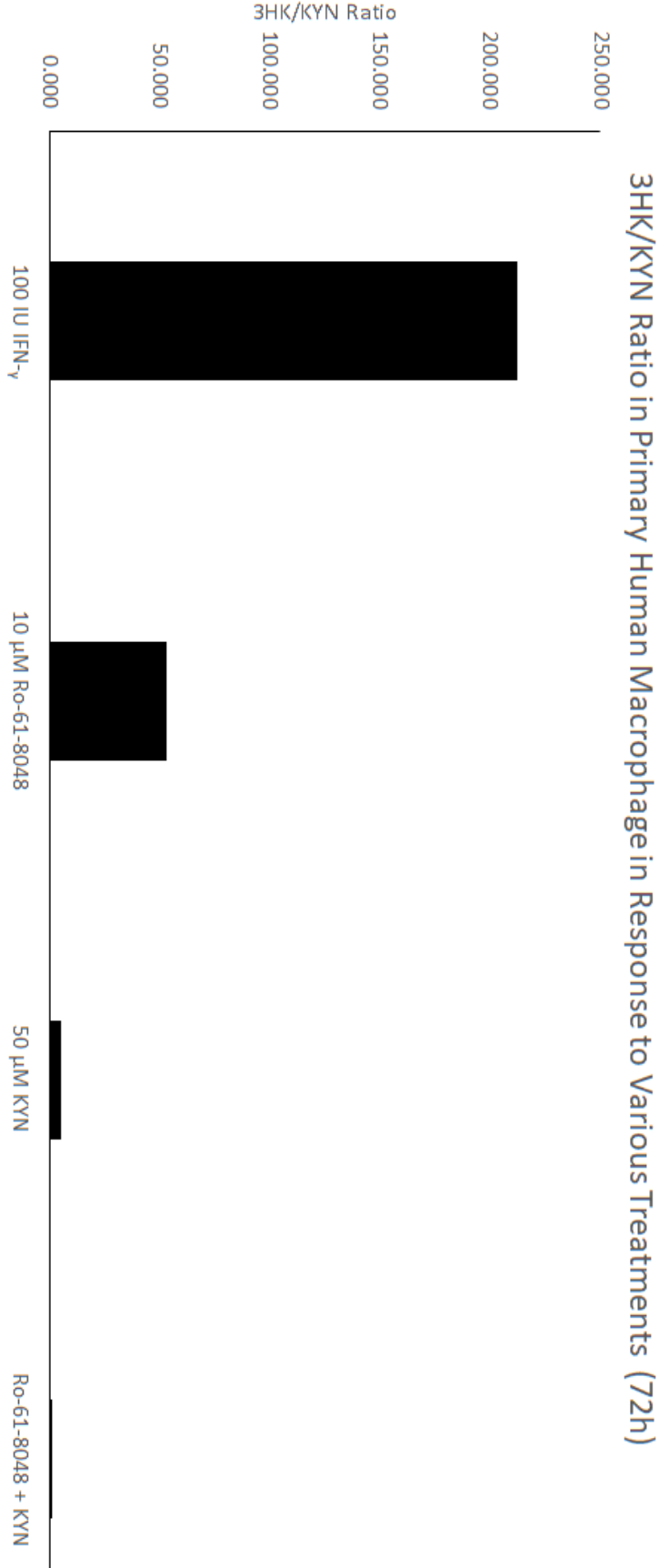


FIGURE 3.17: 3-hydroxykynurenine : Kynurenine ratio in primary human macrophages as a response to KP modulation. All treatments included [IFN γ].

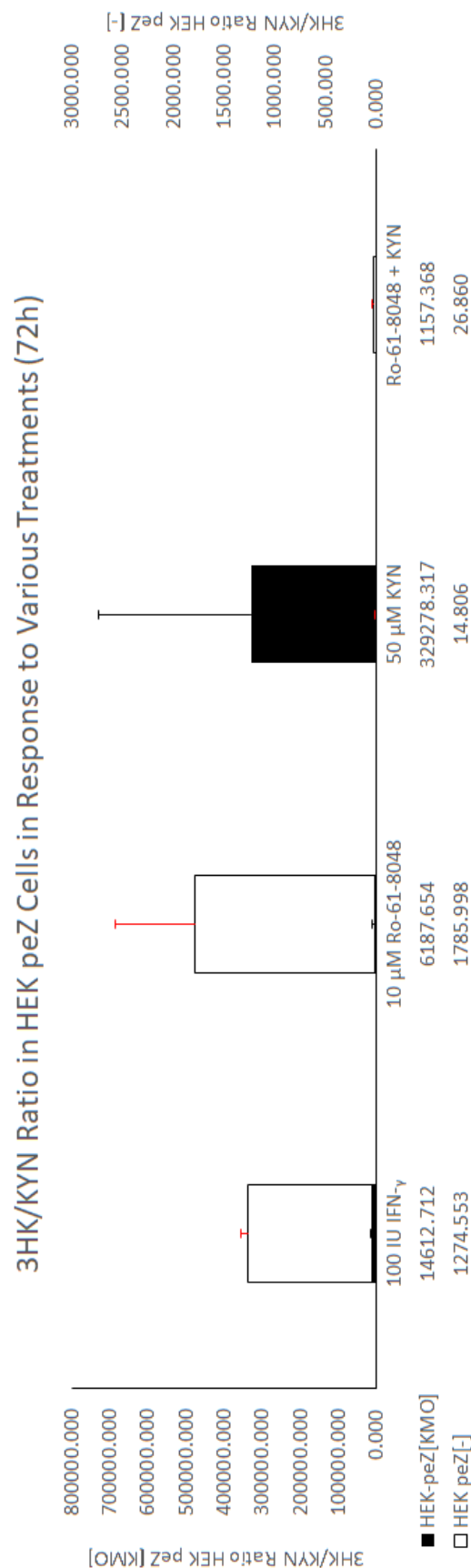


FIGURE 3.18: 3-hydroxykynurenine : Kynurenine ratio in HEK peZ cells as a response to KP modulation. All treatments included [IFN γ .

To finally assess the impact of these KP modulations on tau phosphorylation, cell lysates were isolated and probed for tau phosphorylation with the AT8 antibody as described in the Western blot protocol.

In primary human neurons, KMO inhibition by itself showed no significant change in tau phosphorylation but when coupled with KYN supplementation, a significant decrease in tau phosphorylation was observed (Fig. 3.19). KYNA pre-incubation also showed a noticeable decrease in tau phosphorylation. Most noteworthy was the almost 4-fold decrease in tau phosphorylation when QUIN activity was negated by Ca^{2+} chelation.

Macrophages also demonstrated a significant decrease in tau phosphorylation upon KMO inhibition and KYNA pre-incubation (Fig. 3.20). The significant decrease in QUIN-derived tau phosphorylation upon Ca^{2+} chelation was also evident in macrophages.

HEK peZ cells revealed similar findings, with an observable decrease in tau phosphorylation upon KMO inhibition. Phosphorylation was enhanced by KYN supplementation in HEK peZ [KMO] cells (Fig. 3.21). Antagonising NMDAR with KYNA decreased phosphorylation across both HEK peZ cell lines. Treatment with pathological QUIN concentration further increased tau phosphorylation levels. HEK peZ cells were the only cell lines that demonstrated an increase in tau phosphorylation with KYN treatment. KMO over-expressing HEK peZ cell line significantly increased tau phosphorylation levels.

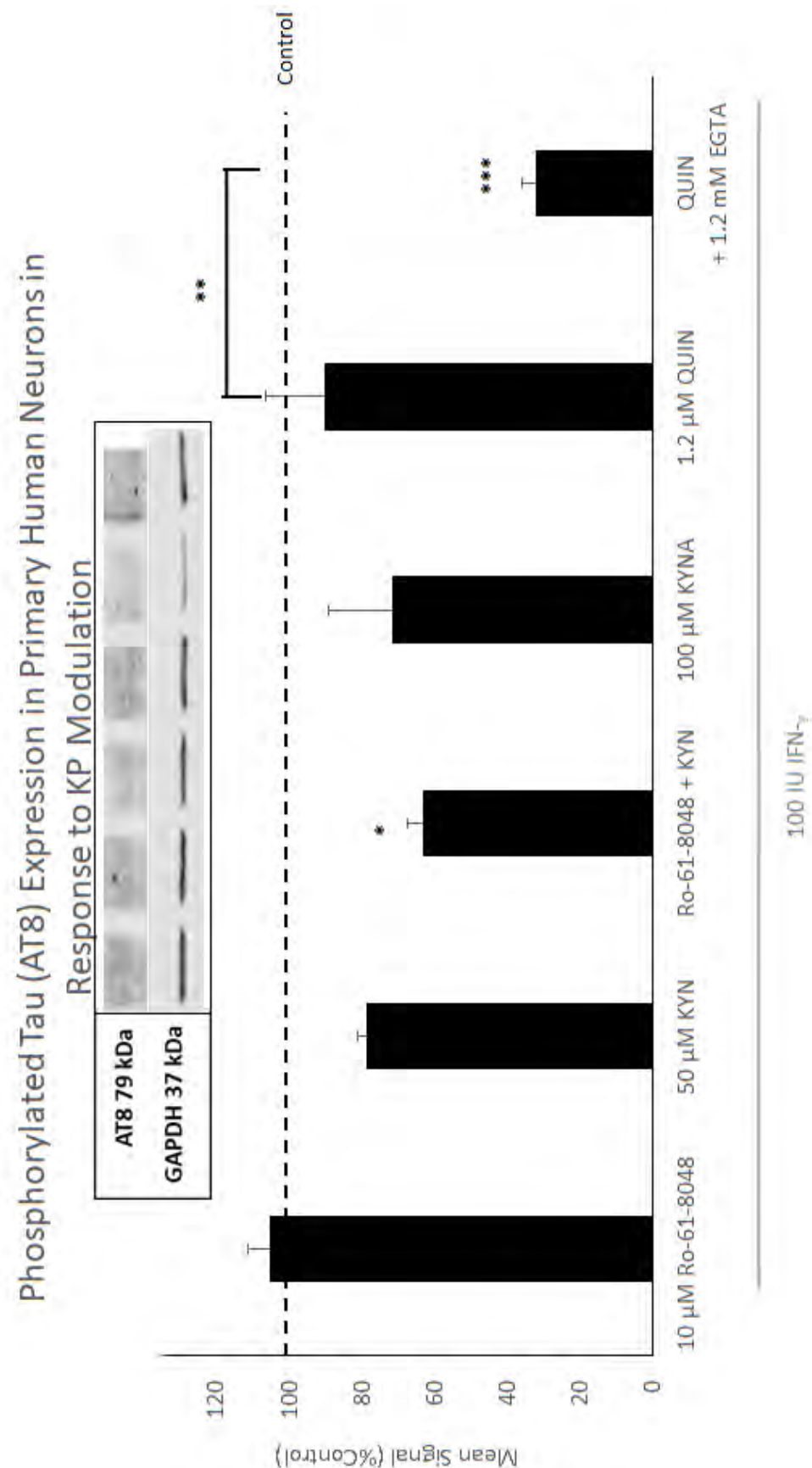


FIGURE 3.19: KYN and KMO treatment showed significant decrease in tau phosphorylation which was also observable in KYN (NMDAR antagonist) treatments. Calcium chelation with EGTA showed a large 3-fold decrease in phosphorylated tau compared QUIN treatments with no Ca^{2+} chelation [One-way ANOVA: * $p < 0.05$, ** $p < 0.001$, *** $p < 0.0001$; $n = 2$ duplicates.]

Phosphorylated Tau (AT8) Expression in Primary Human Macrophages in Response to KP Modulation

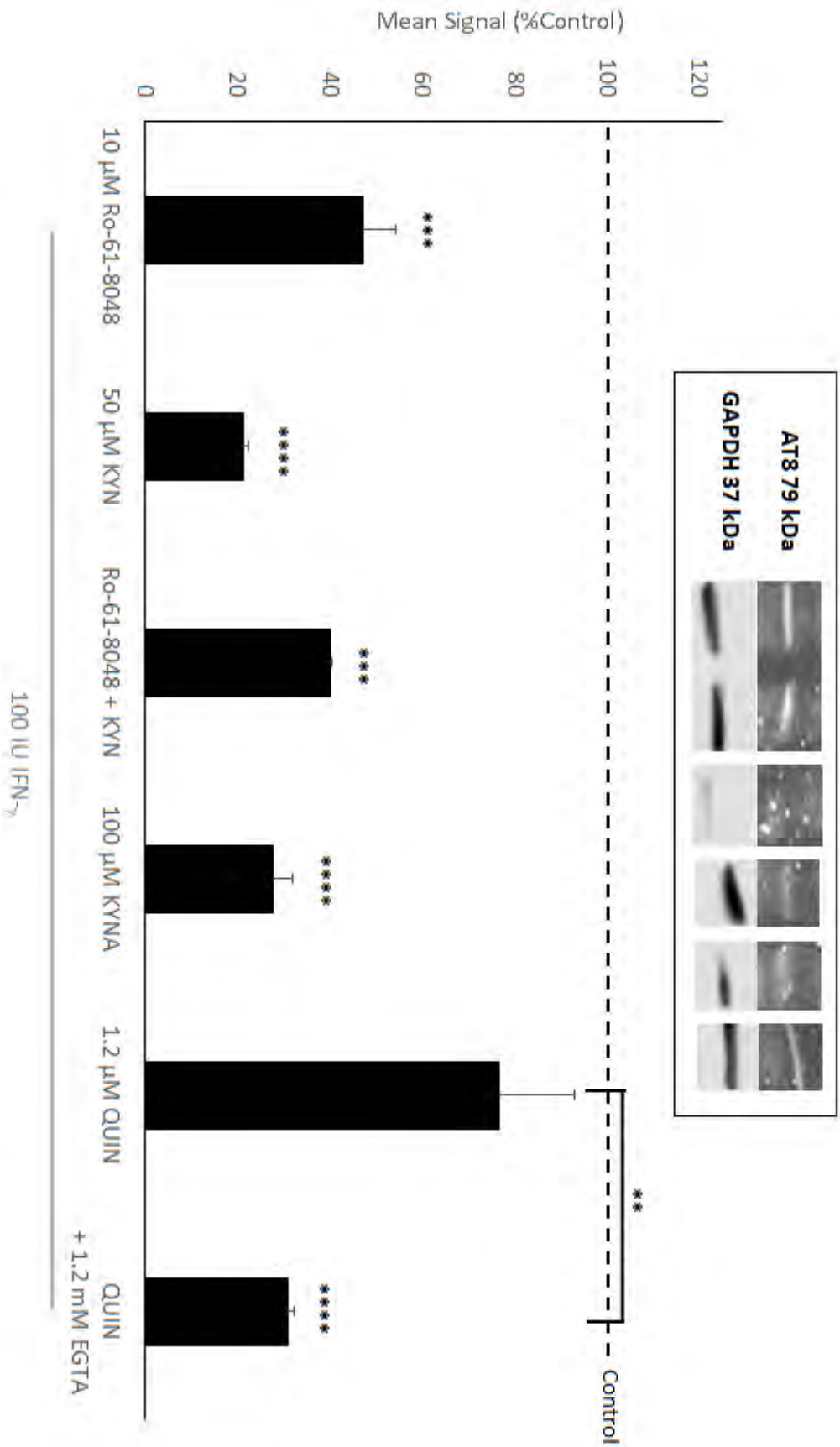


FIGURE 3.20: KMO inhibition, KYNA treatment (NMDAR antagonist), and calcium chelation demonstrated significant decrease in tau phosphorylation. Unexpectedly, so did treatment with KYN. [One-way ANOVA: textbf**p<0.01, ***p<0.001; ****p<0.001n=2 technical duplicates.]

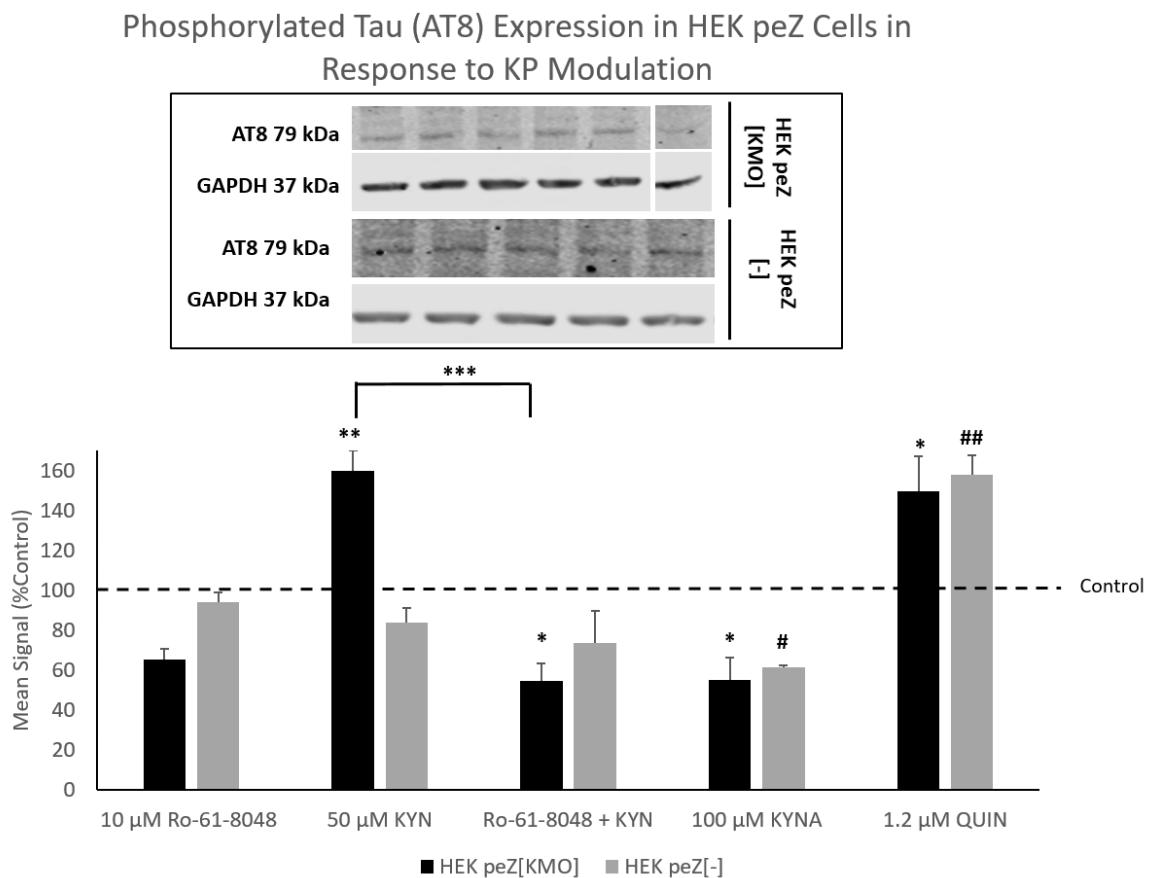


FIGURE 3.21: KMO inhibition and KYNA treatment (NMDAR antagonist) demonstrated significant decrease in tau phosphorylation, while KYN treatment expectantly increased tau phosphorylation [One-way ANOVA: * $p < 0.05$, ** $p < 0.001$, *** $p < 0.0001$ (HEK peZ [KMO]); $p < 0.05$, $p < 0.001$ (HEK peZ [-]); $n = 2$ duplicates].

3.8 Attempted Optimisation of High-Throughput ROS and Ca^{2+} Influx Assays in Various Cell Lines

To further explore how KP metabolites manipulate ROS and Ca^{2+} influx, attempts were made to optimise high throughput DCF-DA and Fura-2AM protocols respectively. Unfortunately, due to project time constraints, optimisation of both DCF-DA and Fura-2AM assays have been unable to successfully reproduce all of the physiological impacts of KP metabolites on these phenomena previously observed in the literature.

Preliminary time-course experiments with DCF-DA (Fig. 3.22) have generally failed to reproduce the previous results reported in the literature [86]. However, the H_2O_2 positive control did demonstrate increased ROS. Specifically, QUIN mediated increased ROS could not be reproduced across all cell lines, dependant on live-trace or end-point assays. KYNA co treatment also do not show statistical significance. HEK peZ cells seemed to be showing resilience to QUIN toxicity. While the vector-only counterpart demonstrated subtle changes, the KMO over-expressing cell line showed little to no difference in fluorescence at all. On the other hand, SH-SY5Y cells showed higher ROS activity with KYNA antagonism than QUIN in three technical replicates, however, this difference was also not statistically significant.

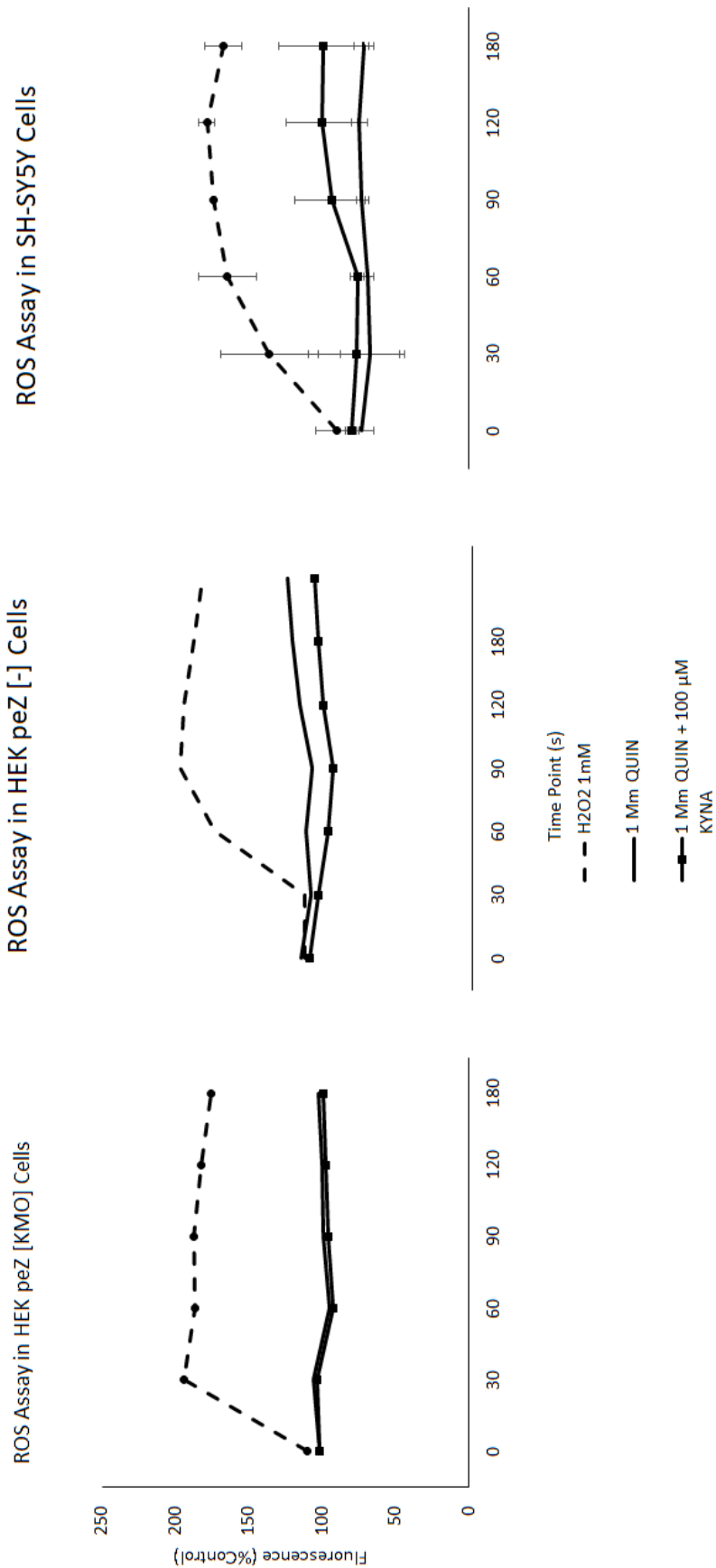


FIGURE 3.22: Time-course of a DCF-DA assay in various cell lines

To record potential long-term physiological effect and to account for auto-fluorescence, end-point assays were conducted following 24-hour treatments in HEK peZ [-] cells (Fig. 3.23) which further incorporated known NMDAR antagonist APV, which achieved limited success. The positive control and a relatively high dose of QUIN (1mM) demonstrated no increase in ROS activity. However, we were able to demonstrate a decrease in ROS activity with calcium chelation and glutamate receptor antagonism with KYNA exhibiting more potency than APV. Stand-alone treatments of APV and EGTA increased ROS activity 2- and 1.5-fold respectively.

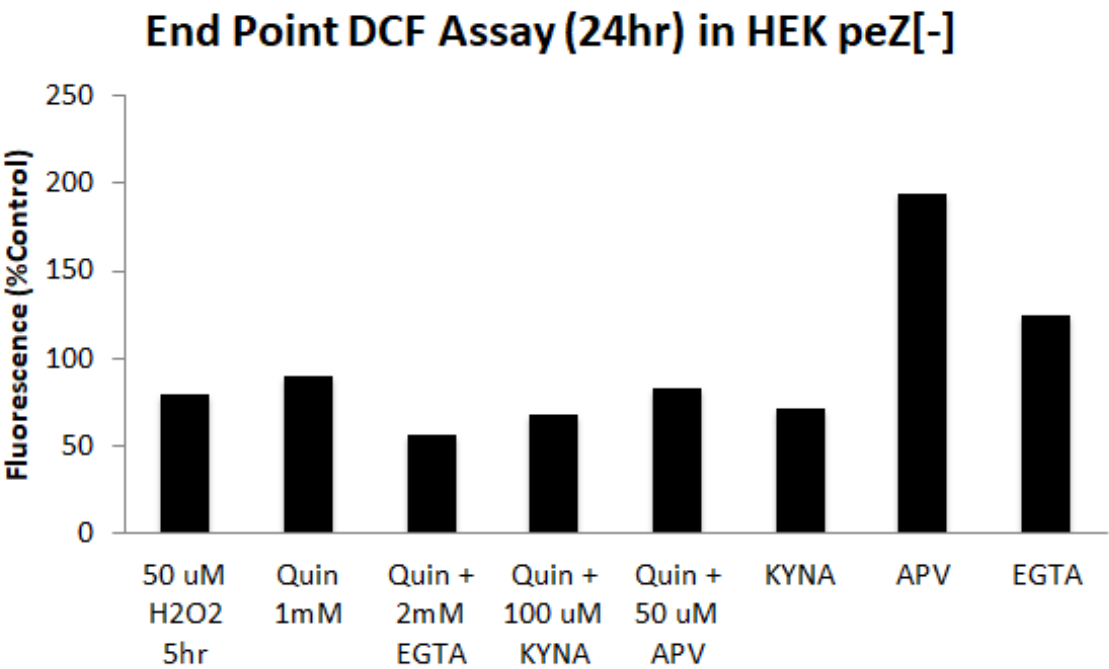


FIGURE 3.23: End-point DCF-DA assay in HEK peZ [-] cells

Similar time-course assays were run using the calcium indicating dye Fura-2AM (Fig. 3.24) in N2a cells. Once again, the high-throughput assay failed to completely reproduce previously reported results, however the positive control did show a marginal increase in Ca^{2+} influx. To record potential long-term physiological effect, the assay was repeated with N2a cells incubated in the treatment conditions for a total of 4h following which a short-term end point assay was conducted. While the calcium positive control did show an increase in Ca^{2+} influx, so too did the negative (vehicle-only) control (Fig. 3.25).

A 24-h end-point assay was conducted using SH-SY5Y cells with a slightly higher QUIN dose and inclusion of NMDAR agonists NMDA and D-Ser (Fig. 3.26). These assays did show a successful positive control result, however QUIN treatment failed to increase Ca^{2+} influx in SH-SY5Y cell lines. Most importantly, the assay's reliability was scrutinised due to the observed increase in Ca^{2+} influx despite KYNA antagonism. However, the inclusion of NMDA and D-Ser in the assay did demonstrate that N2a cells were more susceptible to Ca^{2+} influx than SH-SY5Y cell lines, demonstrated by greater intracellular calcium levels in response to NMDA, NMDA + D-Ser, and QUIN + D-Ser treatments. In summary, assay conditions showed limited sensitivity, (Fig. 3.24, 3.25) which was not improved after a 24-hour exposure period (Fig. 3.26).

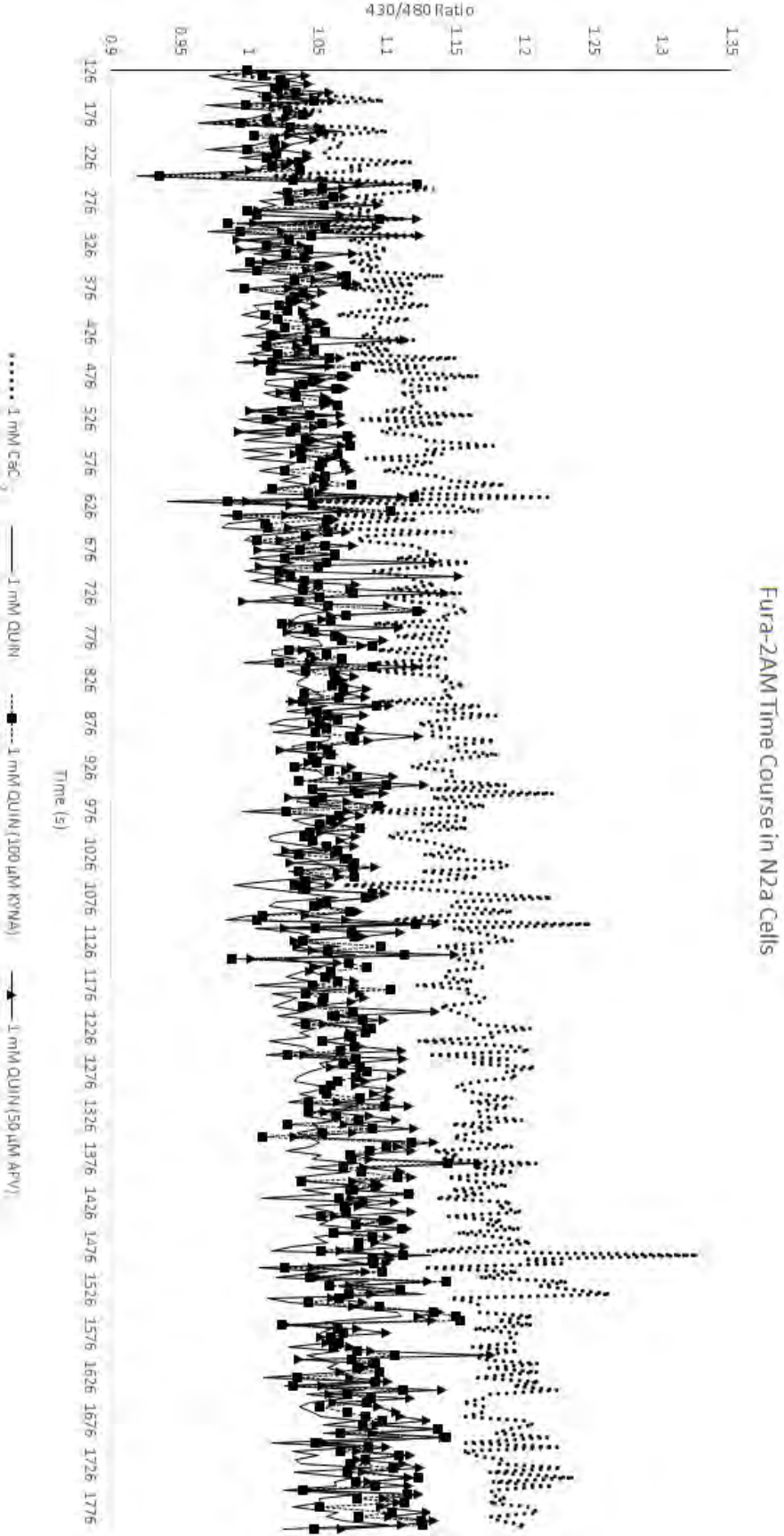


FIGURE 3.24: Time-course of a Fura-2AM assay in N2a cells

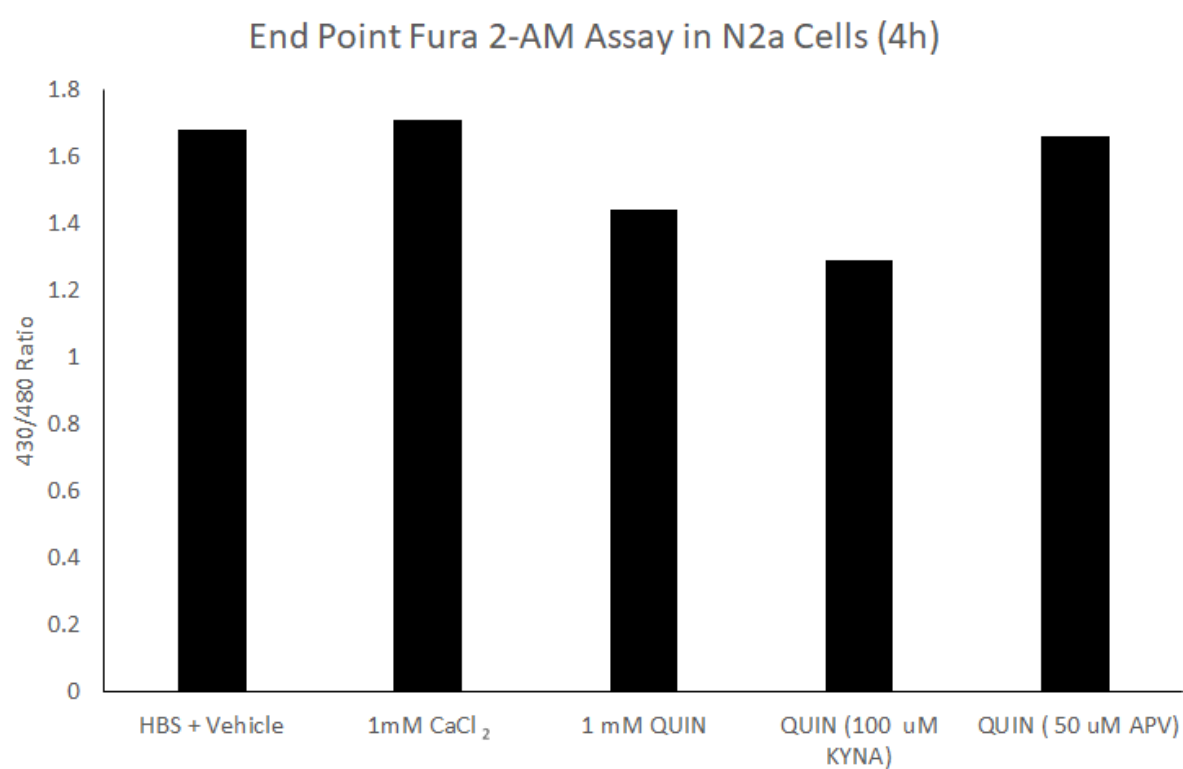


FIGURE 3.25: Short-term end-point of a Fura-2AM assay in N2a cells

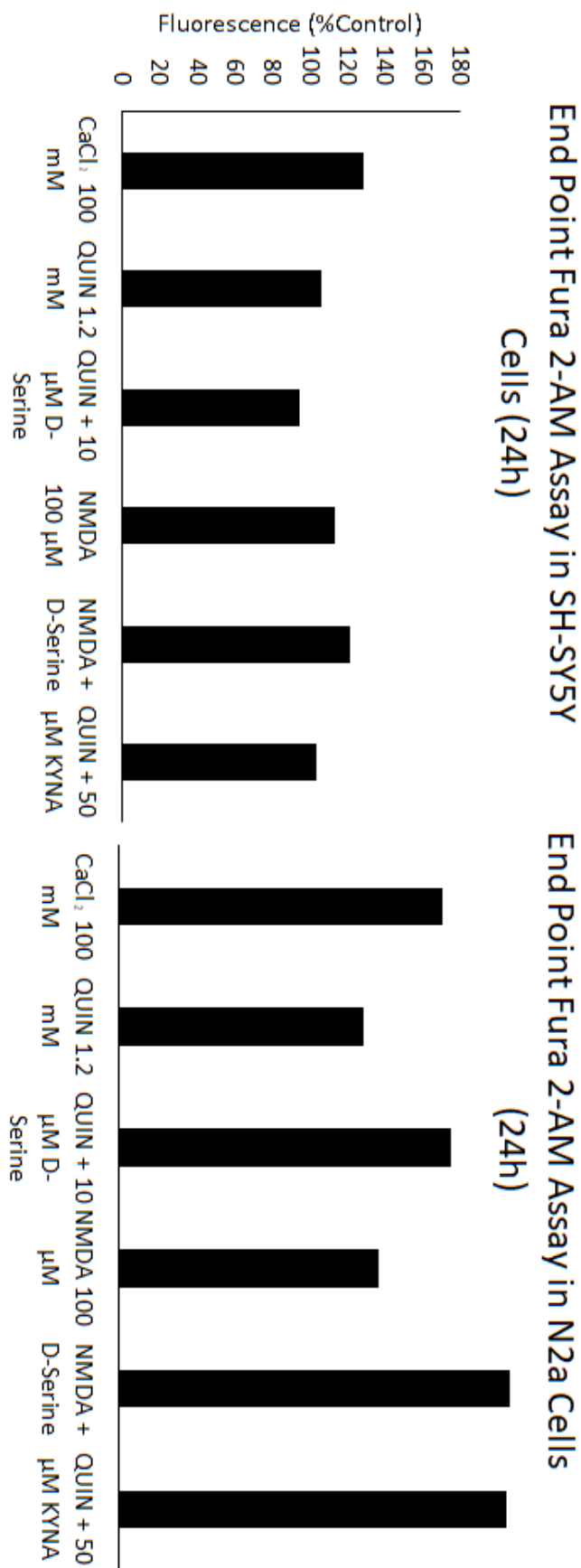


FIGURE 3.26: End-point Fura-2AM assay in SH-SY5Y and N2a cells

4

Discussion

4.1 Interplay Between KP Metabolites, ROS and Ca^{2+} Influx

Cellular KMO and IDO-1 expression was observed in N2a and SH-SY5Y cell lines confirming their suitability as cell models to study the KP (Fig. 3.1, 3.2), although KMO expression in SH-SY5Y and N2a cells did not appear at the expected kDa. However, KMO is known to undergo various post-translational modifications in mammalian cells which include N-glycosylation at three sites, which are known to increase the kDa of the enzyme [94].

Studies in N2a cells confirmed increased QUIN and KP-derived ROS activity increased tau phosphorylation at the Ser202 and Thr205 epitopes (Fig. 3.3), which are considered the key phosphorylation site for NFT formation [39, 40]. DCF-DA assays also showed that NMDAR antagonism with KYNA reduces QUIN-derived ROS activity (Fig. 3.4, 3.5). KMO over-expression was also found to synergistically increase ROS production when exposed to pathological QUIN concentrations (Fig. 3.6). These results confirm that KP modulation, in particular pathological QUIN and 3HK, increase tau phosphorylation by increasing ROS activity.

The HEK peZ model has previously been shown to express high ROS activity at even basal conditions, which correlated with decreased KYN levels and significant up-regulation of 3HK concentrations [86]. Taken together, this demonstrates that KMO over-expression increases ROS activity through 3HK synthesis, leading to increased tau phosphorylation. This is line with data that supports a crucial role for ROS activity in tau phosphorylation and tauopathies. Specifically, the accumulation of ROS is now considered a hallmark of tauopathies [24, 40, 46, 47], although the role of ROS in facilitating neurodegeneration has not been fully elucidated. It is hypothesised that ROS production is simultaneously as a consequence of chronic tau phosphorylation and also a transient response to cellular damage linked to tauopathies [24], known to trigger tau proteolysis [95], which is noteworthy considering that higher molecular weight tau proteins are known to have neuroprotective effects [96]. In short, tau phosphorylation and ROS activity are two elements in a positive feedback loop that lead to tauopathies. The studies reported in this thesis are the first to show, to the best of our knowledge, that the KP metabolites QUIN and 3-HK mediate tau phosphorylation via their capacity to produce intracellular ROS.

Excessive QUIN was also confirmed to increase intracellular Ca^{2+} influx after both acute (Fig. 3.7) and chronic (24-h, Fig. 3.8) exposure periods. Most notably, NMDAR inactivation showed significantly reduced QUIN-derived Ca^{2+} influx (to undetectable levels) at the same focal plane (z-plane). Most significantly, the calcium chelator EGTA also significantly reduced Ca^{2+} influx. Cell treatments that induced excess Ca^{2+} influx, restricted Ca^{2+} localisation to inside the cell body. This redistribution of calcium transport away from axons may be detrimental to neuronal function. Western blot experiments, where cells were treated under similar conditions, demonstrated significantly reduced tau phosphorylation with calcium chelation. That, and the treatment of cells with NMDAR antagonist KYNA also reduced tau phosphorylation, provide the first evidence that QUIN-mediated tau-phosphorylation mediates Ca^{2+} localisation, possibly via NMDAR. Further support of this conclusion is provided by the result that treatment with the KMO inhibitor Ro-61-8048 is also capable of reducing tau phosphorylation.

After establishing that pathological concentrations of QUIN elicit ROS activity and Ca^{2+} influx, both of which correlated with increased tau phosphorylation, HEK peZ cells were employed to model over-expression of the KMO enzyme that favours the QUIN-producing branch of the KP. Baseline tau phosphorylation in these cells was low, however the KMO over-expressing cells showed an almost 4-fold greater level of tau phosphorylation than the vector-only control HEK peZ [-] cells (Fig. 3.13), further adding to the case that QUIN mediates tau phosphorylation.

Primary neurons and HEK peZ [-] cells show low basal expression of KMO [81] and so exhibited limited KMO inhibition with Ro-61-8048 as demonstrated by the 3HK/KYN ratio (Fig. 3.16, 3.18). Conversely, macrophages and HEK peZ [KMO] cells freely express the KMO enzyme [97–99] and so, Ro-61-8048 inhibition of KMO was achieved as reflected by the 3HK/KYN ratio (Fig. 3.17, 3.18). Despite variable KMO expression, KMO inhibition did show decrease in tau phosphorylation across all cell lines. In the case of macrophages and HEK peZ [KMO] cells, the reduction in tau phosphorylation was significant. Furthermore, NMDAR antagonism with KYNA also demonstrated a

significant decrease in tau phosphorylation in these cell lines. Most interestingly, calcium chelation in all human primary cells also significantly reduced tau phosphorylation 4-fold. Pathological QUIN exposure to primary human cells did not significantly increase tau phosphorylation in this study which was contrary to previous reports [15, 81, 97, 100]. The discrepancy of the presented results may be attributed to technical errors in the experiment, most likely cell seeding density, poor lysate collection, and uneven loading (which can be accounted for by protein normalisation).

Preliminary time-course experiments with DCF-DA (Fig. 3.22) were not fully optimised due to time constraints, and did not always reproduce results previously reported in literature [86]. HEK peZ [KMO] cells were more resistant towards QUIN-derived ROS activity, in line with a study that reported KMO over-expression to be a preventative measure against 3HK-driven ROS activity [101]. End-point ROS assays were conducted following 24-h treatments in HEK peZ [-] cells (Fig. 3.23) which further incorporated known NMDAR antagonist APV. Once again, these assays were not fully optimised due to time constraints. Crucially, the positive control was not strong enough to illicit ROS production, however, calcium chelation and glutamate receptor antagonism with KYNA and APV did decrease ROS signal. KYNA exhibited more potency than APV in ameliorating QUIN toxicity, potentially due to its broad-spectrum antagonism of glutamate receptors [102]. KYNA treatment alone did not increase ROS production, congruent to *in vivo* studies [101], but stand-alone treatments of APV and EGTA increased ROS activity in SH-SY5Y cells. This is in disagreement with reports that show APV to be well tolerated [103], albeit only in combination with other drugs.

To supplement the live cell calcium imaging experiments, we attempted to optimise high-throughput Ca^{2+} influx assays using Fura-2AM (Fig. 3.24, 3.25, 3.26). Due to time constraints, we were unable to optimise the assay but achieve some success. KYNA pre-incubation decreased QUIN-derived Ca^{2+} influx, in line with supporting literature [104–107]. We did attempt to follow previously reported protocols, but it is possible they failed to state all required conditions. Notwithstanding, these experiments did show some success and were only supplemental to our live-cell calcium imaging experiments.

Various avenues present themselves to further optimise both ROS and Ca^{2+} influx high throughput assays. Fura 2-AM is a reliable method of intracellular calcium detection because of its ability to discriminate between intracellular bound calcium and extracellular free calcium. It has also previously been employed to record QUIN-mediated intracellular calcium changes in primary rat hippocampal neurons NMDAR and QUIN [108], as well as other reported studies previously identified. Incorporating reliable blockers of store operate Ca^{2+} influx may also assist in validating the experiments [109], however, its reliability in modulating Ca^{2+} influx is controversial [110]. Both DCF-DA and Fura 2-AM assays demonstrated greater discrimination between treatments when combined with phenol-red-free and FBS-free media, which has the added benefit of forcing the cells to remain in the same stage of the cell cycle. Otherwise, already optimised and commercially-available assays can also be considered.

While the present study showed statistically significant findings, in some cases, analyses were limited by the limited number of experimental replicates. This may mask truly significant results and highlight the need to conduct more experiments to support the presented findings. Despite these caveats in place, this study was for the first time able to link KMO activity, QUIN production, and resulting Ca^{2+} influx to tau phosphorylation, and suggests further avenues for mechanistic investigation.

4.2 Calcium Signalling in Tau Phosphorylation

No single kinase or phosphatase is responsible for the phosphorylation state of all tau epitopes. Rather, it is now accepted that phosphorylation occurs in a sequential manner - i.e. phosphorylation at one epitope facilitates secondary phosphorylation at another. This is best demonstrated by GSK3 β . It has been noted that when phosphorylated first by CDK5 or CaMKII, and then GSK3 β , tau experiences rapid phosphorylation at Thr 231 and Ser 235 epitopes [111]. The order in which enzymes phosphorylate tau has not been actively studied within the literature, though the "kinase cascade", a phenomena by which kinase activation up-regulates multiple secondary kinases, is well accepted as a factor in tauopathies.

The interplay between these kinases and KP modulating enzymes may pose an interesting avenue for research. Phosphatase activity has also been linked to decreased tau phosphorylation mediated through NMDARs, which are deregulated by receptor interactions with QUIN [12–16]. GSK3 β , CDK, CamK, and PPs have previously been known to show a delicate interplay in NMDAR activation, possibly through the N2RA receptor [32, 50–52, 64, 67, 112, 113]. Advancing these findings to include KP enzyme activity may establish a direct link in QUIN-NMDAR interaction. with respect to tau phosphorylation, ROS production and Ca²⁺ influx. Indeed, tau induced CAMK activation increases tau phosphorylation [64, 114], a known precursor to A β accumulation [62]. Considering observations reported in this thesis, that QUIN was shown to lead to both Ca²⁺ influx and ROS production, that KMO over-expression lead to increased ROS activity [86] and 3HK synthesis, and that 3HK and GSK3 β both have demonstrated redox activity [24, 72], future studies should look at how GSK3 β mediates calcium signalling and tau phosphorylation in response to redox conditions mediated by 3HK activity.

NMDAR Ca²⁺ signalling and its relation to tau phosphorylation was the leading hypothesis of this study. However, the literature also reports rapid Ca²⁺ signalling between AMPAR (AMPA receptors) and NMDAR, whereby which AMPA activated the NMDAR by dislodging the Mg²⁺ blockade and inducing Ca²⁺ influx [59]. This potential mechanisms were outside the scope of the present study. The relationship between AMPAR activation and QUIN-induced excitotoxicity has yet to be explored in the current literature.

In the experiments presented in this thesis, glutamate was used to activate the NMDAR in primary mouse neurons, which is known to also activate AMPARs[115]. The effects of NMDAR modulation was studied using memantine, a known NMDAR antagonist. Memantine is an uncompetitive antagonist that mimics the mechanism by which free Mg²⁺ blocks the NMDAR mechanism which relies on electro-chemical potential [116, 117]. Therefore, memantine will block NMDAR during chronic activation of the receptor [118], where Mg²⁺ is dislodged from the NMDAR. However, inhibition

with KYNA does not directly prove NMDAR-specific mediation of Ca^{2+} influx when we consider that KYNA is known to be the only endogenous inhibitor of not only NMDARs but also AMPARs and other kainate receptors as well as all ionotropic glutamate receptors [102].

KYNA antagonism of AMPARs is well established. At the micromolar concentrations, KYNA demonstrates antagonistic effects on NMDAR and AMPAR. In lower, nanomolar concentrations, KYNA allosterically modulates the increase in post-synaptic potential (i.e. increase Ca^{2+} influx) [119, 120]. This dose-dependant behaviour and its potential effects on p-Tau warrants further study, however, this was outside the scope of the present study.

Interestingly, QUIN-mediated toxicity at NMDAR is inhibited when the receptor is pre-conditioned with NMDA. [121]. In essence, NMDA preconditioning of the NMDAR facilitates homeostasis which is protective against QUIN-derived deregulation. This indicates that NMDA, while being an agonist of Ca^{2+} influx, does not mediate excitotoxicity like QUIN. This may be attributed to the preference of the molecules towards specific receptor sub-types [122].

$\text{A}\beta$ plaques also increase intra-cellular Ca^{2+} levels, making cells more prone to the effects of glutamate toxicity, thereby increasing tau phosphorylation [12]. This is supported by observations indicating that phosphorylated tau impairs glutamate receptors in dendrites [24]. Findings also show that QUIN promotes glutamate release and inhibits its re-uptake at the NMDAR receptor [79], thereby increasing the potential that glutamate will mediate excitotoxicity through AMPAR and other receptors. This may be relevant to other paradigms of tauopathies. Excess extra-cellular glutamate could agonise AMPAR as readily as NMDAR, reiterating the need for further studies to focus on AMPAR-mediated confounding factors on the QUIN-NMDAR hypothesis. Presently, the literature is ambiguous in this regard.

Studies indicate that inhibiting calcium influx at either NMDAR or AMPAR can have therapeutic benefits [123]. The most comprehensive study found to date looked at QUIN toxicity and cytoskeletal phosphorylation in astrocytes [124]. This study assessed the effects of inhibition in both NMDAR, using NMDAR-specific antagonists, and other general glutamate receptors, using an array of non-specific glutamate receptor antagonists. Both groups of experiments showed successful decrease of Ca^{2+} . Interestingly, the effect of calcium chelation was also assessed in the study, showing both intra- and extra-cellular calcium chelation prevented QUIN-mediated Ca^{2+} influx. This supports the findings presented in this thesis which showed a significant increase in Ca^{2+} influx which correlated with an increase in tau phosphorylation. The study also assessed enzyme activation in response to QUIN mediated NMDAR activation, finding that PKA and PKC were up-regulated, supporting the current understanding of the literature. The study further identified that the Voltage-gated Calcium Channel (VGCC)-type L was not being involved in mediating increased intracellular calcium. A separate study also confirmed that QUIN does not mediate Ca^{2+} influx via VGCCs [108], suggesting that VGCC-mediated calcium influx is not solely responsible for QUIN-mediated Ca^{2+} influx.

Recent studies have shown that the polyphenol curcumin protects neurons from glutamate-driven Ca^{2+} influx [125]. While acknowledging that NMDAR activation may be involved, the study focused solely on AMPAR activation but did not assess effects on tau phosphorylation. Notwithstanding, the study adds weight to the importance of further assessing the role of AMPA in Ca^{2+} influx. While NMDAR is known to be the most sensitive to Ca^{2+} influx out of all glutamate receptors [118], making it a desirable model to study Ca^{2+} influx, the broad-spectrum activity of the KP metabolites must also be fully explored to discriminate between different glutamate receptor activity. The need for this study is highlighted by another study that assessed the structure of the tau cytoskeleton. This study found that QUIN-mediated Ca^{2+} influx was ameliorated by the broad spectrum antagonism of KYNA, but not by the known NMDAR antagonist MK-801 [88].

The primary mouse neuron live cell calcium imaging and Fura-2AM calcium assays in this study also did not consider the potential for QUIN-driven AMPAR activation, although, they did incorporate known NMDAR-specific antagonist APV to confirm NMDAR-mediated effects. It should be noted that while the NMDAR-mediated QUIN activity is widely supported in the literature, there still remains speculation that QUIN may have direct intra-cellular effects, including tau phosphorylation, independently of NMDAR activation [15, 126].

4.3 The Role of the KP and KMO Inhibition in Tauopathy

KMO inhibition has long been speculated to hold therapeutic benefits since a landmark study reported reported KMO inhibition had therapeutic results in murine model of degenerative disease [127]. Not only physiological markers of inflammation, but also reduced markers of psychological disturbances have also highlighted as therapeutic impacts of KMO inhibition in acute spinal cord injury [128]. It was also noted that multiple studies have reported KMO inhibition to ameliorate neurodegeneration in mouse models of various tauopathies. Similarly, KMO inhibition is also believed to hold therapeutic effects in multiple sclerosis [129], spinal cord injury [128], and in Schizophrenia [130].

The work presented in this thesis supports a recent study that assessed the KP in cerebrospinal fluid (CSF) of human AD patients [131]. This study demonstrated that multiple instances of KP metabolite correlation with tau phosphorylation. Interestingly, AD patients demonstrated high KYNA concentrations in the CSF, which was attributed to compensatory mechanisms acting to reduce chronic excitotoxicity at the NMDAR. However, elevated KYNA levels are known to cause motor-cognitive impairments [83], indicating that basal KYNA concentrations maintain neuroprotective effects, where KYNA elevation may present with pathological impairments not uncommon in AD and other tauopathies. Indeed, tauopathies manifest within the CSF,

with increased phosphorylation correlating with increased brain atrophy and cognitive impairments [24]. Importantly AD, CSF showed increased 3HK/KYN ratio, representative of KMO activity, correlating with increased p-Tau in humans [131].

It should be noted that while the work reported in this thesis supports the notion that modulating the KP may hold therapeutic benefits, it is reasonable to consider contradictions in the data. Collectively, the data supports the strong possibility that KP modulation may hold therapeutic benefits in neurodegenerative disease, especially those characterised by tauopathies. None the less, there are conflicting data in the literature. For instance, a study showed KMO inhibition with Ro-61-8048 producing no significant decrease in QUIN concentrations in the brain [132]. However, this does not take into consideration the inability of current synthetic KMO inhibitors to cross the blood-brain barrier (BBB) [72]. It is well-appreciated that KMO inhibition up-regulates the neuroprotective metabolite KYNA in the brain [72, 127].

Several reports suggest investigating tau phosphorylation by assessing specific residues is not representative of true physiological manifestations of tauopathies [24]. Notwithstanding this point of view, the results presented in this thesis indicate that KP modulation can impact on glutamate receptor activity to 1) increase both ROS production and Ca^{2+} influx and 2) up-regulate tau phosphorylation at the Ser202/Thr 205 epitopes. These epitopes are recognised as key phosphorylation sites for NFT formation [39–41]. However, it should be noted that the AT8 antibody has been reported to bind non-specifically [133]. Additional Western blots examining p-Tau using the AT8 antibody also showed non-specific banding when the membrane transfer systems was changed to another manufacturer. *In vitro* studies have achieved desirable specificity with whole-cell assays [134]. The results reported in this thesis can therefore be further validated by In-Cell assays in the Odyssey CLx Imaging System. Alternatively, novel methods such as Phos-tag SDS-PAGE have been proven to be more specific than AT8 and yield new insights into phosphorylation in tauopathies [135].

4.4 Conclusion

This study has contributed several significant results relevant to our understanding of the mechanisms by which QUIN mediates tau phosphorylation. Previously, while it has been shown that QUIN colocalises with phosphorylated tau, and that QUIN treatment of primary human neurons directly causes an increase in tau phosphorylation, no studies have addressed the mechanisms by which QUIN mediates tau phosphorylation. Considering the known links between tau phosphorylation, ROS production, and cellular Ca^{2+} influx, we, for the first time, investigated whether there was a direct mechanistic link between KMO enzyme activity, QUIN production, and tau phosphorylation. The work reported in this thesis showed: 1) that KMO inhibition significantly decreased tau phosphorylation; 2) that QUIN increased tau phosphorylation which correlated with an increased ROS production and intracellular Ca^{2+} influx; and 3) these findings were supported by experiments showing that inhibition of NMDAR prevented QUIN-mediated tau phosphorylation.

However, these promising results need to be considered in the context that other avenues by which QUIN mediate tau phosphorylation need to be explored. More specifically, there exists the potential that QUIN and other KP metabolites may mediate Ca^{2+} influx through other mechanisms including AMPARs. Additionally, explorations of the role of enzymes involved in the phosphorylation process are warranted. Collectively, the results in this thesis add to the substantial evidence that therapeutic modulation of the KP may be beneficial in neurodegenerative conditions, especially tauopathies. A remaining challenge is the lack of BBB-permeable KMO inhibitors that have the potential to potentially reduce NFT burden.



Appendix

A.1 Real-Time Videos of Ca^{2+} Influx

Real-time videos of live calcium signalling in primary mouse hippocampal neurons can be found embedded in the PDF (Fig. 3.9, 3.10, 3.11, 3.12). A compilation of the real-time videos can be viewed by [clicking here](#), or through this URL: <https://vimeo.com/375572911/b95a07a8f2>.

References

- [1] D. S. Rivera, C. Lindsay, J. F. Codocedo, I. Morel, C. Pinto, P. Cisternas, F. Bozinovic, and N. C. Inestrosa. *Andrographolide recovers cognitive impairment in a natural model of Alzheimer’s disease (Octodon degus)*. *Neurobiology of aging* **46**, 204 (2016). 1
- [2] C. A. Lane, J. Hardy, and J. M. Schott. *Alzheimer’s disease*. *European journal of neurology* **25**(1), 59 (2018). 1
- [3] Z. Mueed, P. Tandon, S. K. Maurya, R. Deval, M. A. Kamal, and N. K. Poddar. *Tau and mTOR: The Hotspots for Multifarious Diseases in Alzheimer’s Development*. *Front Neurosci* **12**, 1017 (2018). 1
- [4] P. Saha and N. Sen. *Tauopathy: A common mechanism for neurodegeneration and brain aging*. *Mech Ageing Dev* **178**, 72 (2019). 2, 4
- [5] M. G. Spillantini and M. Goedert. *Tau pathology and neurodegeneration*. *The Lancet Neurology* **12**(6), 609 (2013). URL <http://www.sciencedirect.com/science/article/pii/S1474442213700905>. 2, 3, 4, 6, 7, 9
- [6] R. M. Nisbet, J.-C. Polanco, L. M. Ittner, and J. Gotz. *Tau aggregation and its interplay with amyloid-beta*. *Acta neuropathologica* **129**(2), 207 (2015). 2
- [7] J. P. Brion. *Neurofibrillary tangles and Alzheimer’s disease*. *Eur Neurol* **40**(3), 130 (1998). 2

- [8] J. A. Fein, S. Sokolow, C. A. Miller, H. V. Vinters, F. Yang, G. M. Cole, and K. H. Gyls. *Co-localization of amyloid beta and tau pathology in Alzheimer's disease synaptosomes*. The American journal of pathology **172**(6), 1683 (2008). 2
- [9] S. A. Frautschy, F. Yang, M. Irizarry, B. Hyman, T. C. Saido, K. Hsiao, and G. M. Cole. *Microglial response to amyloid plaques in APP^{sw} transgenic mice*. American Journal of Pathology **152**(1), 307 (1998). 2
- [10] M. C. Irizarry, M. McNamara, K. Fedorchak, K. Hsiao, and B. T. Hyman. *APP(Sw) transgenic mice develop age-related A β deposits and neuropil abnormalities, but no neuronal loss in CA1*. Journal of Neuropathology and Experimental Neurology **56**(9), 965 (1997).
- [11] M. C. Irizarry, F. Soriano, M. McNamara, K. J. Page, D. Schenk, D. Games, and B. T. Hyman. *A β deposition is associated with neuropil changes, but not with overt neuronal loss in the human amyloid precursor protein V717F (PDAPP) transgenic mouse*. Journal of Neuroscience **17**(18), 7053 (1997). 2
- [12] M. P. Mattson, B. Cheng, D. Davis, K. Bryant, I. Lieberburg, and R. E. Rydel. *beta-Amyloid peptides destabilize calcium homeostasis and render human cortical neurons vulnerable to excitotoxicity*. J Neurosci **12**(2), 376 (1992). 2, 13, 68, 69
- [13] S. F. Chan and N. J. Sucher. *An NMDA Receptor Signaling Complex with Protein Phosphatase 2A*. The Journal of Neuroscience **21**(20), 7985 (2001). URL <http://www.jneurosci.org/content/21/20/7985.abstract>. 12
- [14] L. Minghetti, M. A. Ajmone-Cat, M. A. De Berardinis, and R. De Simone. *Microglial activation in chronic neurodegenerative diseases: roles of apoptotic neurons and chronic stimulation*. Brain Research Reviews **48**(2), 251 (2005). URL <http://www.sciencedirect.com/science/article/pii/S0165017304001924>.

- [15] A. Rahman, K. Ting, K. M. Cullen, N. Braidy, B. J. Brew, and G. J. Guillemin. *The excitotoxin quinolinic acid induces tau phosphorylation in human neurons*. PLoS ONE **4**(7), e6344 (2009). 16, 17, 18, 66, 71
- [16] P. Pierozan, A. Zamoner, K. Soska, B. O. de Lima, K. P. Reis, F. Zamboni, M. Wajner, and R. Pessoa-Pureur. *Signaling mechanisms downstream of quinolinic acid targeting the cytoskeleton of rat striatal neurons and astrocytes*. Experimental Neurology **233**(1), 391 (2012). URL <http://www.sciencedirect.com/science/article/pii/S0014488611004092>. 2, 19, 68
- [17] S. Okuda, N. Nishiyama, H. Saito, and H. Katsuki. *3-Hydroxykynurenine, an Endogenous Oxidative Stress Generator, Causes Neuronal Cell Death with Apoptotic Features and Region Selectivity*. Journal of Neurochemistry **70**(1), 299 (1998). URL <https://doi.org/10.1046/j.1471-4159.1998.70010299.x>. 2, 19
- [18] A. L. Colin-Gonzalez, M. Maya-Lopez, J. Pedraza-Chaverri, S. F. Ali, A. Chavarria, and A. Santamaria. *The Janus faces of 3-hydroxykynurenine: dual redox modulatory activity and lack of neurotoxicity in the rat striatum*. Brain Res **1589**, 1 (2014). 2, 19
- [19] N. N. Naseri, H. Wang, J. Guo, M. Sharma, and W. Luo. *The complexity of tau in Alzheimer's disease*. Neurosci Lett **705**, 183 (2019). 3, 4, 7
- [20] Y. Fichou, Y. K. Al-Hilaly, F. Devred, C. Smet-Nocca, P. O. Tsvetkov, J. Verelst, J. Winderickx, N. Geukens, E. Vanmechelen, A. Perrotin, L. Serpell, B. J. Hanseeuw, M. Medina, L. Buee, and I. Landrieu. *The elusive tau molecular structures: can we translate the recent breakthroughs into new targets for intervention?* Acta Neuropathol Commun **7**(1), 31 (2019). 4, 5, 8, 9
- [21] P. W. Baas and L. Qiang. *Tau: It's Not What You Think*. Trends in Cell Biology **29**(6), 452 (2019). URL <http://www.sciencedirect.com/science/article/pii/S0962892419300388>. 4, 8

- [22] A. Venkatramani and D. Panda. *Regulation of neuronal microtubule dynamics by tau: Implications for tauopathies*. Int J Biol Macromol **133**, 473 (2019). 4, 7
- [23] S. Maeda and L. Mucke. *Tau Phosphorylation-Much More than a Biomarker*. Neuron **92**(2), 265 (2016). 4
- [24] S. M. Alavi Naini and N. Soussi-Yanicostas. *Tau Hyperphosphorylation and Oxidative Stress, a Critical Vicious Circle in Neurodegenerative Tauopathies?* Oxidative medicine and cellular longevity **2015**, 151979 (2015). URL <https://www.ncbi.nlm.nih.gov/pubmed/26576216><https://www.ncbi.nlm.nih.gov/pmc/articles/PMC4630413/>. 4, 5, 7, 9, 10, 11, 12, 64, 68, 69, 72
- [25] M. Rankovic and M. Zweckstetter. *Upregulated levels and pathological aggregation of abnormally phosphorylated Tau-protein in children with neurodevelopmental disorders*. Neurosci Biobehav Rev **98**, 1 (2019). 4
- [26] S. Taniguchi-Watanabe, T. Arai, F. Kametani, T. Nonaka, M. Masuda-Suzukake, A. Tarutani, S. Murayama, Y. Saito, K. Arima, and M. Yoshida. *Biochemical classification of tauopathies by immunoblot, protein sequence and mass spectrometric analyses of sarkosyl-insoluble and trypsin-resistant tau*. Acta Neuropathologica **131**(2), 267 (2016). 5
- [27] S. L. DeVos, D. K. Goncharoff, G. Chen, C. S. Kebodeaux, K. Yamada, F. R. Stewart, D. R. Schuler, S. E. Maloney, D. F. Wozniak, F. Rigo, C. F. Bennett, J. R. Cirrito, D. M. Holtzman, and T. M. Miller. *Antisense Reduction of Tau in Adult Mice Protects against Seizures*. The Journal of Neuroscience **33**(31), 12887 (2013). URL <http://www.jneurosci.org/content/33/31/12887.abstract>. 5
- [28] D. M. Holtzman, M. C. Carrillo, J. A. Hendrix, L. J. Bain, A. M. Catafau, L. M. Gault, M. Goedert, E. Mandelkow, E.-M. Mandelkow, D. S. Miller, S. Ostrowitzki, M. Polydoro, S. Smith, M. Wittmann, and M. Hutton. *Tau: From research to clinical development*. Alzheimer's & Dementia **12**(10), 1033 (2016). URL <http://www.sciencedirect.com/science/article/pii/S155252601630019X>. 5

- [29] S.-W. Min, X. Chen, T. E. Tracy, Y. Li, Y. Zhou, C. Wang, K. Shirakawa, S. S. Minami, E. Defensor, S. A. Mok, P. D. Sohn, B. Schilling, X. Cong, L. Ellerby, B. W. Gibson, J. Johnson, N. Krogan, M. Shamloo, J. Gestwicki, E. Masliah, E. Verdin, and L. Gan. *Critical role of acetylation in tau-mediated neurodegeneration and cognitive deficits*. *Nature Medicine* **21**, 1154 (2015). URL <https://doi.org/10.1038/nm.3951>. 5
- [30] M. Morris, S. Maeda, K. Vossel, and L. Mucke. *The Many Faces of Tau*. *Neuron* **70**(3), 410 (2011). URL <http://www.sciencedirect.com/science/article/pii/S0896627311003114>. 5
- [31] M. E. Orr, A. C. Sullivan, and B. Frost. *A Brief Overview of Tauopathy: Causes, Consequences, and Therapeutic Strategies*. *Trends in pharmacological sciences* **38**(7), 637 (2017). URL <https://www.ncbi.nlm.nih.gov/pubmed/28455089https://www.ncbi.nlm.nih.gov/pmc/articles/PMC5476494/>. 7
- [32] Y. Chen, X. Chen, Z. Yao, Y. Shi, J. Xiong, J. Zhou, Z. Su, and Y. Huang. *Tau Interaction and Tau Amyloidogenesis*. *J Mol Neurosci* (2019). 8, 9, 68
- [33] K. Yamada. *Extracellular Tau and Its Potential Role in the Propagation of Tau Pathology*. *Front Neurosci* **11**, 667 (2017). 8
- [34] M. Usenovic, S. Niroomand, R. E. Drolet, L. Yao, R. C. Gaspar, N. G. Hatcher, J. Schachter, J. J. Renger, and S. Parmentier-Batteur. *Internalized Tau Oligomers Cause Neurodegeneration by Inducing Accumulation of Pathogenic Tau in Human Neurons Derived from Induced Pluripotent Stem Cells*. *The Journal of Neuroscience* **35**(42), 14234 LP (2015). URL <http://www.jneurosci.org/content/35/42/14234.abstract>. 8
- [35] S. S. Shafiei, M. J. Guerrero-Muñoz, and D. L. Castillo-Carranza. *Tau Oligomers: Cytotoxicity, Propagation, and Mitochondrial Damage*. *Frontiers in aging neuroscience* **9**, 83 (2017). URL <https://www.ncbi.nlm.nih.gov/pubmed/28420982https://www.ncbi.nlm.nih.gov/pmc/articles/PMC5378766/>.

- [36] C. A. Lasagna-Reeves, D. L. Castillo-Carranza, U. Sengupta, J. Sarmiento, J. Troncoso, G. R. Jackson, and R. Kayed. *Identification of oligomers at early stages of tau aggregation in Alzheimer's disease*. FASEB journal : official publication of the Federation of American Societies for Experimental Biology **26**(5), 1946 (2012). URL <https://www.ncbi.nlm.nih.gov/pubmed/22253473><https://www.ncbi.nlm.nih.gov/pmc/articles/PMC4046102/>.
- [37] K. Iqbal, C.-X. Gong, and F. Liu. *Hyperphosphorylation-induced tau oligomers*. Frontiers in neurology **4**, 112 (2013). URL <https://www.ncbi.nlm.nih.gov/pubmed/23966973><https://www.ncbi.nlm.nih.gov/pmc/articles/PMC3744035/>. 8
- [38] S. Narasimhan, J. L. Guo, L. Changolkar, A. Stieber, J. D. McBride, L. V. Silva, Z. He, B. Zhang, R. J. Gathagan, J. Q. Trojanowski, and V. M. Y. Lee. *Pathological Tau Strains from Human Brains Recapitulate the Diversity of Tauopathies in Nontransgenic Mouse Brain*. J Neurosci **37**(47), 11406 (2017). 8
- [39] L. Martin, X. Latypova, C. M. Wilson, A. Magnaudeix, M. L. Perrin, C. Yardin, and F. Terro. *Tau protein kinases: involvement in Alzheimer's disease*. Ageing Res Rev **12**(1), 289 (2013). 8, 9, 64, 72
- [40] M. M. Haque, D. P. Murale, Y. K. Kim, and J. S. Lee. *Crosstalk between Oxidative Stress and Tauopathy*. Int J Mol Sci **20**(8) (2019). 10, 64
- [41] C. Despres, C. Byrne, H. Qi, F.-X. Cantrelle, I. Huvent, B. Chambraud, E.-E. Baulieu, Y. Jacquot, I. Landrieu, G. Lippens, and C. Smet-Nocca. *Identification of the Tau phosphorylation pattern that drives its aggregation*. Proceedings of the National Academy of Sciences of the United States of America **114**(34), 9080 (2017). URL <https://www.ncbi.nlm.nih.gov/pubmed/28784767><https://www.ncbi.nlm.nih.gov/pmc/articles/PMC5576827/>. 72
- [42] K. H. Strang, M. S. Goodwin, C. Riffe, B. D. Moore, P. Chakrabarty, Y. Levites, T. E. Golde, and B. I. Giasson. *Generation and characterization of new monoclonal antibodies targeting the PHF1 and AT8 epitopes on human tau*. Acta

- Neuropathologica Communications **5**(1), 58 (2017). URL <https://doi.org/10.1186/s40478-017-0458-0>. 8
- [43] Y. Carlomagno, D. e. C. Chung, M. Yue, M. Castanedes-Casey, B. J. Madden, J. Dunmore, J. Tong, M. DeTure, D. W. Dickson, L. Petrucelli, and C. Cook. *An Acetylation-phosphorylation switch that regulates tau aggregation propensity and function*. Journal of Biological Chemistry **292**(37), 15277 (2017). 9
- [44] M. Platten, E. A. A. Nollen, U. F. Röhrig, F. Fallarino, and C. A. Opitz. *Tryptophan metabolism as a common therapeutic target in cancer, neurodegeneration and beyond*. Nature Reviews Drug Discovery (2019). URL <https://doi.org/10.1038/s41573-019-0016-5>. 9
- [45] F. Liu, I. Grundke-Iqbal, K. Iqbal, and C.-X. Gong. *Contributions of protein phosphatases PP1, PP2A, PP2B and PP5 to the regulation of tau phosphorylation*. European Journal of Neuroscience **22**(8), 1942 (2005). URL <https://doi.org/10.1111/j.1460-9568.2005.04391.x>. 9, 10, 11
- [46] V. Bonet-Costa, L. C. Pomatto, and K. J. Davies. *The Proteasome and Oxidative Stress in Alzheimer's Disease*. Antioxid Redox Signal **25**(16), 886 (2016). 9, 11, 64
- [47] J. M. van der Harg, L. Eggels, F. N. Bangel, S. R. Ruigrok, R. Zwart, J. J. M. Hoozemans, S. E. la Fleur, and W. Scheper. *Insulin deficiency results in reversible protein kinase A activation and tau phosphorylation*. Neurobiol Dis **103**, 163 (2017). 9, 11, 64
- [48] M. Gratuze, J. Julien, F. R. Petry, F. Morin, and E. Planel. *Insulin deprivation induces PP2A inhibition and tau hyperphosphorylation in hTau mice, a model of Alzheimer's disease-like tau pathology*. Scientific reports **7**, 46359 (2017). URL <https://doi.org/10.1038/srep46359>. 10

- [49] C.-X. Gong, T. Lidsky, J. Wegiel, L. Zuck, I. Grundke-Iqbal, and K. Iqbal. *Phosphorylation of Microtubule-associated Protein Tau Is Regulated by Protein Phosphatase 2A in Mammalian Brain: IMPLICATIONS FOR NEUROFIBRILLARY DEGENERATION IN ALZHEIMER'S DISEASE*. Journal of Biological Chemistry **275**(8), 5535 (2000). URL <http://www.jbc.org/content/275/8/5535.abstract>. 10
- [50] J.-M. Sontag and E. Sontag. *Protein phosphatase 2A dysfunction in Alzheimer's disease*. Frontiers in Molecular Neuroscience **7**(16) (2014). URL <https://www.frontiersin.org/article/10.3389/fnmol.2014.00016>. 10, 68
- [51] W. Qian, J. Shi, X. Yin, K. Iqbal, I. Grundke-Iqbal, C. X. Gong, and F. Liu. *PP2A regulates tau phosphorylation directly and also indirectly via activating GSK-3beta*. J Alzheimers Dis **19**(4), 1221 (2010). 10, 11
- [52] T. Ponce-Lopez, E. Hong, M. Abascal-D^aaz, and A. Meneses. *Role of GSK3-beta and PP2A on Regulation of Tau Phosphorylation in Hippocampus and Memory Impairment in ICV-STZ Animal Model of Alzheimer's Disease*. Advances in Alzheimer's Disease **Vol.06No.0**, 19 (2017). URL <file://www.scirp.org/journal/PaperInformation.aspx?PaperID=74645>. 10, 11, 68
- [53] S. Jang and S.-H. Park. *Antidiabetic Drug Metformin Protects Neuronal Cells against Quinolinic Acid-Induced Excitotoxicity by Decreasing Intracellular Calcium*. Chonnam Medical Journal **54**(1), 24 (2018). 11
- [54] S. M. De La Monte and J. R. Wands. *Alzheimer's disease is type 3 diabetes-evidence reviewed* (2008). 11
- [55] M. Manczak, T. S. Anekonda, E. Henson, B. S. Park, J. Quinn, and P. H. Reddy. *Mitochondria are a direct site of A β accumulation in Alzheimer's disease neurons: implications for free radical generation and oxidative damage in disease progression*. Human Molecular Genetics **15**(9), 1437 (2006). URL <https://doi.org/10.1093/hmg/ddl066>. 12

- [56] L. Pagani and A. Eckert. *Amyloid-Beta interaction with mitochondria*. International journal of Alzheimer's disease **2011**, 925050 (2011). URL <https://www.ncbi.nlm.nih.gov/pubmed/21461357><https://www.ncbi.nlm.nih.gov/pmc/articles/PMC3065051/>. 12
- [57] Z. T. Kincses, J. Toldi, and L. Vécsei. *Kynurenines, neurodegeneration and Alzheimer's disease*. Journal of cellular and molecular medicine **14**(8), 2045 (2010). URL <https://www.ncbi.nlm.nih.gov/pubmed/20629991><https://www.ncbi.nlm.nih.gov/pmc/articles/PMC3822995/>. 12, 18
- [58] M. Terunuma, K. J. Vargas, M. E. Wilkins, O. A. Ramírez, M. Jaureguiberry-Bravo, M. N. Pangalos, T. G. Smart, S. J. Moss, and A. Couve. *Prolonged activation of NMDA receptors promotes dephosphorylation and alters postendocytic sorting of GABA_B receptors*. Proceedings of the National Academy of Sciences **107**(31), 13918 (2010). URL <http://www.pnas.org/content/107/31/13918.abstract>. 12
- [59] J. Liu, L. Chang, Y. Song, H. Li, and Y. Wu. *The Role of NMDA Receptors in Alzheimer's Disease*. Frontiers in neuroscience **13**, 43 (2019). URL <https://www.ncbi.nlm.nih.gov/pubmed/30800052><https://www.ncbi.nlm.nih.gov/pmc/articles/PMC6375899/>. 12, 13, 14, 68
- [60] D. M. Kullmann and K. P. Lamsa. *Long-term synaptic plasticity in hippocampal interneurons*. Nature Reviews Neuroscience **8**(9), 687 (2007). URL <https://doi.org/10.1038/nrn2207>. 12
- [61] S. Kocahan and Z. Doğan. *Mechanisms of Alzheimer's Disease Pathogenesis and Prevention: The Brain, Neural Pathology, N-methyl-D-aspartate Receptors, Tau Protein and Other Risk Factors*. Clinical psychopharmacology and neuroscience : the official scientific journal of the Korean College of Neuropsychopharmacology **15**(1), 1 (2017). URL <https://www.ncbi.nlm.nih.gov/pubmed/28138104><https://www.ncbi.nlm.nih.gov/pmc/articles/PMC5290713/>. 12

- [62] N. Pierrot, S. F. Santos, C. Feyt, M. Morel, J.-P. Brion, and J.-N. Octave. *Calcium-mediated Transient Phosphorylation of Tau and Amyloid Precursor Protein Followed by Intraneuronal Amyloid- β Accumulation*. Journal of Biological Chemistry **281**(52), 39907 (2006). URL <http://www.jbc.org/content/281/52/39907.abstract>. 13, 68
- [63] T. Yamamoto and A. Hirano. *A COMPARATIVE STUDY OF MODIFIED BIELSCHOWSKY, BODIAN AND THIOFLAVIN S STAINS ON ALZHEIMER'S NEUROFIBRILLARY TANGLES*. Neuropathology and Applied Neurobiology **12**(1), 3 (1986). URL <https://doi.org/10.1111/j.1365-2990.1986.tb00677.x>. 13
- [64] Y.-P. Wei, J.-W. Ye, X. Wang, L.-P. Zhu, Q.-H. Hu, Q. Wang, D. Ke, Q. Tian, and J.-Z. Wang. *Tau-Induced Ca^{2+} /Calmodulin-Dependent Protein Kinase-IV Activation Aggravates Nuclear Tau Hyperphosphorylation*. Neuroscience bulletin **34**(2), 261 (2018). URL <https://www.ncbi.nlm.nih.gov/pubmed/28646348><https://www.ncbi.nlm.nih.gov/pmc/articles/PMC5856708/>. 13, 68
- [65] J. H. Weiss, C. J. Pike, and C. W. Cotman. *Rapid Communication: Ca^{2+} Channel Blockers Attenuate β -Amyloid Peptide Toxicity to Cortical Neurons in Culture*. Journal of Neurochemistry **62**(1), 372 (1994). URL <https://doi.org/10.1046/j.1471-4159.1994.62010372.x>. 13
- [66] E. Alberdi, M. V. Sanchez-Gomez, F. Cavaliere, A. Perez-Samartin, J. L. Zugaza, R. Trullas, M. Domercq, and C. Matute. *Amyloid beta oligomers induce Ca^{2+} dysregulation and neuronal death through activation of ionotropic glutamate receptors*. Cell Calcium **47**(3), 264 (2010). 13
- [67] A. De Montigny, I. Elhiri, J. Allyson, M. Cyr, and G. Massicotte. *NMDA reduces Tau phosphorylation in rat hippocampal slices by targeting NR2A receptors, GSK3 β , and PKC activities*. Neural plasticity **2013**, 261593 (2013).

- URL <https://www.ncbi.nlm.nih.gov/pubmed/24349798><https://www.ncbi.nlm.nih.gov/pmc/articles/PMC3856160/>. 13, 68
- [68] J. J. Palop and L. Mucke. *Amyloid-beta-induced neuronal dysfunction in Alzheimer's disease: from synapses toward neural networks*. Nature neuroscience **13**(7), 812 (2010). URL <https://www.ncbi.nlm.nih.gov/pubmed/20581818><https://www.ncbi.nlm.nih.gov/pmc/articles/PMC3072750/>. 14
- [69] J. J. Palop, J. Chin, E. D. Roberson, J. Wang, M. T. Thwin, N. Bien-Ly, J. Yoo, K. O. Ho, G.-Q. Yu, A. Kreitzer, S. Finkbeiner, J. L. Noebels, and L. Mucke. *Aberrant Excitatory Neuronal Activity and Compensatory Remodeling of Inhibitory Hippocampal Circuits in Mouse Models of Alzheimer's Disease*. Neuron **55**(5), 697 (2007). URL <https://doi.org/10.1016/j.neuron.2007.07.025>. 14
- [70] A. D. Bachstetter, B. Xing, L. de Almeida, E. R. Dimayuga, D. M. Watterson, and L. J. Van Eldik. *Microglial p38 α MAPK is a key regulator of proinflammatory cytokine up-regulation induced by toll-like receptor (TLR) ligands or beta-amyloid (A β)*. Journal of Neuroinflammation **8**(1), 79 (2011). URL <https://doi.org/10.1186/1742-2094-8-79>. 14
- [71] R. S. Phillips, E. C. Iradukunda, T. Hughes, and J. P. Bowen. *Modulation of Enzyme Activity in the Kynurenine Pathway by Kynurenine Monoxygenase Inhibition*. Frontiers in molecular biosciences **6**, 3 (2019). URL <https://www.ncbi.nlm.nih.gov/pubmed/30800661><https://www.ncbi.nlm.nih.gov/pmc/articles/PMC6376250/>. 14
- [72] K. R. Jacobs, G. Castellano-Gonzalez, G. J. Guillemin, and D. B. Lovejoy. *Major Developments in the Design of Inhibitors along the Kynurenine Pathway*. Curr Med Chem **24**(23), 2471 (2017). 14, 18, 68, 72
- [73] M. D. Lovelace, B. Varney, G. Sundaram, M. J. Lennon, C. K. Lim, K. Jacobs, G. J. Guillemin, and B. J. Brew. *Recent evidence for an expanded role*

- of the kynurenine pathway of tryptophan metabolism in neurological diseases.* Neuropharmacology **112**, 373 (2017). URL <http://www.sciencedirect.com/science/article/pii/S002839081630096X>. 14
- [74] C. K. Lim, F. J. Fernández-Gomez, N. Braidy, C. Estrada, C. Costa, S. Costa, A. Bessede, E. Fernandez-Villalba, A. Zinger, M. T. Herrero, and G. J. Guillemin. *Involvement of the kynurenine pathway in the pathogenesis of Parkinson's disease.* Progress in Neurobiology **155**, 76 (2017). URL <http://www.sciencedirect.com/science/article/pii/S0301008215300551>. 14
- [75] W. Wu, J. A. Nicolazzo, L. Wen, R. Chung, R. Stankovic, S. S. Bao, C. K. Lim, B. J. Brew, K. M. Cullen, and G. J. Guillemin. *Expression of tryptophan 2,3-dioxygenase and production of kynurenine pathway metabolites in triple transgenic mice and human Alzheimer's disease brain.* PLoS ONE **8**(4), e59749 (2013). 14, 16, 18
- [76] B. I. Aldana. *Microglia-Specific Metabolic Changes in Neurodegeneration.* Journal of Molecular Biology (2019). URL <http://www.sciencedirect.com/science/article/pii/S002228361930124X>. 15
- [77] G. J. Guillemin and B. J. Brew. *Implications of the kynurenine pathway and quinolinic acid in Alzheimer's disease.* Redox Rep **7**(4), 199 (2002). 16, 18, 19
- [78] E. Gulaj, K. Pawlak, B. Bien, and D. Pawlak. *Kynurenine and its metabolites in Alzheimer's disease patients.* Advances in medical sciences **55**(2), 204 (2010). 16
- [79] M. J. Schwarz, G. J. Guillemin, S. J. Teipel, K. Buerger, and H. Hampel. *Increased 3-hydroxykynurenine serum concentrations differentiate Alzheimer's disease patients from controls.* European archives of psychiatry and clinical neuroscience **263**(4), 345 (2013). 16, 69
- [80] G. S. Deora, S. Kantham, S. Chan, S. N. Dighe, S. K. Veliyath, G. McColl, M.-O. Parat, R. P. McGeary, and B. P. Ross. *Multifunctional Analogs of Kynurenic*

- Acid for the Treatment of Alzheimer's Disease: Synthesis, Pharmacology, and Molecular Modeling Studies*. ACS chemical neuroscience **8**(12), 2667 (2017). 16
- [81] G. J. Guillemin, K. M. Cullen, C. K. Lim, G. A. Smythe, B. Garner, V. Kapoor, O. Takikawa, and B. J. Brew. *Characterization of the kynurenine pathway in human neurons*. The Journal of neuroscience : the official journal of the Society for Neuroscience **27**(47), 12884 (2007). URL <https://www.ncbi.nlm.nih.gov/pubmed/18032661><https://www.ncbi.nlm.nih.gov/pmc/articles/PMC6673280/>. 16, 28, 34, 65, 66
- [82] A. L. Guillozet, S. Weintraub, D. C. Mash, and M. M. Mesulam. *Neurofibrillary tangles, amyloid, and memory in aging and mild cognitive impairment*. Archives of neurology **60**(5), 729 (2003). 16
- [83] J. M. Parrott and J. C. O'Connor. *Kynurenine 3-Monooxygenase: An Influential Mediator of Neuropathology*. Frontiers in Psychiatry **6**(116) (2015). URL <https://www.frontiersin.org/article/10.3389/fpsyt.2015.00116>. 18, 19, 71
- [84] D. J. Bonda, M. Mailankot, J. G. Stone, M. R. Garrett, M. Staniszevska, R. J. Castellani, S. L. Siedlak, X. Zhu, H.-g. Lee, G. Perry, R. H. Nagaraj, and M. A. Smith. *Indoleamine 2,3-dioxygenase and 3-hydroxykynurenine modifications are found in the neuropathology of Alzheimer's disease*. Redox Report **15**(4), 161 (2010). URL <https://doi.org/10.1179/174329210X12650506623645>. 19
- [85] G. Mazarei, D. P. Budac, G. Lu, H. Lee, T. Möller, and B. R. Leavitt. *The absence of indoleamine 2,3-dioxygenase expression protects against NMDA receptor-mediated excitotoxicity in mouse brain*. Experimental Neurology **249**, 144 (2013). URL <http://www.sciencedirect.com/science/article/pii/S0014488613002471>. 19
- [86] G. Castellano-Gonzalez, K. R. Jacobs, E. Don, N. J. Cole, S. Adams, C. K. Lim, D. B. Lovejoy, and G. J. Guillemin. *Kynurenine 3-Monooxygenase Activity in Human Primary Neurons and Effect on Cellular Bioenergetics Identifies New*

- Neurotoxic Mechanisms*. Neurotoxicity Research **35**(3), 530 (2019). URL <https://doi.org/10.1007/s12640-019-9997-4>. 19, 20, 25, 36, 56, 64, 66, 68
- [87] G. A. Zakharov, A. V. Popov, E. V. Savvateeva-Popova, and B. F. Shchegolev. *The role of stacking interactions in the mechanisms of binding of the glycine site of NMDA-receptor with antagonists and 3-hydroxykynurenine*. Biofizika **53**(1), 22 (2008). 19
- [88] P. Pierozan, H. Biasibetti-Brendler, F. Schmitz, F. Ferreira, R. Pessoa-Pureur, and A. T. Wyse. *Kynurenic Acid Prevents Cytoskeletal Disorganization Induced by Quinolinic Acid in Mixed Cultures of Rat Striatum*. Molecular Neurobiology **55**(6), 5111 (2018). 25, 70
- [89] N. Braidy, R. Grant, S. Adams, and G. J. Guillemin. *Neuroprotective effects of naturally occurring polyphenols on quinolinic acid-induced excitotoxicity in human neurons*. The FEBS Journal **277**(2), 368 (2010). URL <https://doi.org/10.1111/j.1742-4658.2009.07487.x>. 26
- [90] J. Kovalevich and D. Langford. *Considerations for the use of SH-SY5Y neuroblastoma cells in neurobiology*. Methods in molecular biology (Clifton, N.J.) **1078**, 9 (2013). URL <https://www.ncbi.nlm.nih.gov/pubmed/23975817https://www.ncbi.nlm.nih.gov/pmc/PMC5127451/>. 34
- [91] H. Xicoy, B. Wieringa, and G. J. M. Martens. *The SH-SY5Y cell line in Parkinson's disease research: a systematic review*. Molecular neurodegeneration **12**(1), 10 (2017). URL <https://www.ncbi.nlm.nih.gov/pubmed/28118852https://www.ncbi.nlm.nih.gov/pmc/PMC5259880/>.
- [92] H.-r. Xie, L.-s. Hu, and G.-y. Li. *SH-SY5Y human neuroblastoma cell line: in vitro cell model of dopaminergic neurons in Parkinson's disease*. Chinese medical journal **123**(8), 1086 (2010).
- [93] J. I. Forster, S. Köglsberger, C. Trefois, O. Boyd, A. S. Baumuratov, L. Buck, R. Balling, and P. M. A. Antony. *Characterization of Differentiated SH-SY5Y*

- as Neuronal Screening Model Reveals Increased Oxidative Vulnerability*. Journal of Biomolecular Screening **21**(5), 496 (2016). URL <https://doi.org/10.1177/1087057115625190>. 34
- [94] K. Wilson, D. J. Mole, M. Binnie, N. Z. M. Homer, X. Zheng, B. A. Yard, J. P. Iredale, M. Auer, and S. P. Webster. *Bacterial expression of human kynurenine 3-monooxygenase: Solubility, activity, purification*. Protein Expression and Purification **95**, 96 (2014). URL <http://www.sciencedirect.com/science/article/pii/S1046592813002593>. 63
- [95] P. K. Krishnamurthy, J. L. Mays, G. N. Bijur, and G. V. W. Johnson. *Transient oxidative stress in SH-SY5Y human neuroblastoma cells results in caspase dependent and independent cell death and tau proteolysis*. Journal of Neuroscience Research **61**(5), 515 (2000). URL [https://doi.org/10.1002/1097-4547\(20000901\)61:52-#](https://doi.org/10.1002/1097-4547(20000901)61:52-#). 64
- [96] Y. Zhou, J. Shi, D. Chu, W. Hu, Z. Guan, C.-X. Gong, K. Iqbal, and F. Liu. *Relevance of Phosphorylation and Truncation of Tau to the Etiopathogenesis of Alzheimer's Disease* (2018). URL <https://www.frontiersin.org/article/10.3389/fnagi.2018.00027>. 64
- [97] G. J. Guillemin, D. G. Smith, G. A. Smythe, P. J. Armati, and B. J. Brew. *Expression of the kynurenine pathway enzymes in human microglia and macrophages*. Advances in experimental medicine and biology **527**, 105 (2003). 65, 66
- [98] R. G. Ferrario, S. Baratté, C. Speciale, and P. Salvati. *Kynurenine enzymatic pathway in human monocytes-macrophages. Effect of interferon-gamma activation*. Advances in experimental medicine and biology **398**, 167 (1996).
- [99] S. P. Jones, N. F. Franco, B. Varney, G. Sundaram, D. A. Brown, J. de Bie, C. K. Lim, G. J. Guillemin, and B. J. Brew. *Expression of the Kynurenine Pathway in Human Peripheral Blood Mononuclear Cells: Implications*

- for Inflammatory and Neurodegenerative Disease*. PloS one **10**(6), e0131389 (2015). URL <https://www.ncbi.nlm.nih.gov/pubmed/26114426><https://www.ncbi.nlm.nih.gov/pmc/articles/PMC4482723/>. 65
- [100] M. Busse, V. Hettler, V. Fischer, C. Mawrin, R. Hartig, H. Dobrowolny, B. Bogerts, T. Frodl, and S. Busse. *Increased quinolinic acid in peripheral mononuclear cells in Alzheimer’s dementia*. European Archives of Psychiatry and Clinical Neuroscience **268**(5), 493 (2018). 66
- [101] K. Wilson, M. Auer, M. Binnie, X. Zheng, N. T. Pham, J. P. Iredale, S. P. Webster, and D. J. Mole. *Overexpression of human kynurenine-3-monooxygenase protects against 3-hydroxykynurenine-mediated apoptosis through bidirectional nonlinear feedback*. Cell death & disease **7**(4), e2197 (2016). URL <https://www.ncbi.nlm.nih.gov/pubmed/27077813><https://www.ncbi.nlm.nih.gov/pmc/articles/PMC4855666/>. 66
- [102] Z. Majláth, N. Török, J. Toldi, and L. Vécsei. *Memantine and Kynurenic Acid: Current Neuropharmacological Aspects*. Current Neuropharmacology **14**(2), 200 (2016). 66, 69
- [103] T. Scott, C. Garris, M. Rogers, N. Graham, L. Garrett, and L. Pedneault. *Safety profile and tolerability of amprenavir in patients enrolled in an early access program*. Clinical Therapeutics **23**(2), 252 (2001). 66
- [104] M. A. B. MacKay, M. Kravtsenyuk, R. Thomas, N. D. Mitchell, S. M. Dursun, and G. B. Baker. *D-serine: Potential therapeutic agent and/or biomarker in schizophrenia and depression?* (2019). 66
- [105] A. Mozzarelli and R. S. Phillips. *Editorial: Enzymes Regulating the Homeostasis of Agonists and Antagonists of the N-Methyl D-Aspartate Receptors*. Frontiers in Molecular Biosciences **6** (2019). URL <https://www.frontiersin.org/article/10.3389/fmolb.2019.00037/full>.

- [106] F. Št'astný, V. Lisý, V. Mareš, V. Lisá, V. J. Balcar, and A. Santamaría. *Quinolinic acid induces NMDA receptor-mediated lipid peroxidation in rat brain microvessels*. Redox Report **9**(4), 229 (2004).
- [107] K. H. Jhamandas, R. J. Boegman, R. J. Beninger, A. F. Miranda, and K. A. Lipic. *Excitotoxicity of quinolinic acid: Modulation by endogenous antagonists*. Neurotoxicity Research **2**(2-3), 139 (2000). 66
- [108] K. Tsuzuki, M. Iino, and S. Ozawa. *Change in calcium permeability caused by quinolinic acid in cultured rat hippocampal neurons*. Neuroscience Letters **105**(3), 269 (1989). 67, 70
- [109] M. D. Bootman, T. J. Collins, L. Mackenzie, H. Llewelyn Roderick, M. J. Berridge, and C. M. Peppiatt. *2-Aminoethoxydiphenyl borate (2-APB) is a reliable blocker of store-operated Ca²⁺ entry but an inconsistent inhibitor of InsP₃-induced Ca²⁺ release* (2002). 67
- [110] K. Takahashi, M. Yokota, and T. Ohta. *Molecular mechanism of 2-APB-induced Ca²⁺ influx in external acidification in PC12*. Experimental Cell Research **323**(2), 337 (2014). 67
- [111] A. Sengupta, J. Kabat, M. Novak, Q. Wu, I. Grundke-Iqbal, and K. Iqbal. *Phosphorylation of tau at both Thr 231 and Ser 262 is required for maximal inhibition of its binding to microtubules*. Archives of biochemistry and biophysics **357**(2), 299 (1998). 67
- [112] M. Benneicib, C.-X. Gong, I. Grundke-Iqbal, and K. Iqbal. *Role of protein phosphatase-2A and -1 in the regulation of GSK-3, cdk5 and cdc2 and the phosphorylation of tau in rat forebrain*. FEBS Letters **485**(1), 87 (2000). URL [https://doi.org/10.1016/S0014-5793\(00\)02203-1](https://doi.org/10.1016/S0014-5793(00)02203-1). 68
- [113] E. Sontag, V. Nunbhakdi-Craig, G. Lee, G. S. Bloom, and M. C. Mumby. *Regulation of the Phosphorylation State and Microtubule-Binding Activity of*

- Tau by Protein Phosphatase 2A*. Neuron **17**(6), 1201 (1996). URL <http://www.sciencedirect.com/science/article/pii/S0896627300802500>. 68
- [114] H. Yamamoto, E. Yamauchi, H. Taniguchi, T. Ono, and E. Miyamoto. *Phosphorylation of microtubule-associated protein tau by Ca^{2+} /calmodulin-dependent protein kinase II in its tubulin binding sites*. Arch Biochem Biophys **408**(2), 255 (2002). 68
- [115] H. Guo, L. M. Camargo, F. Yeboah, M. E. Digan, H. Niu, Y. Pan, S. Reiling, G. Soler-Llavina, W. A. Weihofen, H.-R. Wang, Y. G. Shanker, T. Stams, and A. Bill. *A NMDA-receptor calcium influx assay sensitive to stimulation by glutamate and glycine/D-serine*. Scientific Reports **7**(1), 11608 (2017). URL <https://doi.org/10.1038/s41598-017-11947-x>. 68
- [116] S. A. Lipton. *Paradigm shift in neuroprotection by NMDA receptor blockade: Memantine and beyond* (2006). 68
- [117] E. Dominguez, T. Y. Chin, C. P. Chen, and T. Y. Wu. *Management of moderate to severe Alzheimer's disease: Focus on memantine* (2011). 68
- [118] S. A. Lipton. *Failures and Successes of NMDA Receptor Antagonists: Molecular Basis for the Use of Open-Channel Blockers like Memantine in the Treatment of Acute and Chronic Neurologic Insults*. NeuroRx **1**(1), 101 (2004). 68, 70
- [119] C. Prescott, A. M. Weeks, K. J. Staley, and K. M. Partin. *Kynurenic acid has a dual action on AMPA receptor responses*. Neuroscience Letters **402**(1-2), 108 (2006). 69
- [120] Rózsa, H. Robotka, L. Vécsei, and J. Toldi. *The Janus-face kynurenic acid*. Journal of Neural Transmission **115**(8), 1087 (2008). 69
- [121] S. Vandrezen-Filho, P. C. Severino, L. C. Constantino, W. C. Martins, S. Molz, T. Dal-Cim, D. B. Bertoldo, F. R. Silva, and C. I. Tasca. *N-Methyl-D-aspartate Preconditioning Prevents Quinolinic Acid-Induced Deregulation of Glutamate and*

- Calcium Homeostasis in Mice Hippocampus*. Neurotoxicity Research **27**(2), 118 (2014). 69
- [122] A. C. Pawley, S. Flesher, R. J. Boegman, R. J. Beninger, and K. H. Jhamandas. *Differential action of NMDA antagonists on cholinergic neurotoxicity produced by N-methyl-D-aspartate and quinolinic acid*. British Journal of Pharmacology **117**(6), 1059 (1996). 69
- [123] H. n. Xu, L. x. Li, Y. x. Wang, H. g. Wang, D. An, B. Heng, and Y. q. Liu. *Genistein inhibits A β 25–35 -induced SH-SY5Y cell damage by modulating the expression of apoptosis-related proteins and Ca²⁺ influx through ionotropic glutamate receptors*. Phytotherapy Research **33**(2), 431 (2019). 70
- [124] P. Pierozan, F. Ferreira, B. Ortiz de Lima, C. Gonçalves Fernandes, P. Totarelli Monteforte, N. De Castro Medaglia, C. Bincoletto, S. Soubhi Smaili, and R. Pessoa-Pureur. *The phosphorylation status and cytoskeletal remodeling of striatal astrocytes treated with quinolinic acid*. Experimental Cell Research **322**(2), 313 (2014). 70
- [125] K. Chen, Y. An, L. Tie, Y. Pan, and X. Li. *Curcumin Protects Neurons from Glutamate-Induced Excitotoxicity by Membrane Anchored AKAP79-PKA Interaction Network*. Evidence-based complementary and alternative medicine : eCAM **2015**, 706207 (2015). URL <https://www.ncbi.nlm.nih.gov/pubmed/26170881><https://www.ncbi.nlm.nih.gov/pmc/articles/PMC4478437/>. 70
- [126] R. Schwarcz and T. W. Stone. *The kynurenine pathway and the brain: Challenges, controversies and promises* (2017). 71
- [127] D. Zwillling, S. Y. Huang, K. V. Sathyaikumar, F. M. Notarangelo, P. Guidetti, H. Q. Wu, J. Lee, J. Truong, Y. Andrews-Zwillling, E. W. Hsieh, J. Y. Louie, T. Wu, K. Scearce-Levie, C. Patrick, A. Adame, F. Giorgini, S. Moussaoui, G. Laue, A. Rassoulpour, G. Flik, Y. Huang, J. M. Muchowski, E. Masliah, R. Schwarcz, and P. J. Muchowski. *Kynurenine 3-monooxygenase inhibition in blood ameliorates neurodegeneration*. Cell **145**(6), 863 (2011). 71, 72

- [128] K. Jacobs and D. Lovejoy. *Inhibiting the kynurenine pathway in spinal cord injury: Multiple therapeutic potentials?* Neural Regeneration Research **13**(12), 2073 (2018). 71
- [129] M. D. Lovelace, B. Varney, G. Sundaram, N. F. Franco, M. L. Ng, S. Pai, C. K. Lim, G. J. Guillemin, and B. J. Brew. *Current Evidence for a Role of the Kynurenine Pathway of Tryptophan Metabolism in Multiple Sclerosis*. Frontiers in immunology **7**, 246 (2016). URL <https://www.ncbi.nlm.nih.gov/pubmed/27540379><https://www.ncbi.nlm.nih.gov/pmc/articles/PMC4972824/>. 71
- [130] I. Wonodi, O. C. Stine, K. V. Sathyaikumar, R. C. Roberts, B. D. Mitchell, L. E. Hong, Y. Kajii, G. K. Thaker, and R. Schwarcz. *Downregulated Kynurenine 3-Monooxygenase Gene Expression and Enzyme Activity in Schizophrenia and Genetic Association With Schizophrenia Endophenotypes*. Archives of General Psychiatry **68**(7), 665 (2011). URL <https://doi.org/10.1001/archgenpsychiatry.2011.71>. 71
- [131] K. R. Jacobs, C. K. Lim, K. Blennow, H. Zetterberg, P. Chatterjee, R. N. Martins, B. J. Brew, G. J. Guillemin, and D. B. Lovejoy. *Correlation between plasma and CSF concentrations of kynurenine pathway metabolites in Alzheimer’s disease and relationship to amyloid- β and tau*. Neurobiology of Aging **80**, 11 (2019). URL <http://www.sciencedirect.com/science/article/pii/S0197458019301009>. 71, 72
- [132] C. J. Clark, G. M. Mackay, G. A. Smythe, S. Bustamante, T. W. Stone, and R. S. Phillips. *Prolonged Survival of a Murine Model of Cerebral Malaria by Kynurenine Pathway Inhibition*. Infection and Immunity **73**(8), 5249 LP (2005). URL <http://iai.asm.org/content/73/8/5249.abstract>. 72
- [133] F. R. Petry, J. Pelletier, A. Bretteville, F. Morin, F. Calon, S. S. Hébert, R. A. Whittington, and E. Planel. *Specificity of Anti-Tau Antibodies when Analyzing Mice Models of Alzheimer’s Disease: Problems and Solutions*. PLOS ONE **9**(5), e94251 (2014). URL <https://doi.org/10.1371/journal.pone.0094251>. 72

-
- [134] D. Li and Y. K. Cho. *High specificity of widely used phospho-tau antibodies validated using a quantitative whole-cell based assay*. bioRxiv p. 612911 (2019). URL <http://biorxiv.org/content/early/2019/04/18/612911.abstract>. 72
- [135] T. Kimura, G. Sharma, K. Ishiguro, and S.-i. Hisanaga. *Phospho-Tau Bar Code: Analysis of Phosphoisotypes of Tau and Its Application to Tauopathy* (2018). URL <https://www.frontiersin.org/article/10.3389/fnins.2018.00044>. 72